21st course of the International School
of Cosmic-Ray Astrophysics – Erice, 2018 August 2-3

Cosmic-ray direct detection

Lecture I

Pier Simone Marrocchesi - Univ. of Siena and INFN Pisa

Overview

LECTURE-I :

- A brief historical introduction to cosmic rays
- Cosmic-ray detection: from balloons to space
- Electron and positron measurements

LECTURE-II :

- Energy spectra of p, He, light nuclei, sub-Fe nuclei
- Secondary-to-Primary, Primary-to-Primary, Secondary-to-Secondary ratios
- Anti-protons
- Isotope flux ratios, propagation clocks, ultra-heavy nuclei
- A glimpse to future direct measurements of VHE cosmic rays

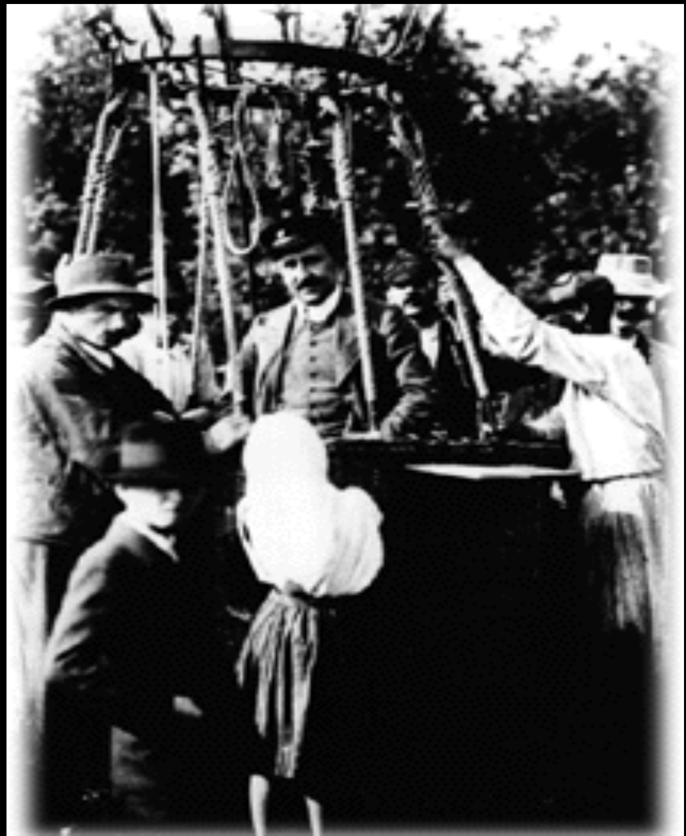 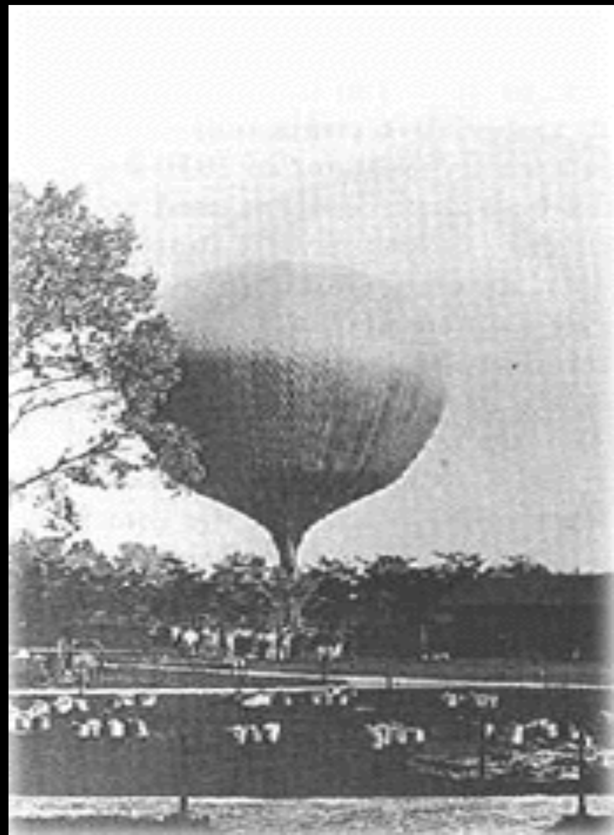

It all started with balloons !

In 1912 the Austrian physicist Victor Hess carried out measurements, at different altitudes in the atmosphere, of the intensity of the misterious ioning radiation that had been observed at sea level. Taking serious risks (no oxygen mask), he reached an altitude ~6500 m aboard a balloon and meaured an INCREASE of the radiation flux with altitude: just the OPPOSITE of what the current expectations were at the time !

GENERATION OF SHOWERS IN THE ATMOSPHERE

- ✧ an example of a hadronics shower generated by a primary proton impinging on top of the atmosphere

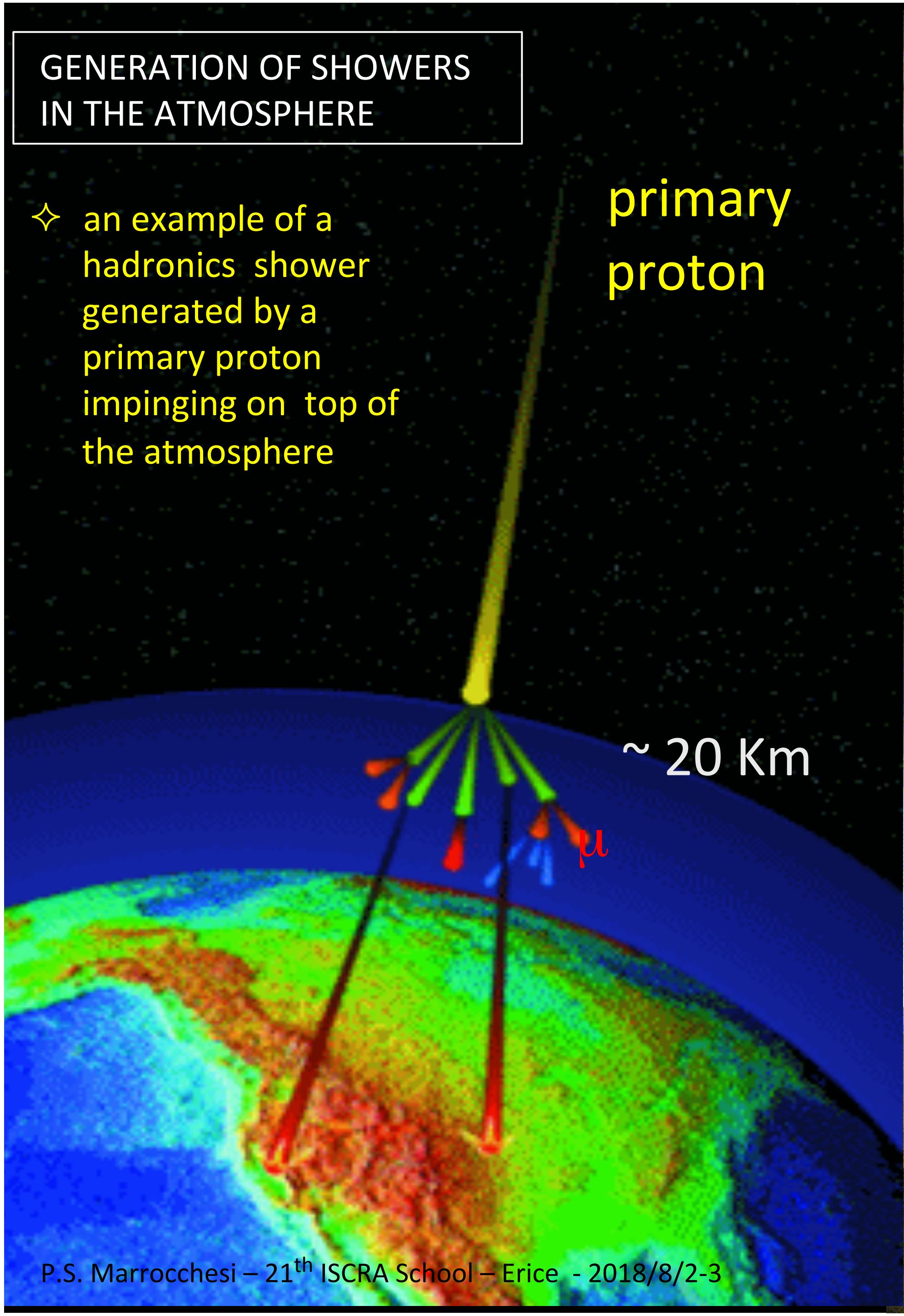

GENERATION OF SHOWERS IN THE ATMOSPHERE

- ✧ an example of the the electromagnetic component of an atmospheric shower

Muons from the cascade decay with τ = 2.2. μs but $\gamma c\tau$ ~ 20 Km for ~3GeV muons -> they can be seen at sea-level

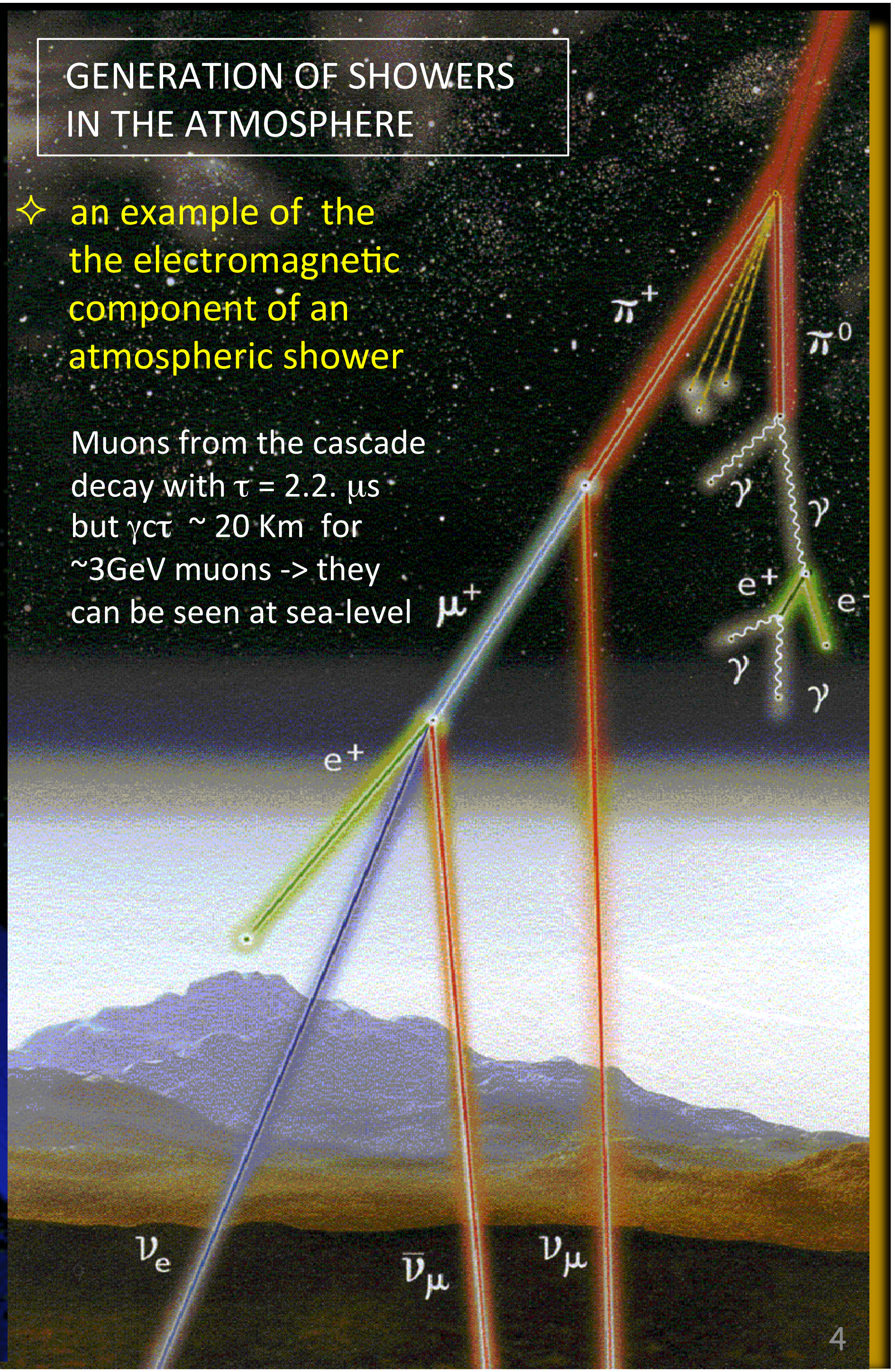

Ground detection of Cherenkov light from atmospheric showers

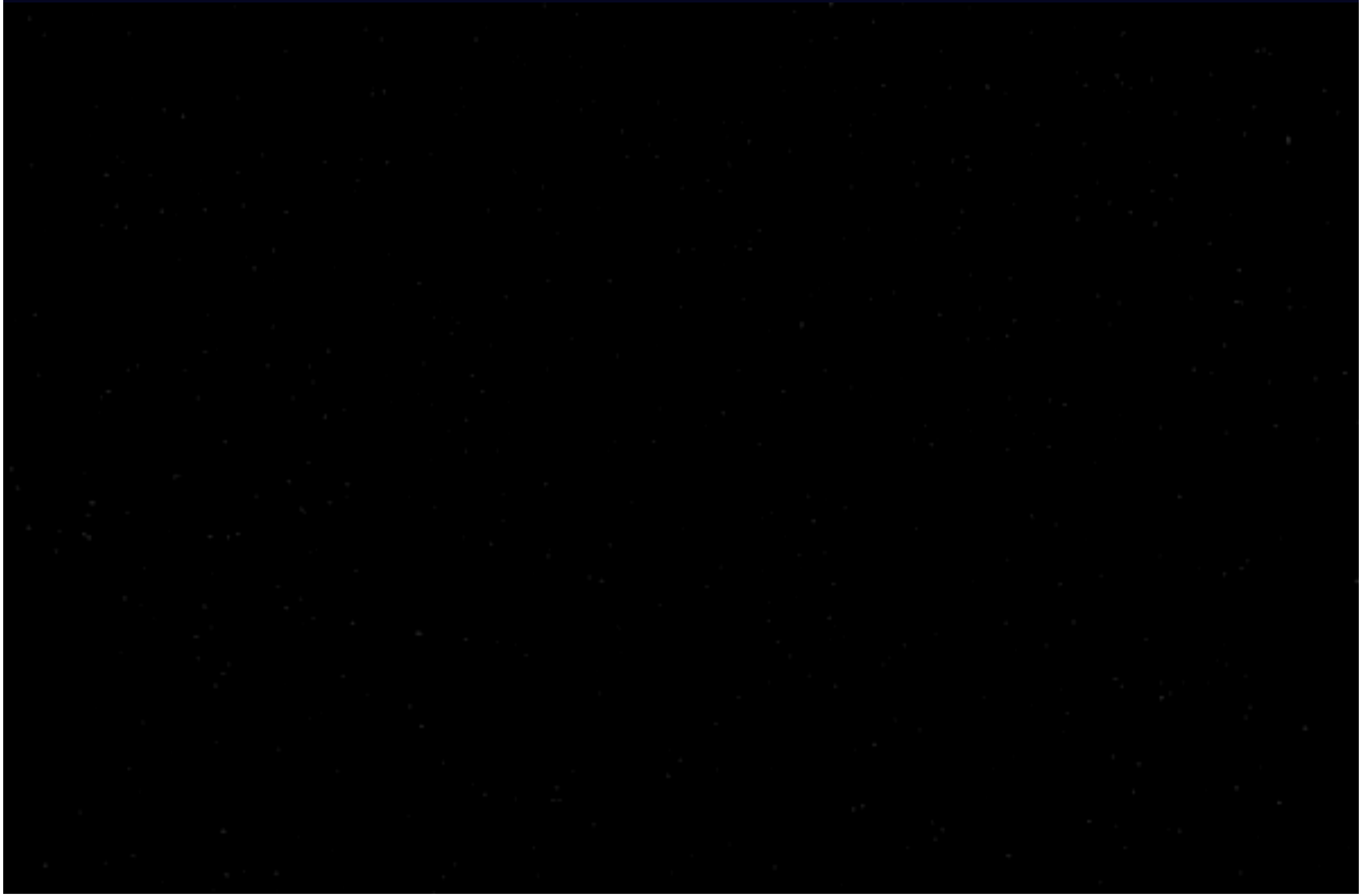

Development of cosmic-ray air showers

GENERATION OF SHOWERS IN THE ATMOSPHERE

an example of shower generated by a primary IRON nucleus impinging at high altitude

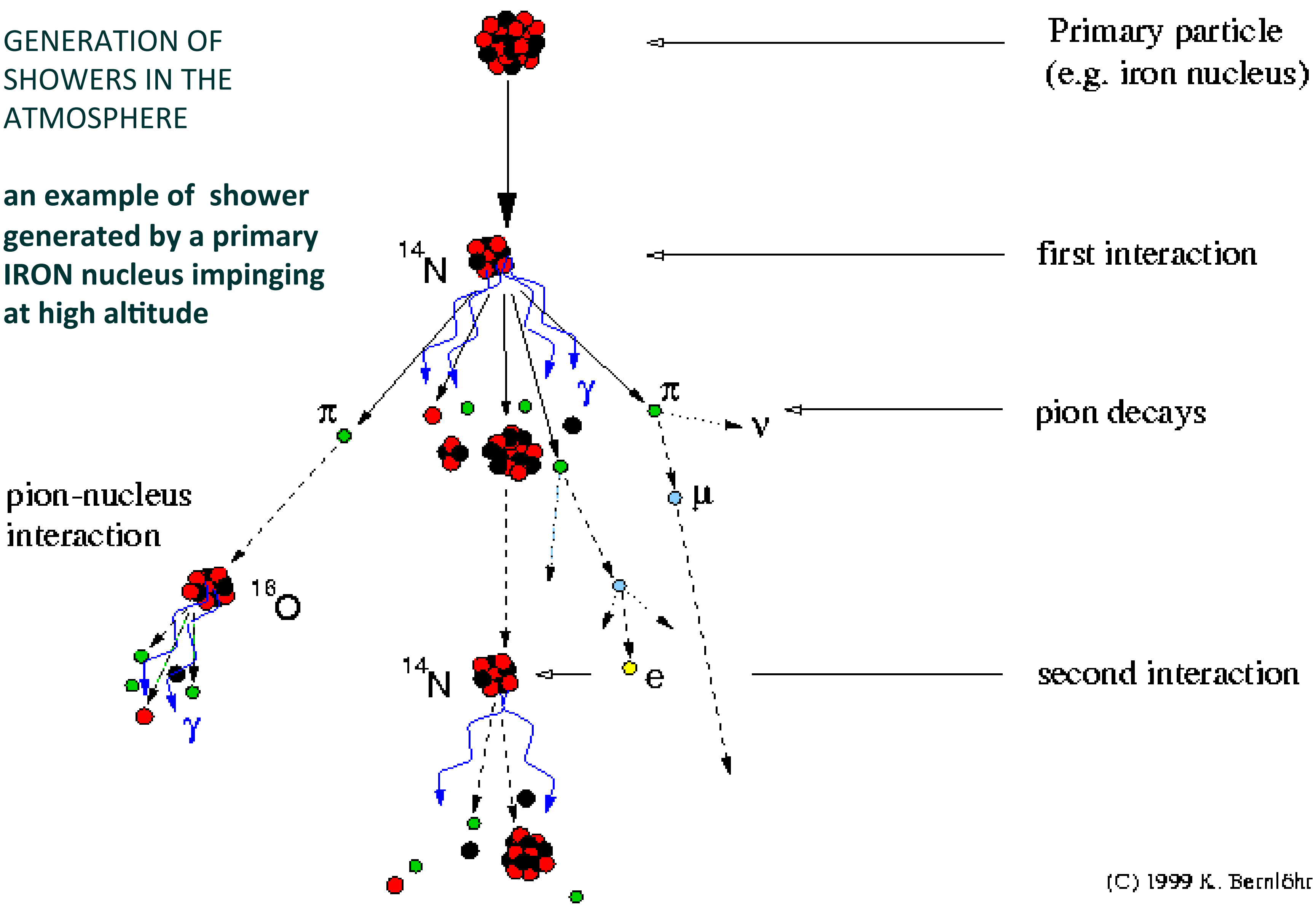

Particle Physics was born AFTER the discovery of COSMIC RAYS

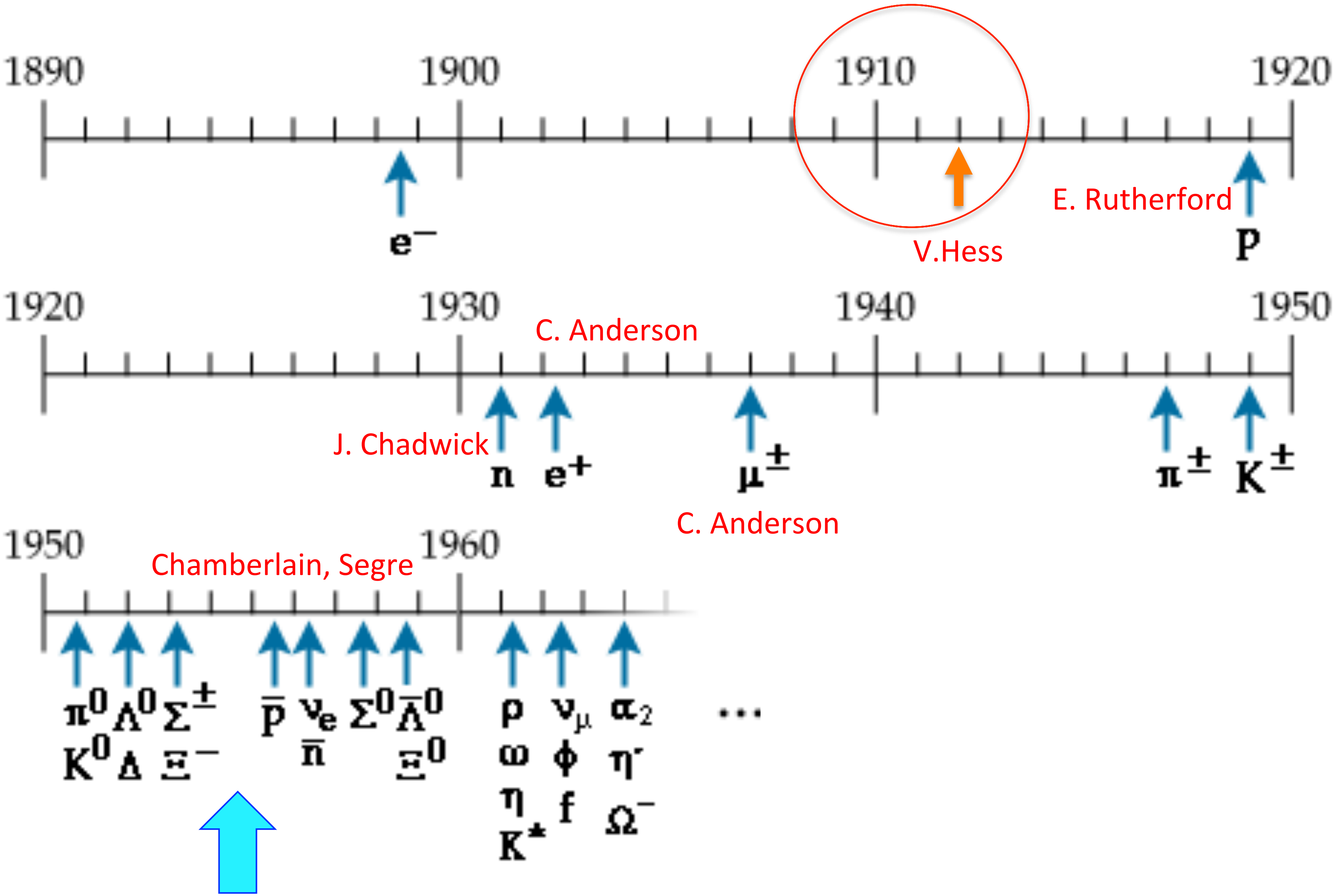

First experiments at particle accelerators

COSMIC RAYS: DIRECT AND INDIRECT MEASUREMENTS

SPACE-BORNE

- free-flyers (satellites)
- International Space Station (ISS)

BALLOON-BORNE

- Long Duration LDB
- Ultra Long (ULDB)

GROUND-BASED

- Air Cherenkov
- Extensive Air Shower
- Under-ground
- Under-water
- Under-ice

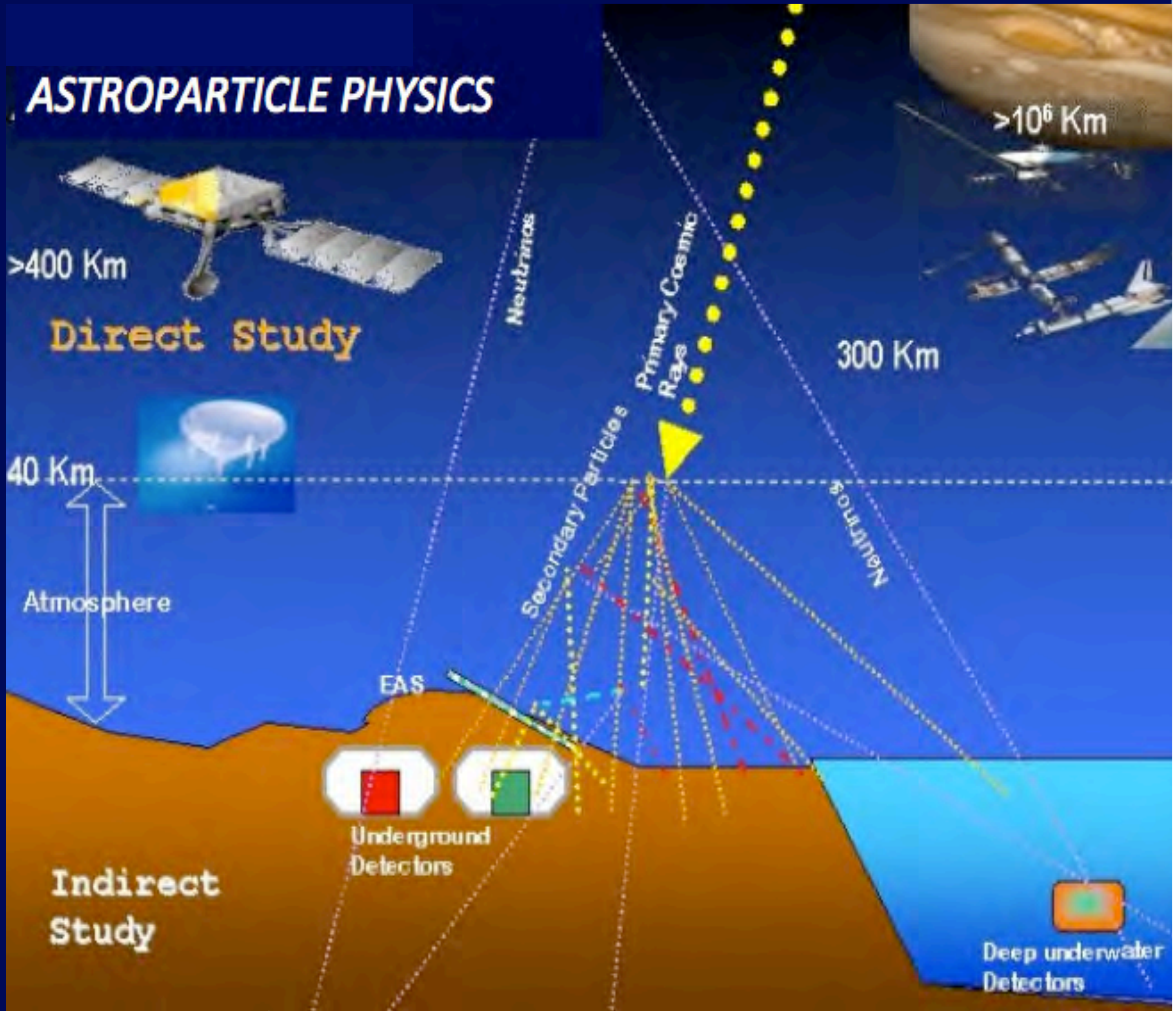

Direct measurements of cosmic rays

Two broad classes of instruments:

- Separation between positive and negative charges:
  - **Magnetic spectrometers**: - permanent magnetization
    - super-conducting coils
  - measurement of momentum

- No sign-of-charge discrimination:
  - **Calorimeters** (mainly, but also TRDs)
  - measurement of energy

(*) another possibility: Fermi experiment uses the Earth magnetic field to separate the two charges, but at low rigidity

Measurement of momentum

① UNIFORM MAGNETIC FIELD $\vec{B}$

- THE TRACK IS BENT IN THE "BENDING PLANE" ORTHOGONAL TO $\vec{B}$
- THE DEFLECTION ANGLE φ OVER THE LENGTH L MEASURES THE TRANSVERSE MOMENTUM P_T

$$\vec{P} = \vec{P}_T + \vec{P}_{//} \qquad P_T = P \sin\theta$$

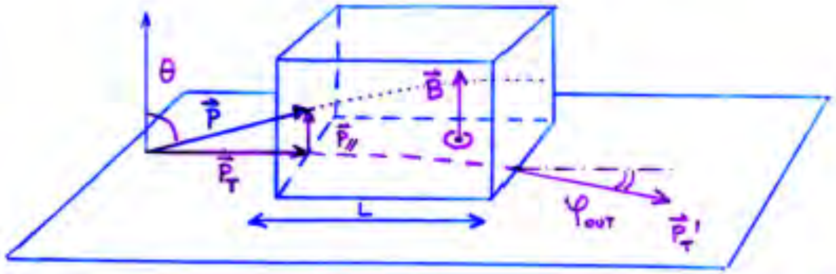

WHERE: θ = POLAR ANGLE $\equiv \measuredangle(\vec{p}, \vec{B})$

λ = DIP ANGLE $\equiv \frac{\pi}{2} - \theta$

ρ = RADIUS OF CURVATURE

q = CHARGE

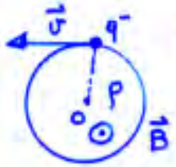

$$q v B = m v^2/\rho$$

$$\boxed{\rho = \frac{P_T}{qB}}$$

- THE DEFLECTION ANGLE φ_{OUT} :

$$\boxed{\sin\varphi_{OUT} = \frac{L}{\rho}}$$

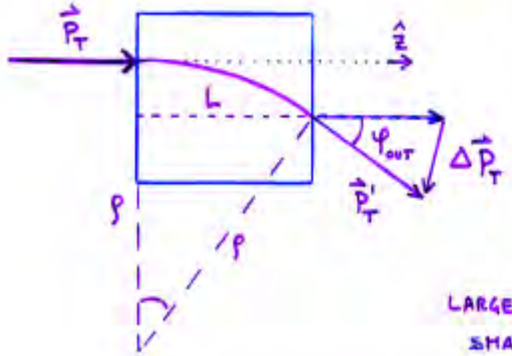

IS A MEASURE OF THE CURVATURE OF THE TRACK :

$$\boxed{\frac{1}{\rho} = \frac{qB}{P_T}}$$

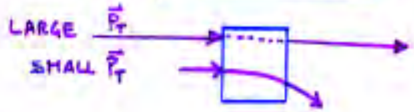

- HIGH MOMENTUM TRACKS : ("STIFF TRACKS") $\begin{cases} \rho & \text{LARGE} \\ 1/\rho & \text{SMALL} \end{cases}$

- LOW MOMENTUM TRACKS : $\begin{cases} \rho & \text{SMALL} \\ 1/\rho & \text{LARGE} \end{cases}$

- THE "MOMENTUM KICK" $\Delta\vec{P}_\perp$ IS PROPORTIONAL TO THE FIELD INTEGRAL $\int_0^L B\,d\ell$:

$$\Delta P_T = \int_{t_1}^{t_2} q v_z B \, dt = q \int_0^L B \, dz =$$

$$= q B L \qquad \text{FOR } \vec{B} \text{ UNIFORM IN } L$$

Example 1. (over simplified)

- One point P_1 known with infinite precision before the magnet
- One point P_2 measured with (point resolution) accuracy $\boxed{\delta x}$ after the magnet

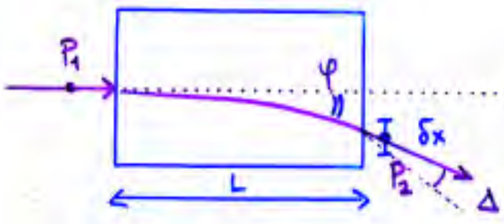

$\Delta\varphi \simeq \frac{\delta x}{L}$ UNCERTAINTY ON THE DEFLECTION

- The uncertainty on the transverse momentum comes from the uncertainty on the deflection

$$\delta\left(\frac{1}{\rho}\right) = \delta\left(\frac{\varphi}{L}\right) = \frac{\delta\varphi}{L} = \frac{\delta x}{L^2}$$

$$\left|\delta\left(\frac{1}{P_T}\right)\right| = \boxed{\frac{\delta P_T}{P_T^2} \cong \frac{1}{0.3\,B}\,\delta\left(\frac{1}{\rho}\right)}$$

B (Tesla)
p_T (GeV/c)
L (m)

ERROR ON TRACK CURVATURE

$$\boxed{\frac{\delta P_T}{P_T} \simeq P_T \, \frac{\delta x}{0.3} \, \frac{1}{BL^2}}$$

important scale factor

Example 2. (neglecting MS)

Reminder

- NO MULTIPLE SCATTERING
- TRACKING SYSTEM WITH N+1 MEASUREMENTS WITH ACCURACY δx

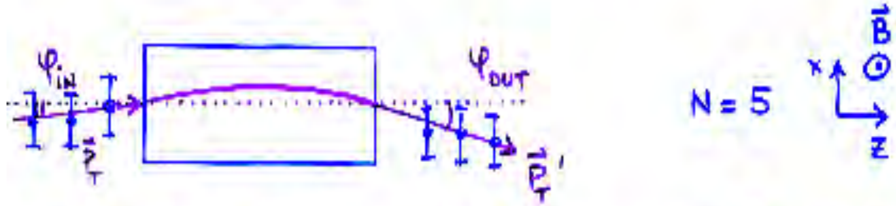

- IN THIS CASE: $\frac{P_T' - P_T}{P_T} = \frac{L}{\rho} = \sin\varphi_{OUT} - \sin\varphi_{IN}$
- THE P_T RELATIVE ERROR: $\frac{\delta P_T}{P_T} \simeq \frac{P_T\,\delta x}{0.3\,BL^2}\sqrt{A_N}$

WHERE A_N IS A STATISTICAL FACTOR THAT DEPENDS ON:

- THE NUMBER N+1 OF INDEPENDENT MEASUREMENTS
- THE GEOMETRY OF THE "TRACKING SYSTEM"

(i) UNIFORM SPACING [GLUCKSTERN, NUCL. INSTR. METHODS 24, 381 (1963)]

$$\delta\left(\frac{1}{\rho}\right) \simeq \frac{\delta x}{L^2}\sqrt{A_N}$$

$$A_N = \frac{720\,N^3}{(N-1)(N+1)(N+2)(N+3)} \xrightarrow{(N \gg 10)} \frac{720}{N+5}$$

Multiple Scattering contribution

- MULTIPLE SCATTERING PRODUCES A DEFLECTION ("APPARENT CURVATURE") OF THE TRACK WHICH AFFECTS MOMENTUM RESOLUTION.
- ANALOGY BETWEEN THE TWO CASES:

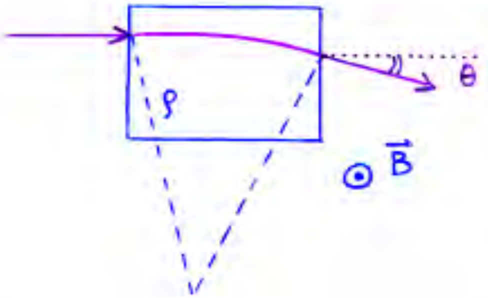

- CURVATURE DUE TO $\vec{B}$:

$$\frac{1}{\rho} \simeq \frac{\theta}{L}$$

$$\delta\left(\frac{1}{\rho}\right) = \frac{\delta\theta}{L} = \frac{\delta x}{L^2}$$

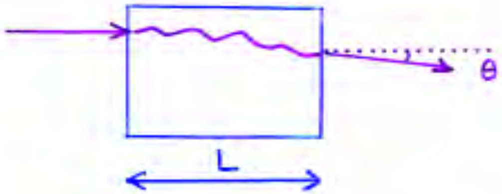

- "APPARENT CURVATURE":

$$\frac{1}{\rho} \simeq \frac{\theta_{MS}}{L}$$

- CURVATURE ERROR:

$$\delta\left(\frac{1}{\rho}\right) = \frac{\delta\theta_{MS}}{L}$$

$$\delta\left(\frac{1}{\rho}\right)_{MS} \simeq \frac{\theta^{RMS}_{PLANE}}{L} \cong \frac{0.015}{\beta p\,(GeV/c)}\sqrt{\frac{L}{X_0}}\cdot\frac{1}{L}$$

$$\left(\frac{\Delta P}{P}\right)_{MS} \cong \frac{0.015}{\beta p}\,\frac{1}{\sqrt{X_0 L}} \propto \frac{1}{\sqrt{L}}$$

- THE RELATIVE ERROR ON MOMENTUM DECREASES (WEAKLY) AS $L^{-1/2}$ TRACK LENGTH IN THE MEDIUM.

Summary:

(i) $\frac{\Delta P_\perp}{P_\perp^2} = \text{const.} \Rightarrow \boxed{\frac{\Delta P_\perp}{P_\perp} \propto P_\perp}$

(ii) $\boxed{\frac{\Delta P_\perp}{P_\perp^2} \propto \frac{1}{BL^2}} \Rightarrow$
- IMPROVES WITH: B LARGE
- IMPROVES MUCH MORE WITH LARGE TRACK LENGTH

⇓

∴ LARGE DETECTORS WITH LARGE TRACKING VOLUME

(iii) $\boxed{\frac{\Delta P_\perp}{P_\perp^2} \propto \delta x}$
- IMPROVES WITH BETTER SPACE RESOLUTION

⇓

∴ HIGH ACCURACY DETECTORS

- THESE RESULTS HOLD WHEN THE CONTRIBUTION OF THE MULTIPLE SCATTERING (MS) IN THE MATERIAL TRAVERSED BY THE PARTICLE IS NEGLIGIBLE
- AT LOW P_T THIS IS NO LONGER TRUE AND $\frac{\Delta P_T}{P_T}$ IS NOT LINEAR IN P_T

$$\boxed{\frac{\delta P_T}{P_T} \sim A \cdot P_T + (B)}$$

Golden's balloon-borne superconducting magnetic spectrometer

[Golden et al. 1984]

- Balloon flight in 1976 from Palestine, U.S.A.
- Exposure time = 19hr
- Altitude: ~5.8g/cm^2
- SΩ = 324 cm^{2}sr
- e$^-$ (separated from e$^+$)

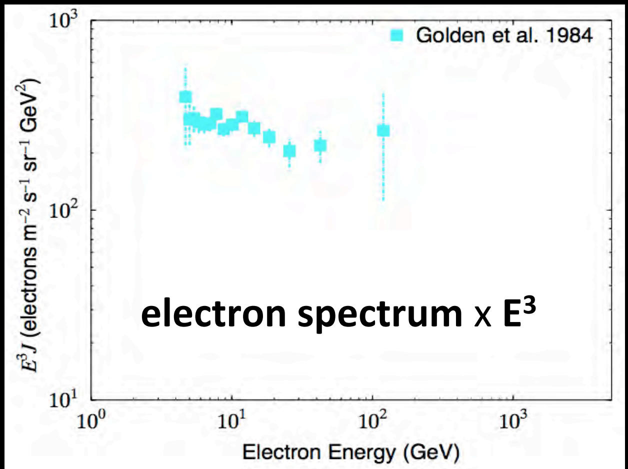

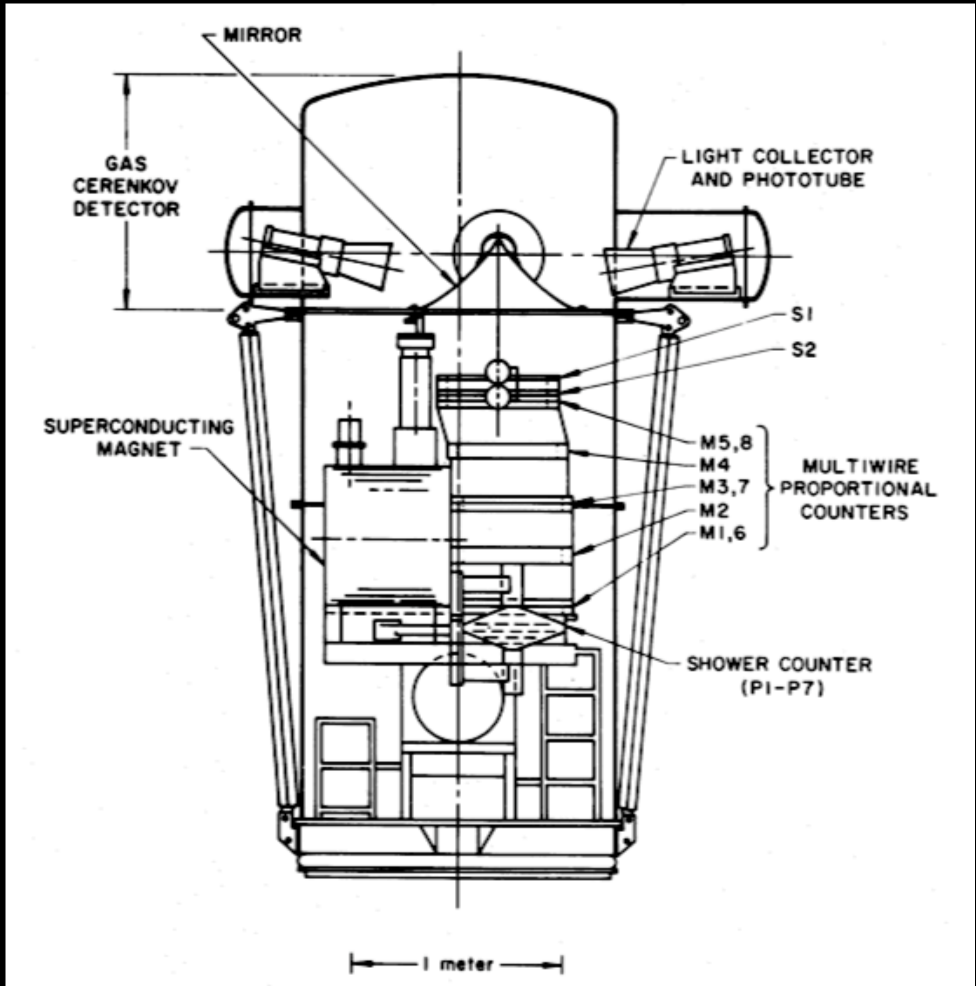

- Flying a super-conducting magnet on a ballon or in space *for a significant amount of time* is a considerable technical challenge

An example: the complexity of the cryostat of the BESS-Polar II balloon experiment

Scientific ballooning

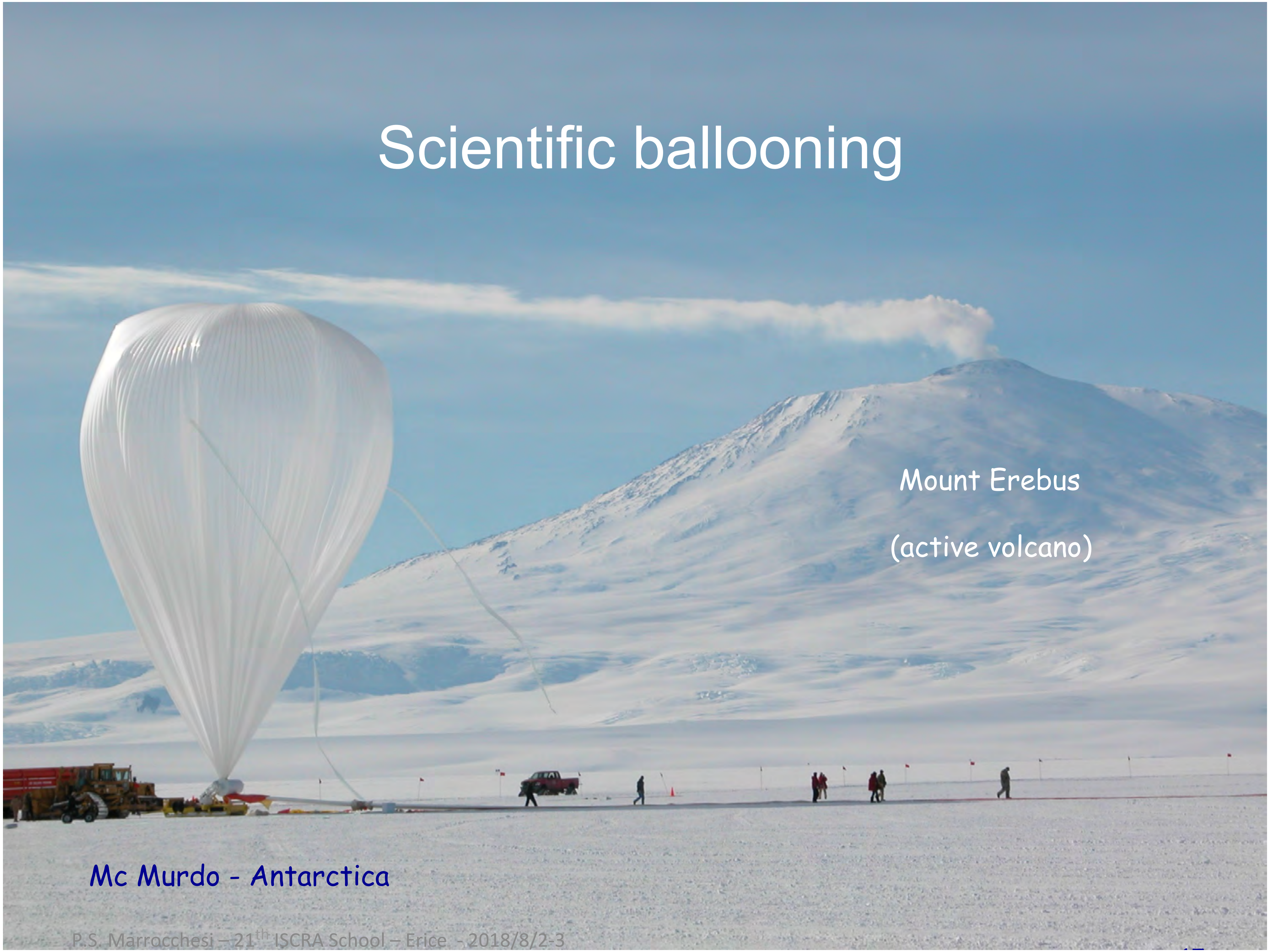

1990s

- Extensive campaign of **daily balloon flights** operated by several groups
  - Wizard (MASS, TS, CAPRICE)
  - BESS
  - Others (HEAT, IMAX...)

- Main instrument characteristics
  - Superconducting magnets ($\sim 1T$ field)
  - MWPC & drift chamber tracking systems ($O(100\mu m)$ resolution)
  - MDR $\sim 100 \div 300\ GV$

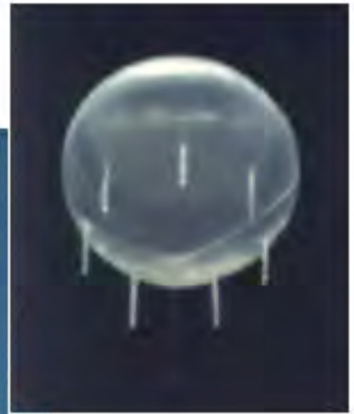

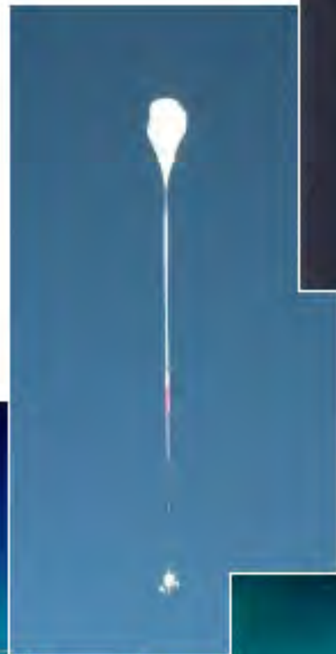

courtesy of
E. Vannuccini
ISSS-2017

MASS-91

[Grimani et al. 2002]

- Balloon flight in 1991
- From Fort Sumner, U.S.A.
- Exposure time = ~10hr
- Altitude = ~5.8 g/cm^2
- SΩ = 182 cm^{2}sr

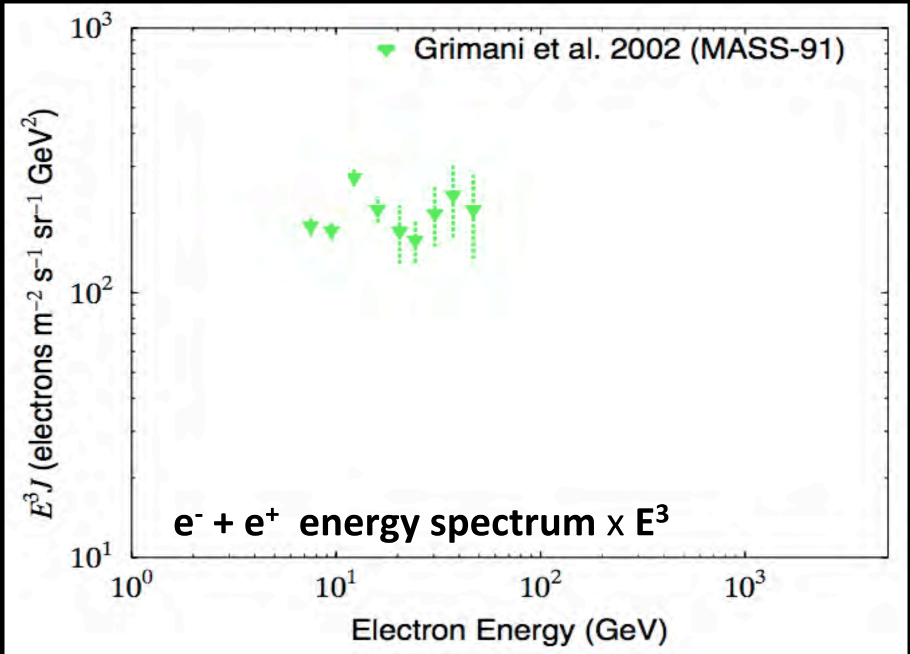

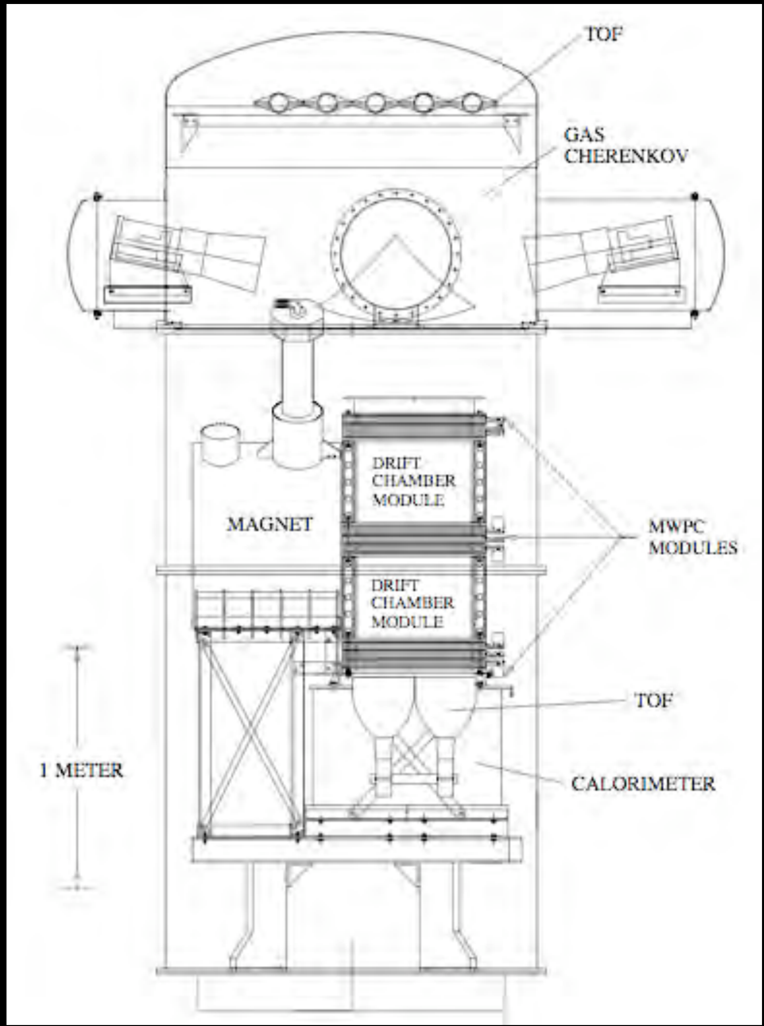

CAPRICE94

[Boezio et al. 2000]

- Balloon flight in 1994
  - From Lynn Lake, Canada
- Exposure time = ~18hr
- Altitude = ~3.9 g/cm^2
- SΩ = ~170 cm^{2}sr
- e-, e+ (separated)

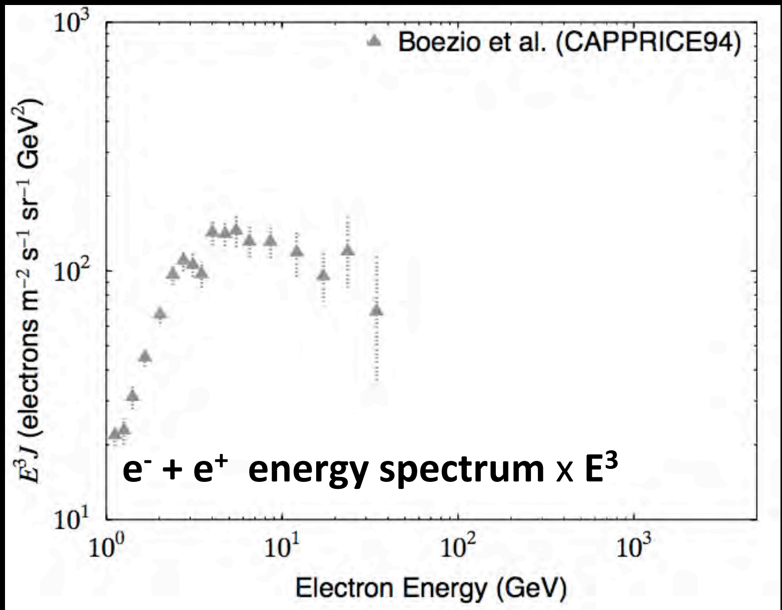

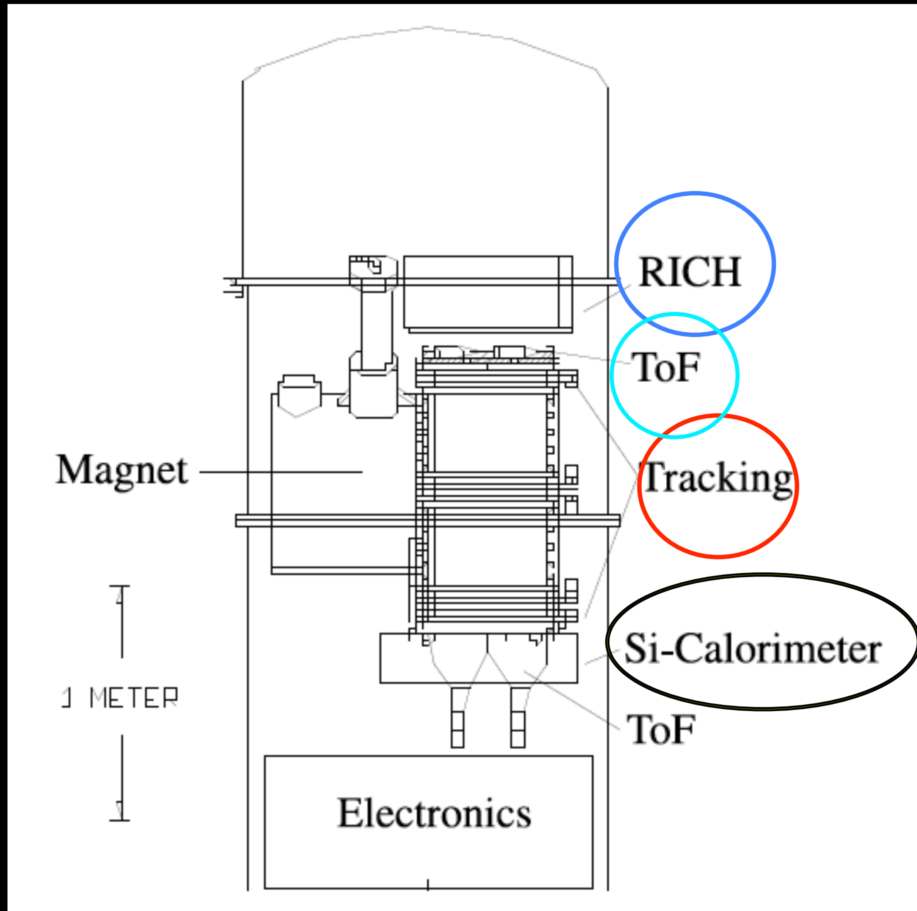

Balloon-borne magnetic spectrometers

HEAT

[DuVernois et al. 2001]

- Balloon flights in 1994,1995
  - From Fort Sumner, Lynn Lake
- Exposure time = 55hr
- Altitude = 5~6 g/cm^2
- $S\Omega$ = 495 cm^{2}sr
- e-, e+ (separated)

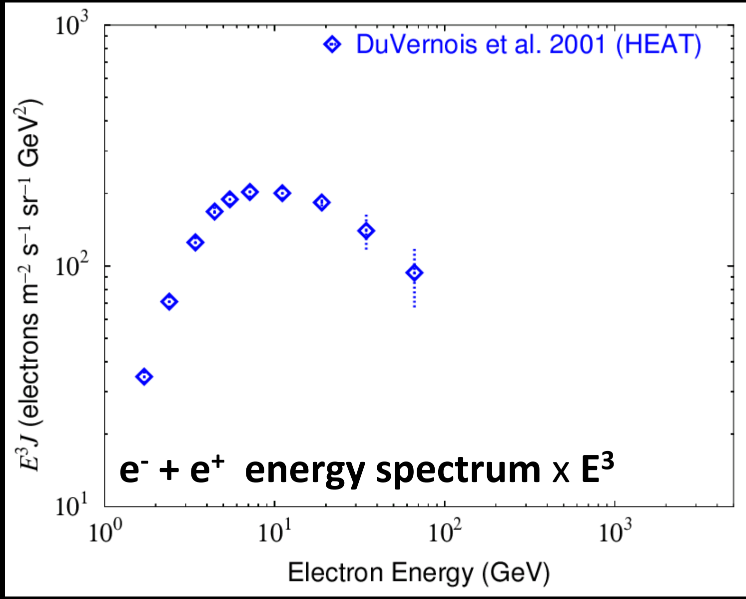

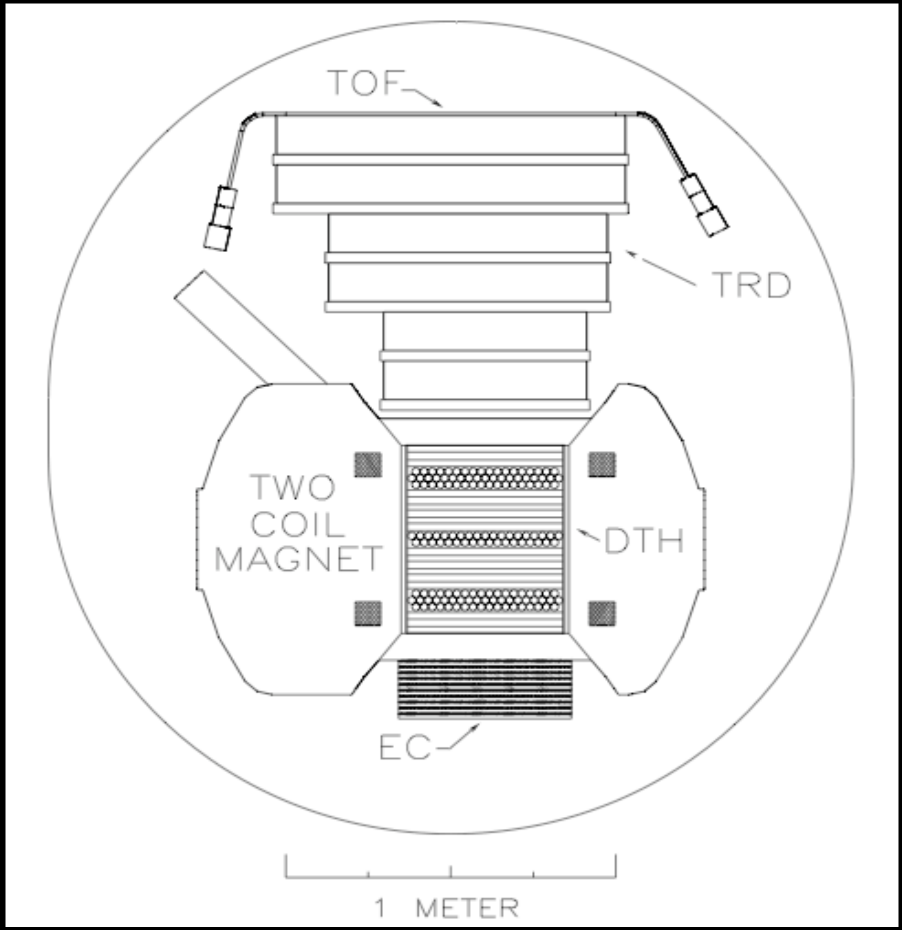

Space-borne magnetic spectrometers

AMS-01

- Space shuttle in 1998
  - 51.7 deg orbit (Discovery)
- Exposure time = ~$1.8x10^2$hr
- Altitude: 320-390km
- $S\Omega$ = ~$1.0x10^3$ cm^2sr
- e-, e+ (separated)

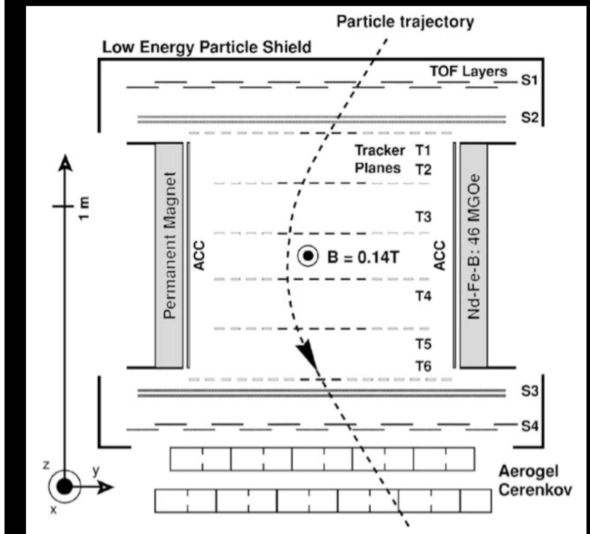

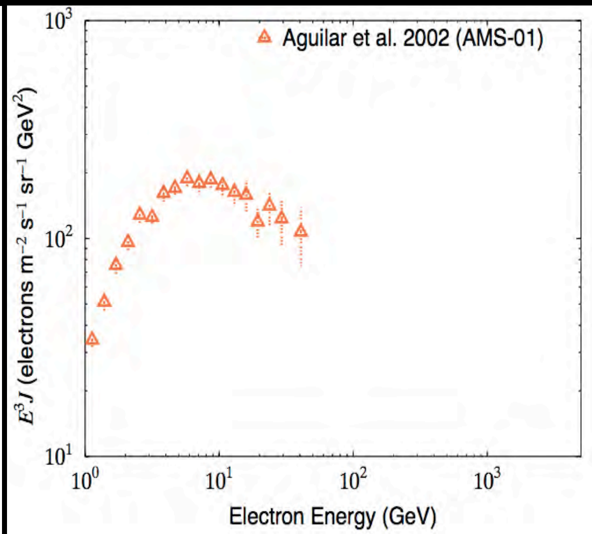

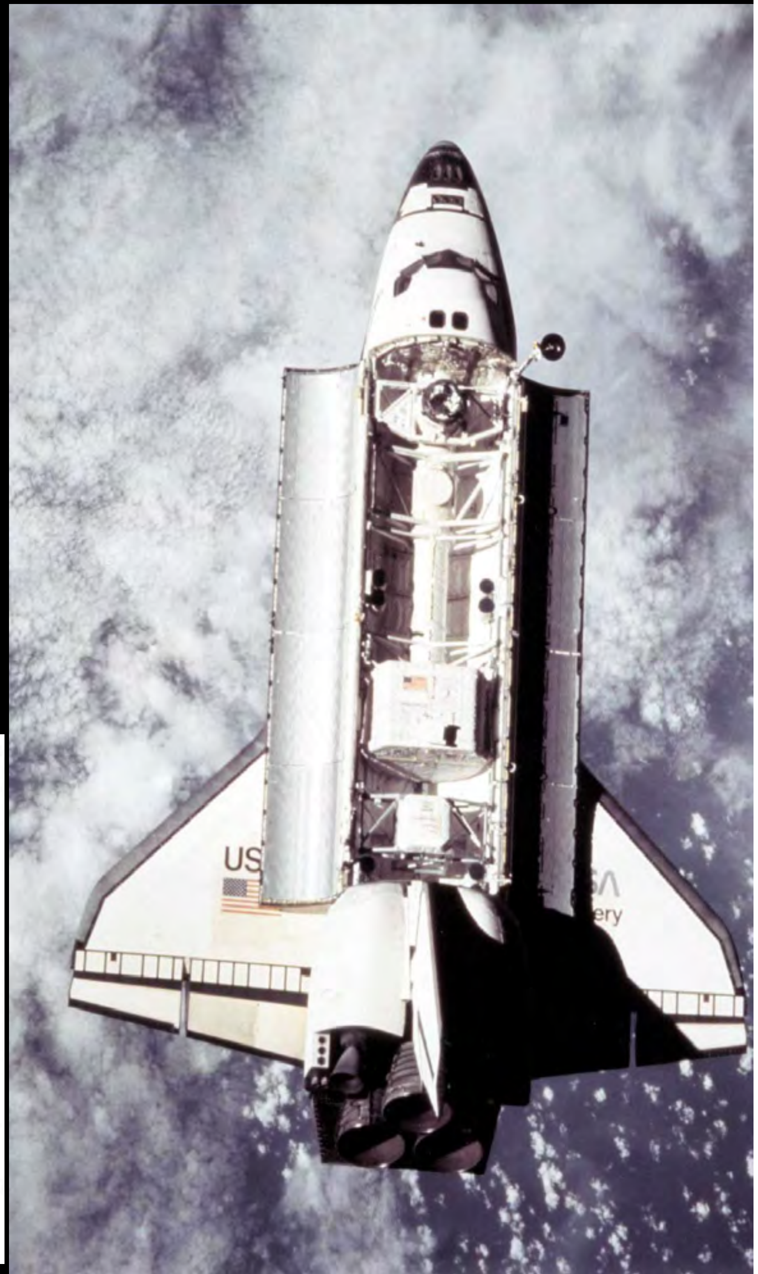

Propagation of cosmic-ray electrons in the Galaxy

- **Energy losses**:
  - **Inverse Compton** scattering with interstellar photons
  - **Synchrotron radiation** in the interstellar magnetic field (B~6μG)

  $\Rightarrow$ $dE/dt = -bE^2$

- Life time of electrons:

  $T=1/(bE) \approx 2.5x\mathbf{10^5 yr}/E(TeV)$

- Propagation distance in the Galaxy:

  $R=(2DT)^{1/2} \approx$ **0.4 ÷ 0.8kpc** (@E=1TeV)

  - Diffusion coeff.: $D=(1\text{-}4)x10^{29}(E/TeV)^{0.3}(cm^2/s)$

Propagation

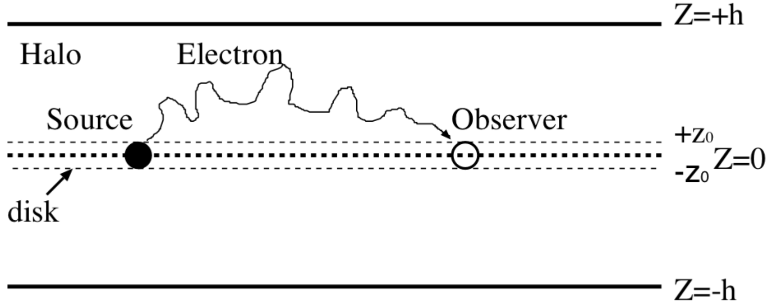

(Diffusion model)

↓

Observations

Constraints on High-Energy Cosmic-Ray Electron Observations

- TeV electrons from distant sources with
  R > ~ 1kpc or T > ~10^5yr
  - Cannot reach the solar system

- TeV electrons from nearby sources with
  R < ~ 1kpc and T < ~10^5yr
  - Identifiable structure(s) in the spectrum
  - Anisotropy of arrival direction of electrons

- *Precision measurements of the electron spectrum* is the key for the identification of cosmic-ray sources where electron acceleration takes place.

Acceleration of CR electrons

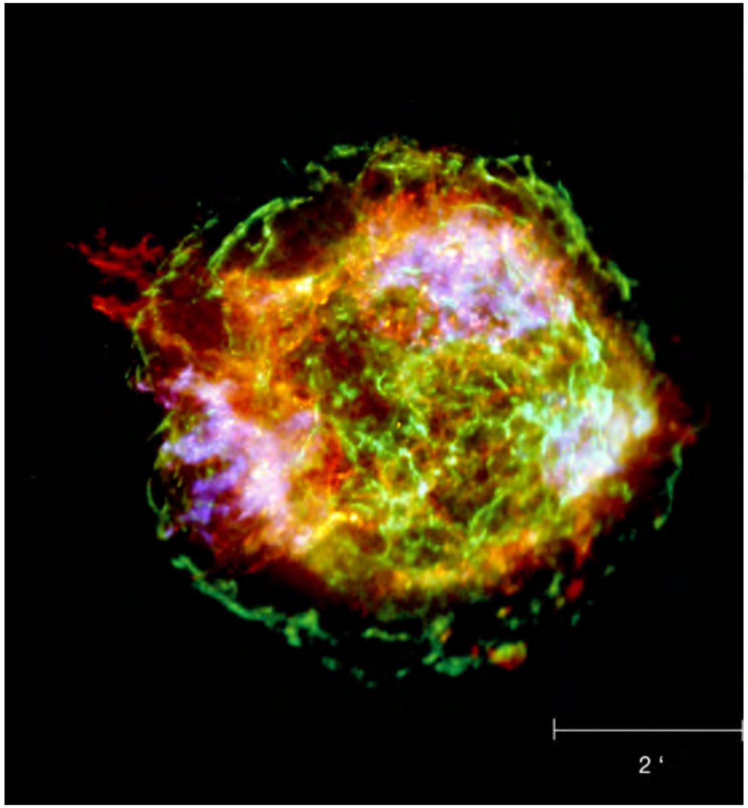

X-ray image of Cas A

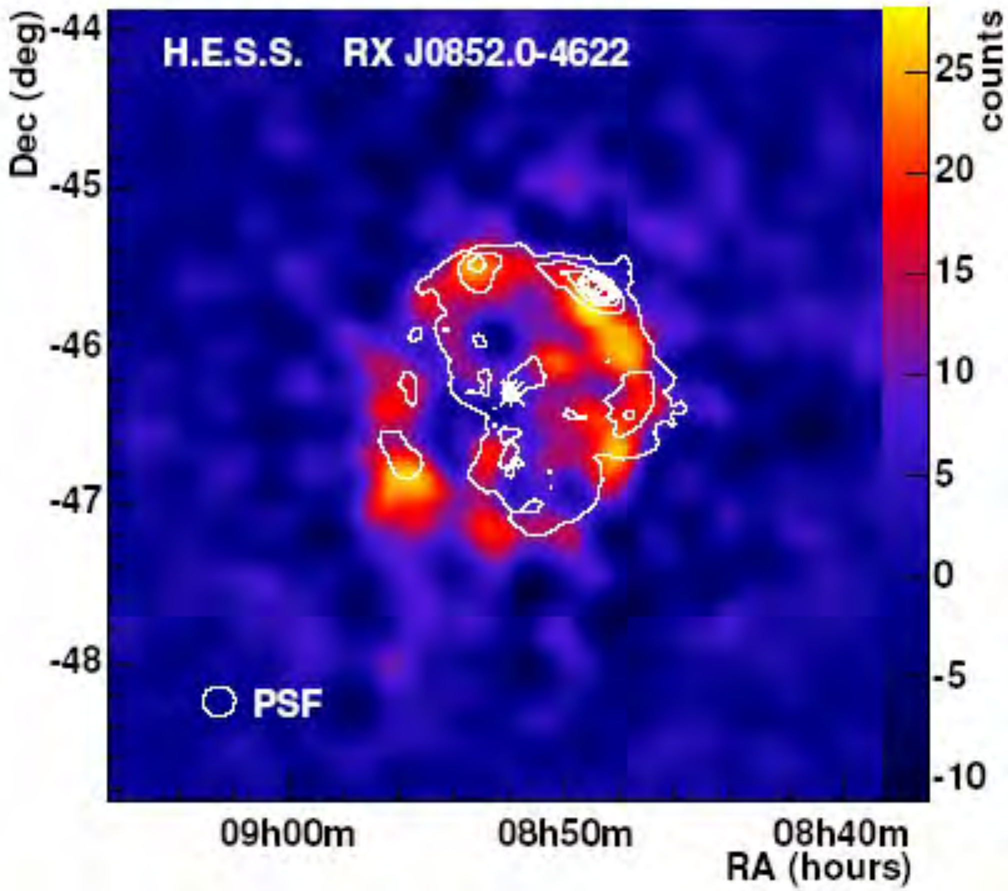

Gamma-ray image of RX J0852.0-4622

- Evidence of high-energy electrons in SNRs from X-ray observations
- Electron or hadron? from gamma-ray observations

Movie: Shock Acceleration by Supernova Remnants

Known Nearby SNRs

Contour of electron flux distance vs. age (E=3TeV)

SNR	R(kpc)	T(yr)
SN185	0.95	1.8×10^3
S147	0.80	4.6×10^3
HB 21	0.80	1.9×10^4
G65.3+5.7	0.80	2.0×10^4
Cygnus Loop	0.44	2.0×10^4
Vela	0.30	1.1×10^4
Monogem	0.30	8.6×10^4
Loop1	0.17	2.0×10^5
Geminga	0.4	3.4×10^5

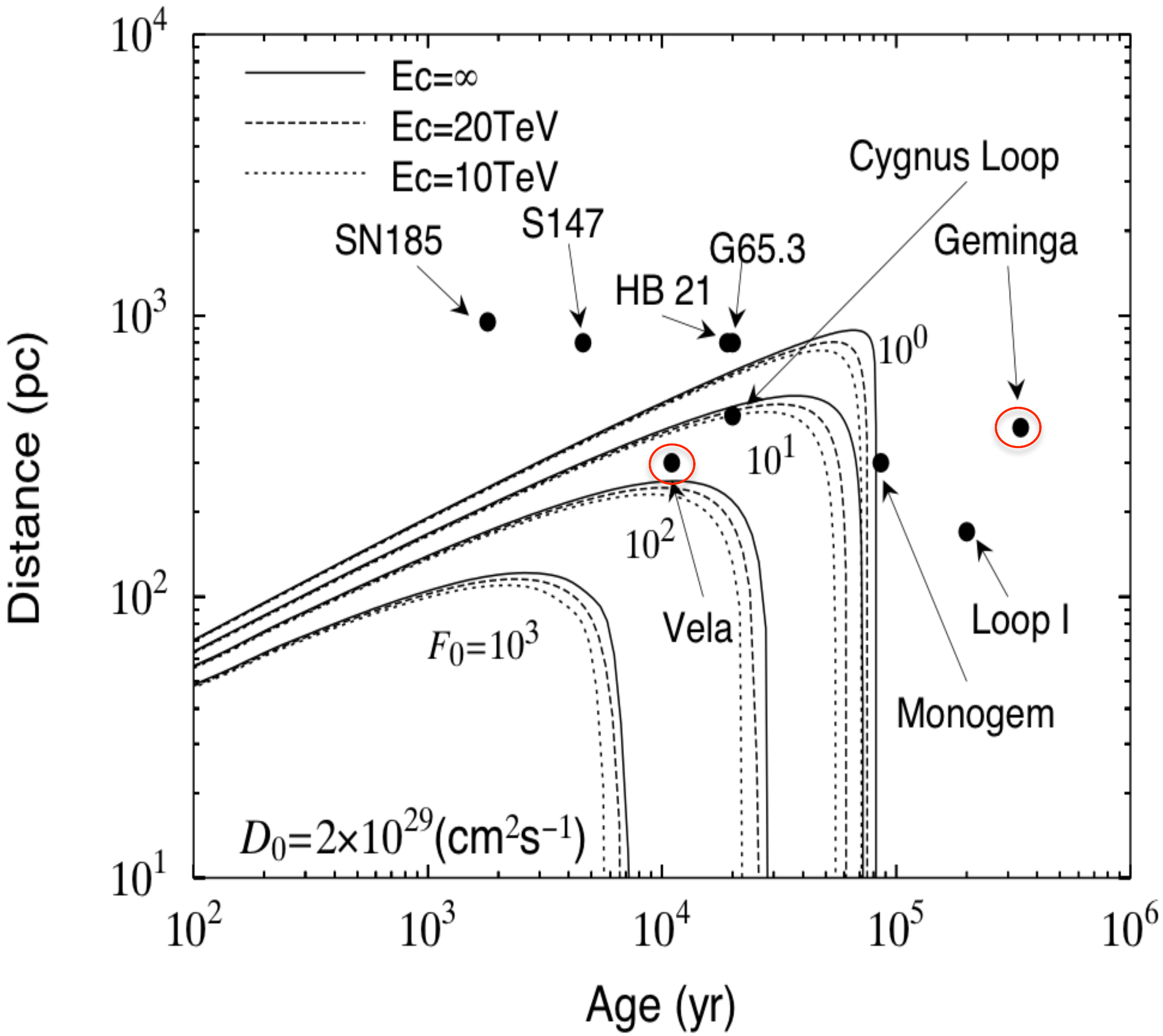

Energy spectra vs. diffusion coefficient

D = 1 x 10^{29} cm^{2}s^{-1}@1TeV K.Yoshida

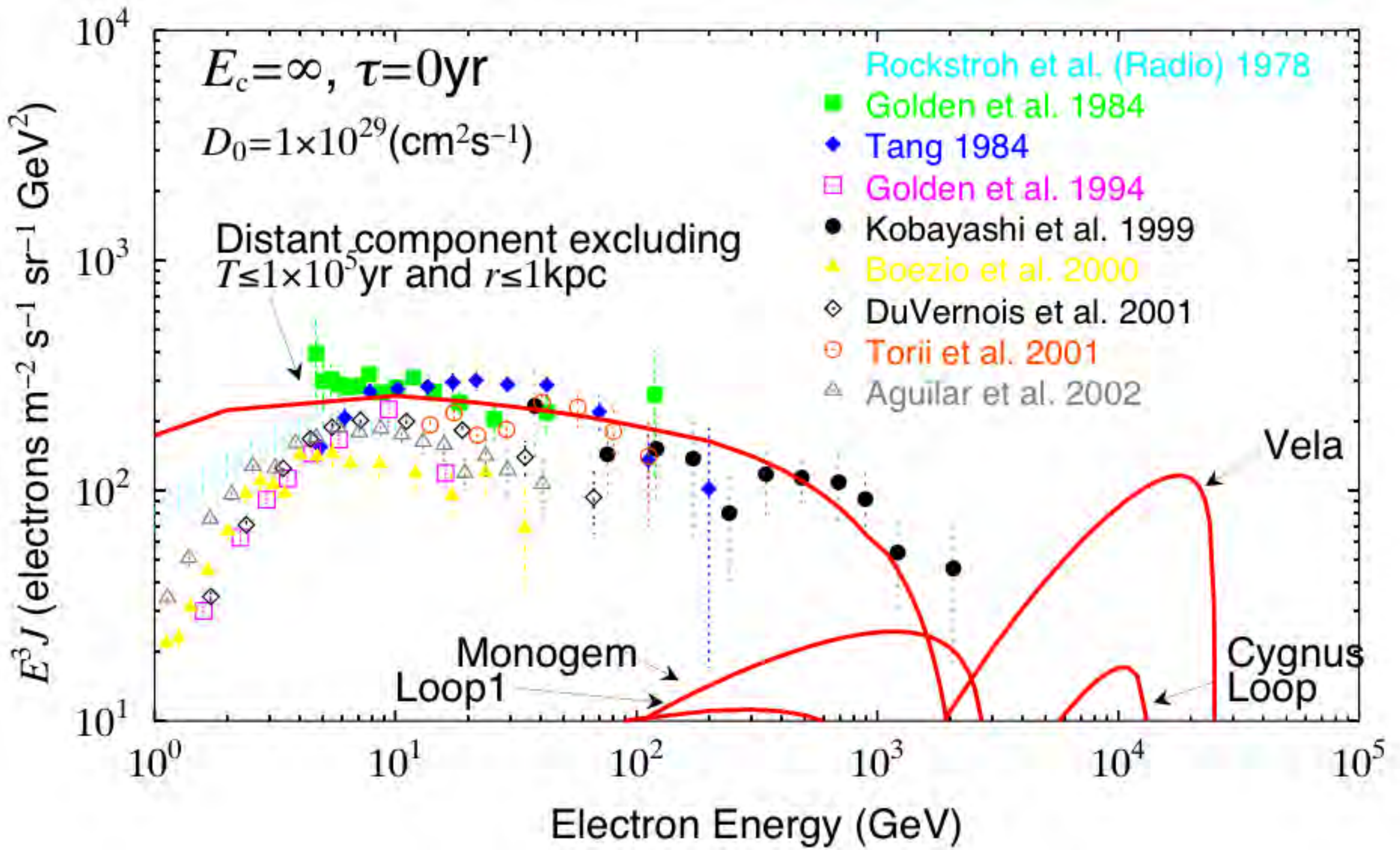

Energy spectra vs. diffusion coefficient

D = 4 x 10^{29} cm^{2}s^{-1}@1TeV K.Yoshida

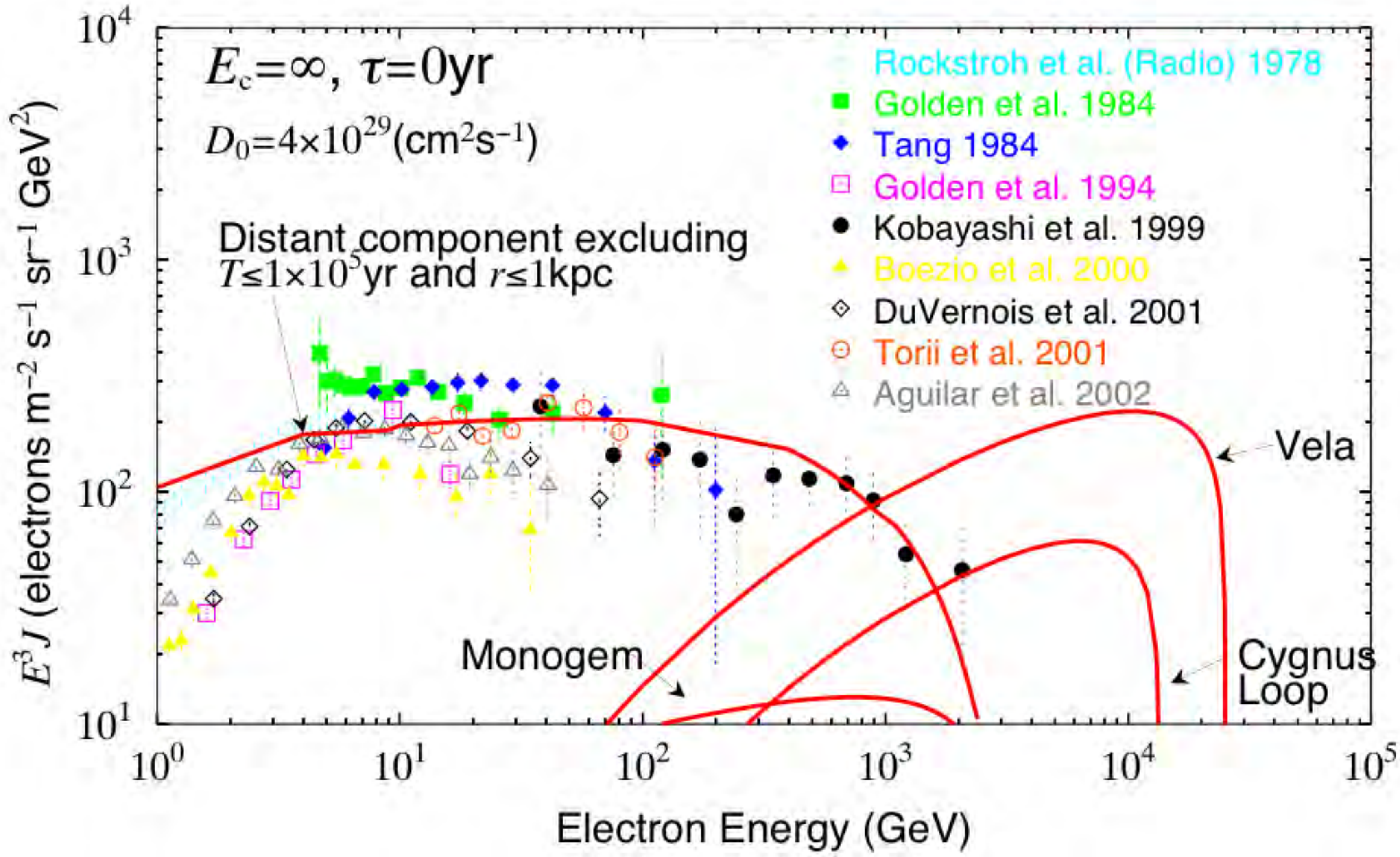

Cutoff in the energy spectrum of electrons at sources

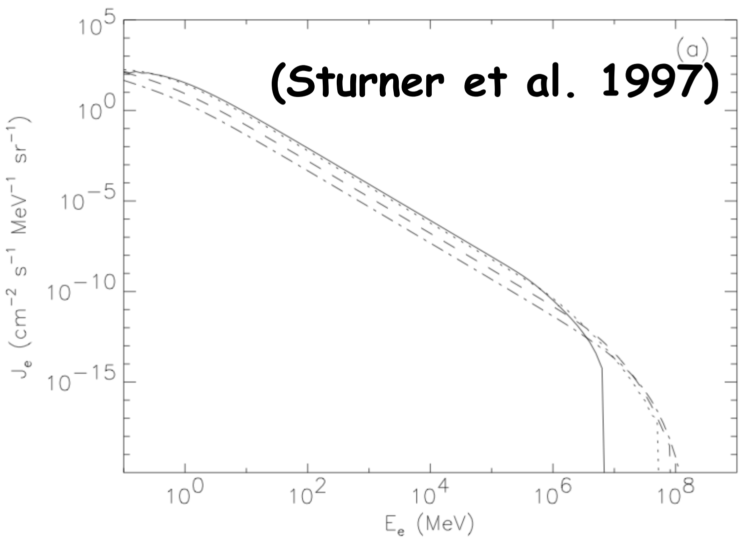

Electron energy spectrum at SNR

$E^{-\gamma}\exp(-E/Ec)$

$\gamma = 2.1\sim2.4$

$E_c = 10 \sim 100$TeV

Rolloff Frequency and Maximum Electron Energy Upper Limits

Object	$\nu_{rolloff}$ (10^{16} Hz)	$\nu_{rolloff}$ (keV)	$E_{max}[(B/10\mu G)]^{1/2}$ (ergs)	$E_{max}[(B/10\mu G)]^{1/2}$ (TeV)
Kes 73[a]	150	6	290	200
Cas A	32	1	130	80
Kepler	11	0.5	79	50
Tycho	8.8	0.4	70	40
G352.7−0.1	6.6	0.3	60	40
SN 1006[b]	6	0.2	57	40
3C 397	3.4	0.1	43	30
W49 B	2.4	0.1	36	20
G349.7+0.2	1.8	0.07	31	20
3C 396	1.6	0.07	30	20
G346.6−0.2	1.5	0.06	29	20
3C 391	1.4	0.06	28	20
SN 386[a]	1.2	0.05	26	20
RCW 103[a]	1.2	0.05	26	20

(Reynolds et al. 1999)

Higher cut-off energies => Higher flux in TeV region

E_c=infty K.Yoshida

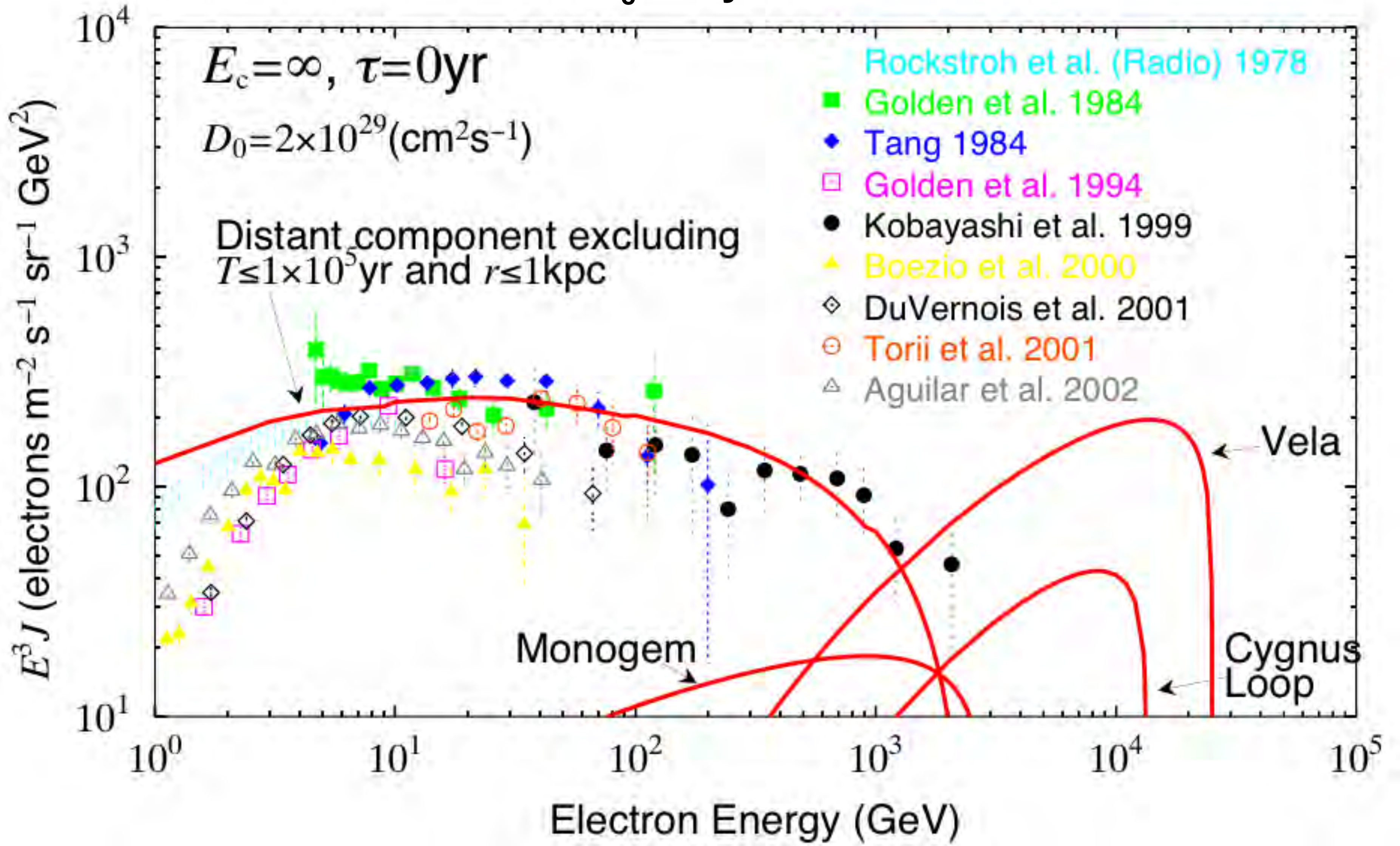

Electron spectra vs. cut-off energies

E_c=10TeV K.Yoshida

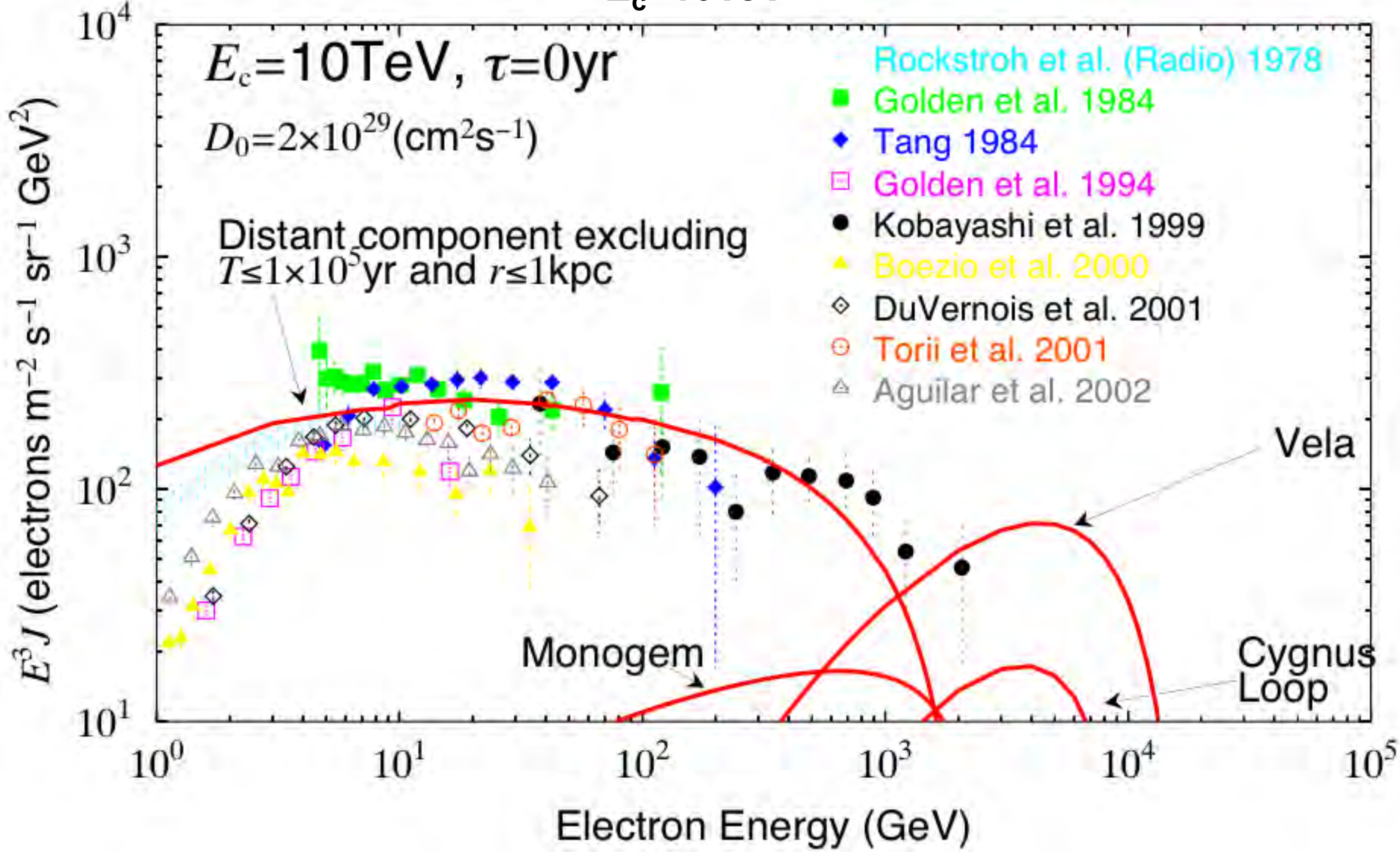

Electron spectra vs. release time delay from SNR

T = 5 x 10^3 yr K.Yoshida

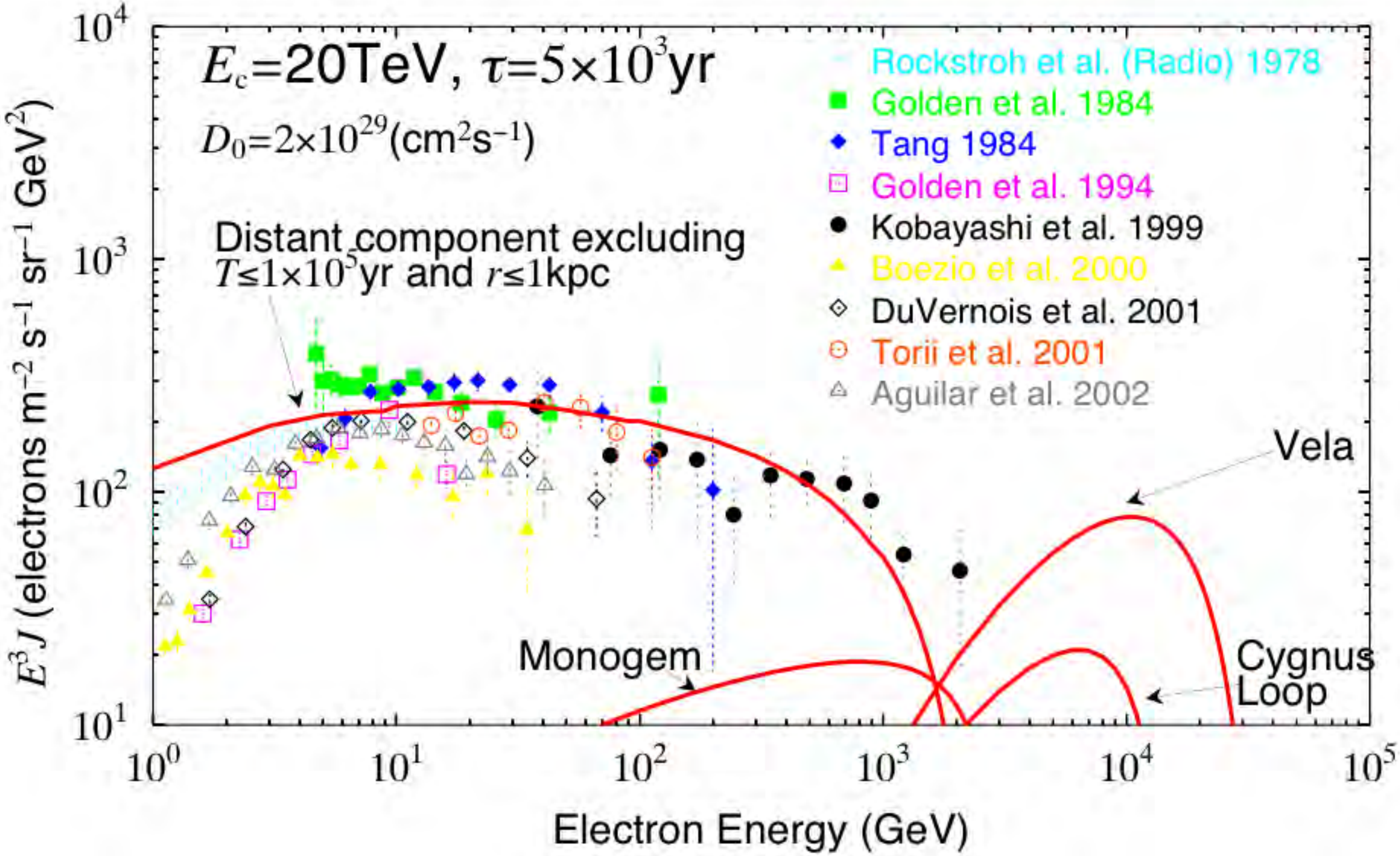

Electron spectra vs. release time delay from SNR

=> Large impact on the flux in TeV region

$T = 1 \times 10^5$ yr

K.Yoshida

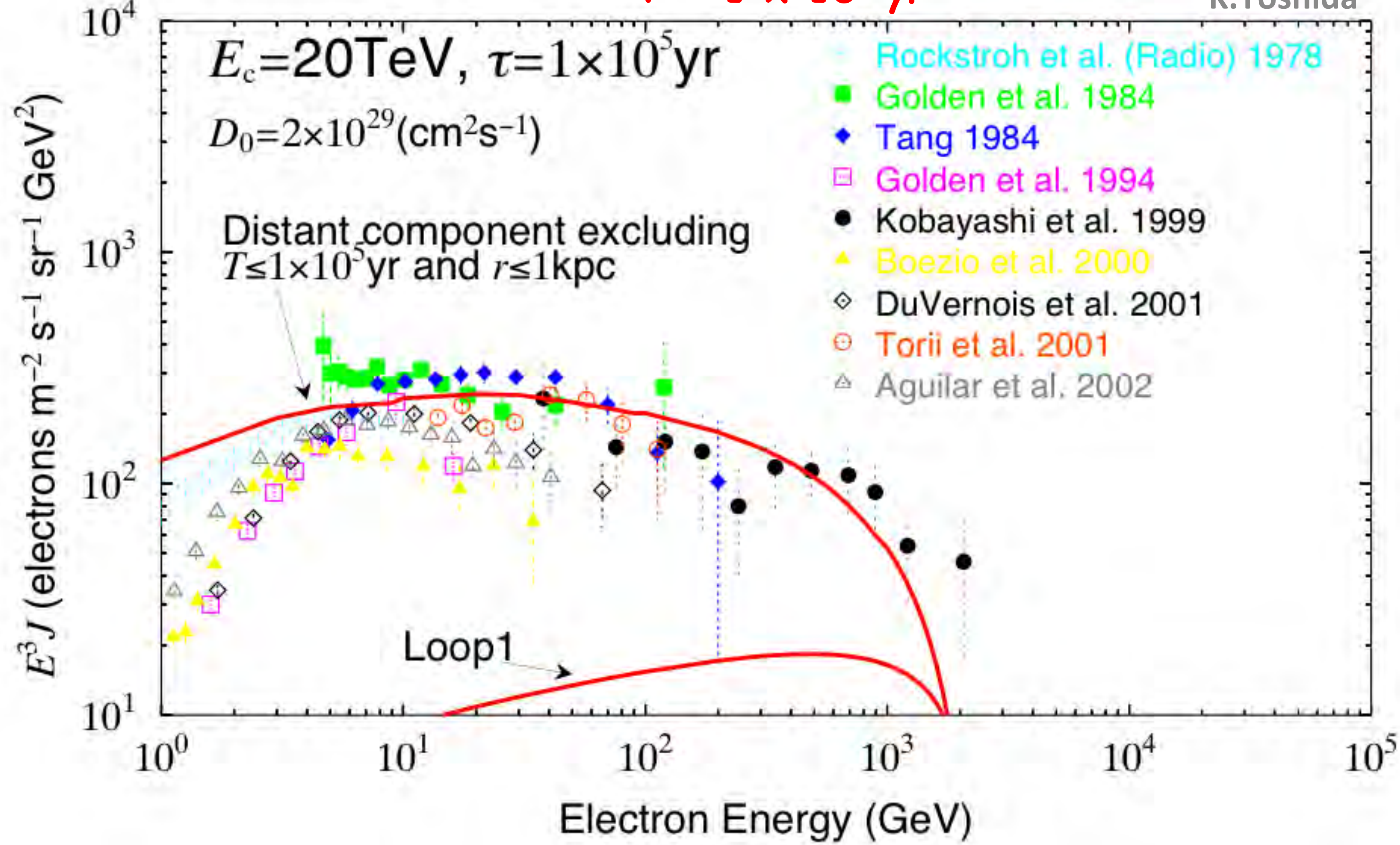

e^+, e^- from Dark Matter annihilation ?

SUSY Dark Matter

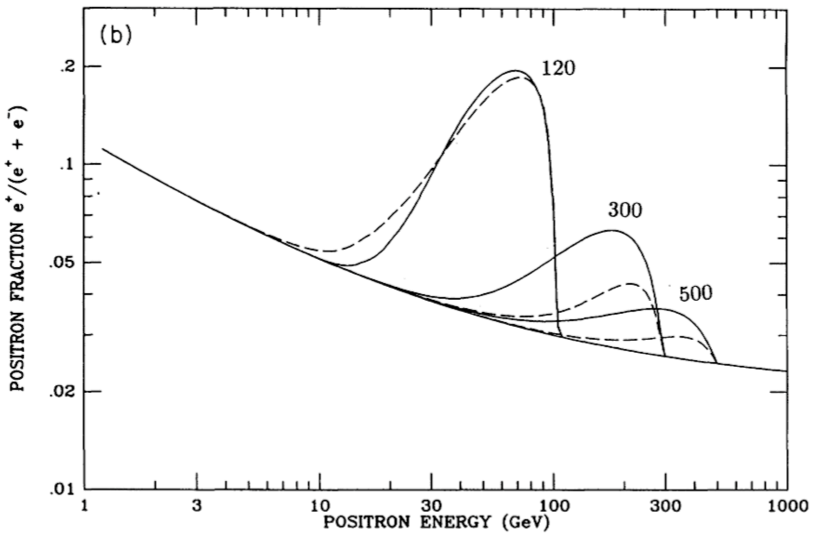

Kamionkwoski et al. (1991)

Kaluza-Klein Dark Matter

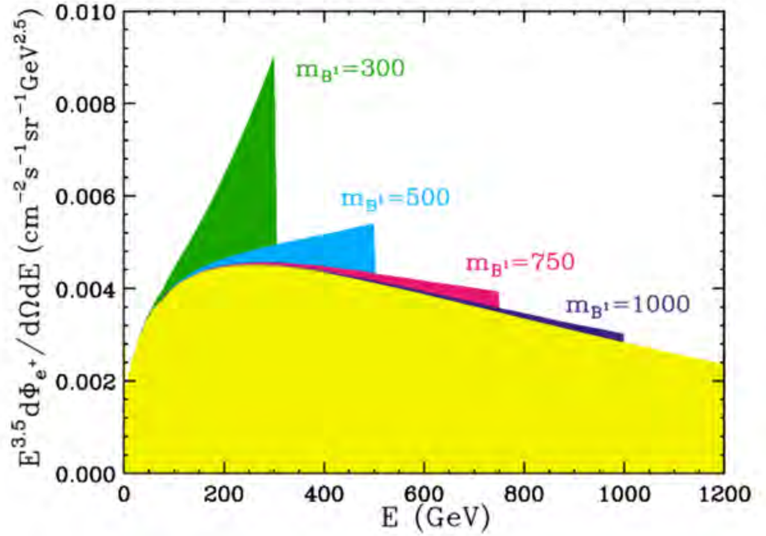

Cheng et al. (2002)

- Distinctive spectral structures expected from D.M. annihilation
- Dark matter searches via e^-,e^+ observations

Indirect dark matter search with electrons

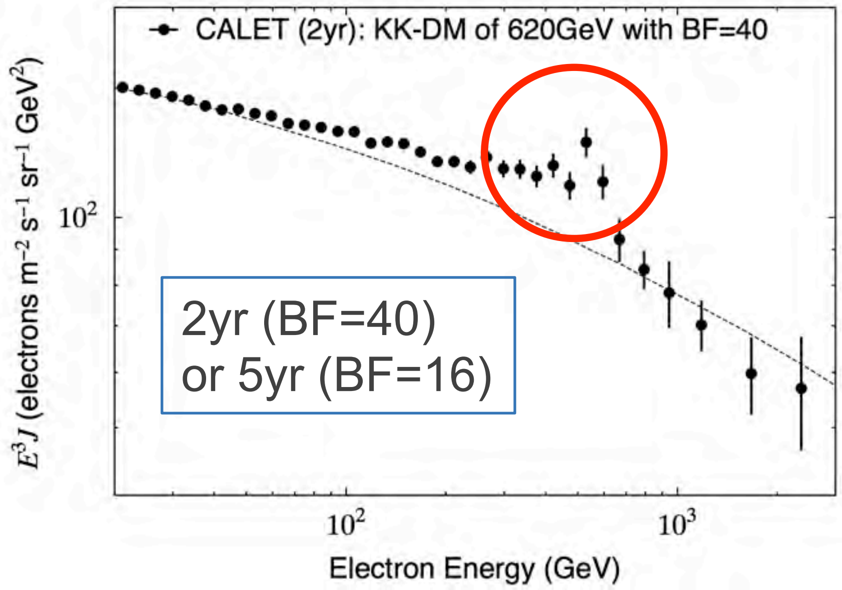

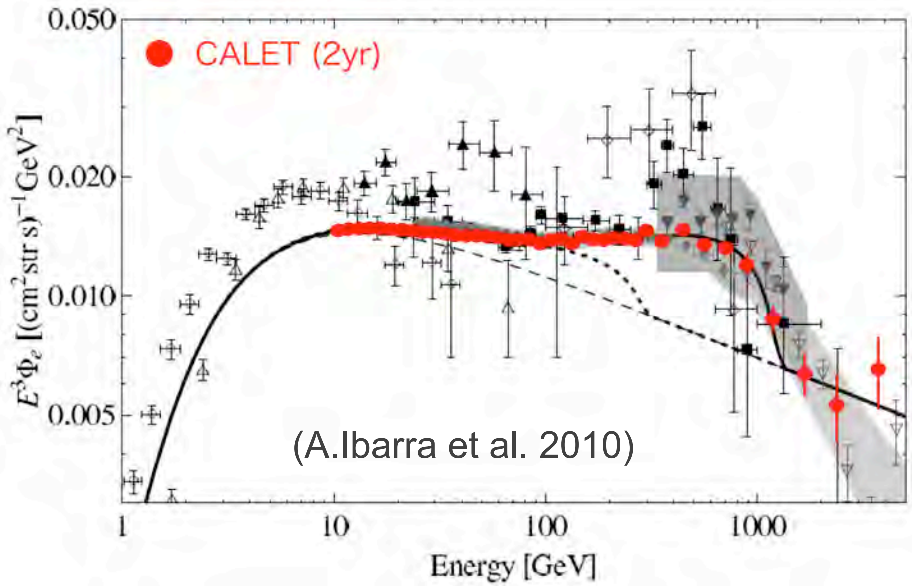

Simulated e^++e^- spectrum for 2yr from Kaluza-Klein dark matter annihilations with m = 620GeV and BF=40.

Simulated e^++e^- spectrum for 2yr from decaying dark matter for a decay channel of D.M.-> $l^+l^-\nu$ with:

M = 2.5TeV

$\tau = 2.1 \times 10^{26}$ s

Observations of High-Energy Electrons

- Direct electron observations since 1960's
  - Daniel&Stephens 1965, Bleeker 1965,…
- As the energy increases:
  - Lower electron flux (falls as E^{-3})
  - Larger proton backgrounds (of order 10^3 to 10^4)
- Requirements for the experiments:
  - Large geometrical factor ($S\Omega$) (from tens of $cm^2 sr$ to $m^2 sr$?)
  - Long exposures (from several tens of days on ballons to years in space ?)
  - High proton rejection power (of order10^5)

❑ **Let's cast an historical look at the instrumentation in the 80's and at the very important advances achieved since then.**

Cosmic-ray electron observations in different energy domains

< 10 GeV

– Solar modulation

- E = 10 GeV-1000 GeV
  – Propagation in the Galaxy
  – Information on sources
  – Dark matter search

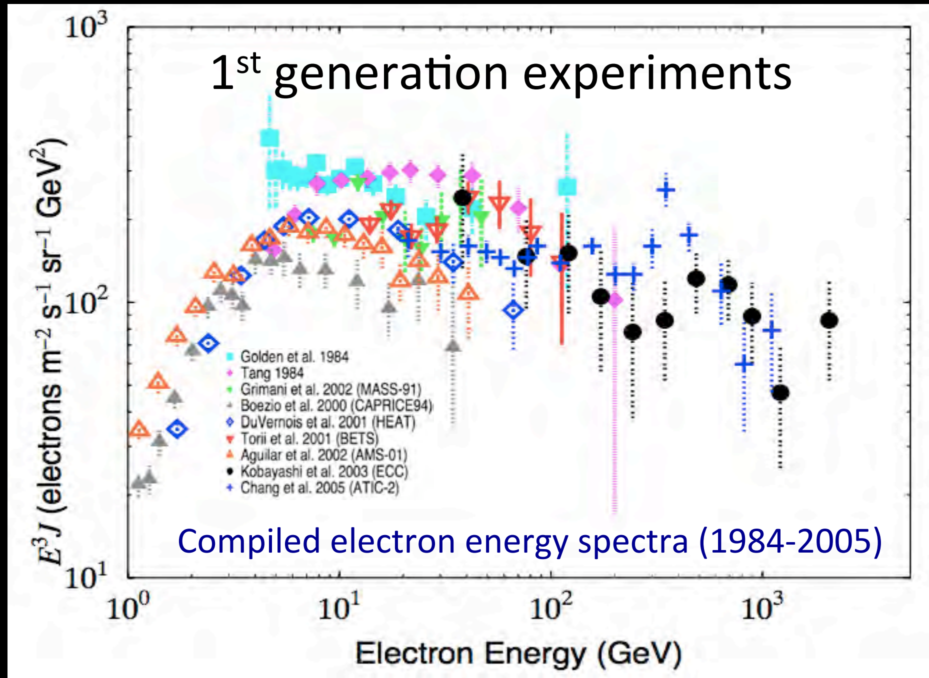

- Variation of the flux: factor 2~3
- Few observations above 100 GeV region

- E > 1 TeV
  – Identification of cosmic-ray source(s)
  – Dark matter search
  – Acceleration mechanism(s)

The era of passive imaging instruments

- 13 Balloon flights in 1968-2001
  - From Sanriku, Japan, etc.
- Exposure time = 270hr
- Altitude = ~4-9 g/cm^2
- $S\Omega$ = ~$3.8x10^3$ cm^2sr
- e- + e+ (no separation)

Emulsion Chambers

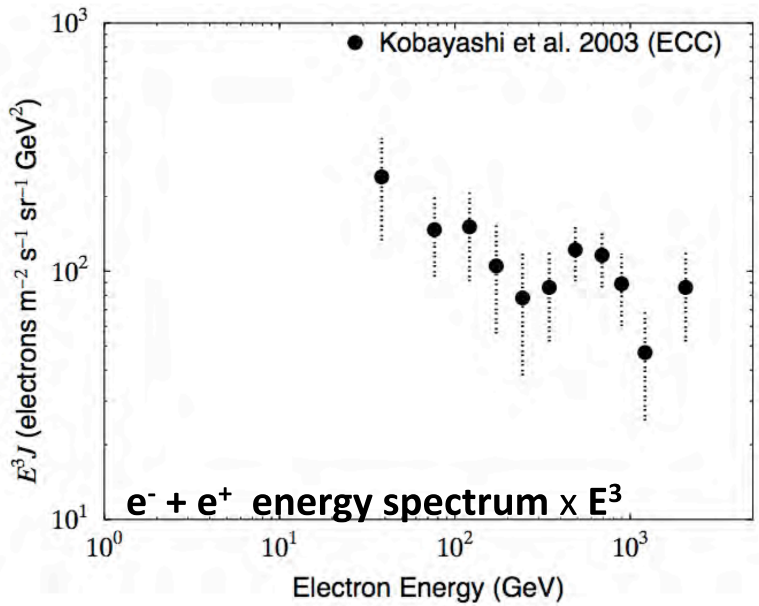

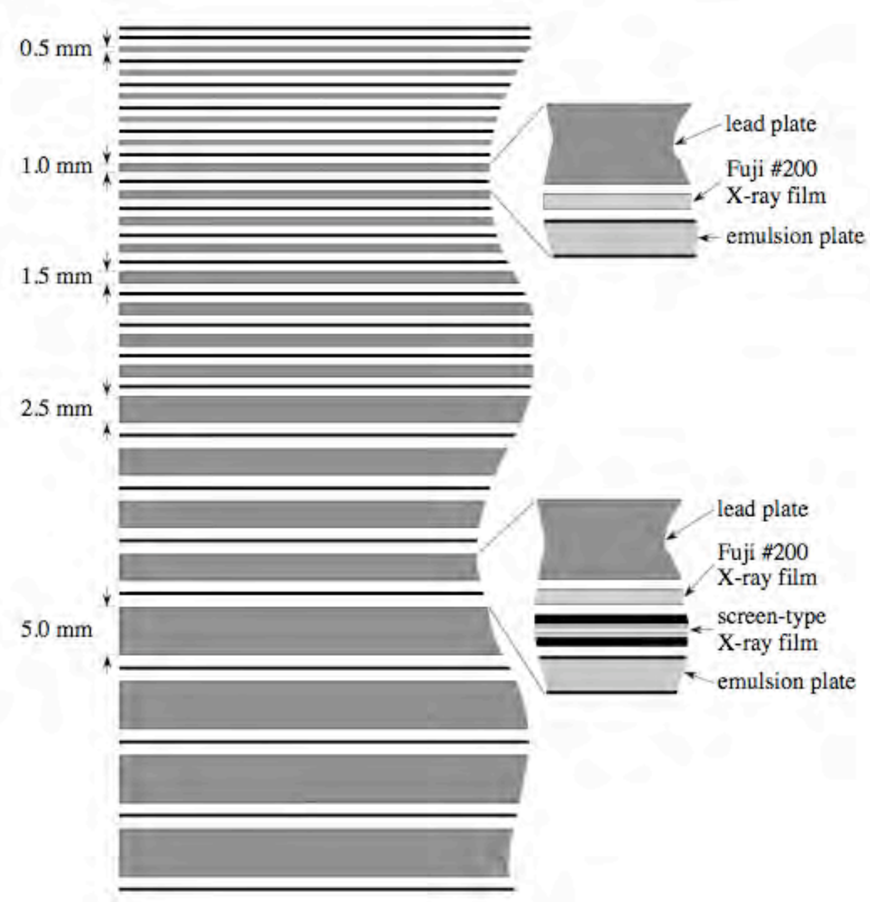

Modern CR Instrumentation in a nutshell

Modern **active** cosmic-ray experiments have a large number of electronics channels therefore power budget is a constant concern in the design.

Charged Particle Tracking, first implemented with **MWPC** and **drift chambers**, has evolved with the more frequent use today of:

- **silicon strip** detectors
- **silicon pixel** detectors
- straw tubes (mainly in TRD detectors)
- **scintillating fibers** readout by segmented photosensors including:
  - **MAPMT** = Multi-Anode PMT
  - **HPD** = Hybrid Photo-Diode
  - **APD** = Avalanche PhotoDiode;
  - **PD** = PhotoDiode;
  - **SiPM** = Silicon PhotoMultiplier;
  - **MCP** = Micro Channel Plate
  - **ICCD** = Image Intensified CCD

Silicon Position Sensitive Detectors

segmented ELECTRODES

single-sided Si-strip
single cooordinate

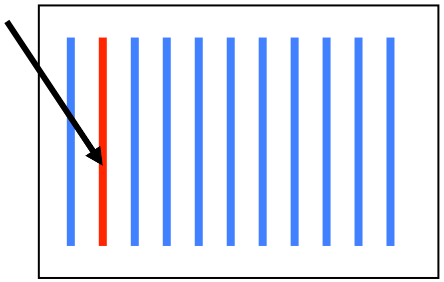

double-sided Si-strip detectors
measure 2 cooordinates

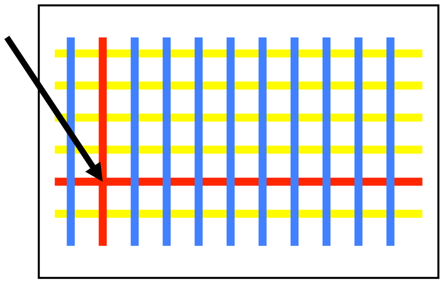

othogonal

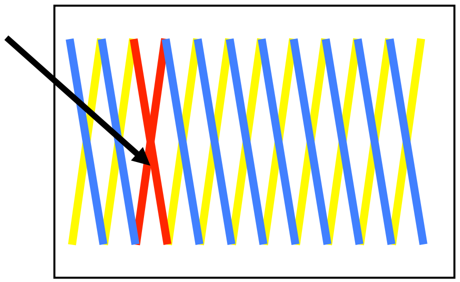

stereo

Pixel detectors

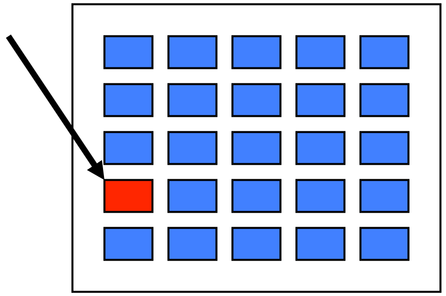

measure 2 cooordinates
(fast readout but large number of channels)

For PID based on **charge detectors** the pixel size has to be optimized to avoid misidentification due to backscattered radiation (predominantly from the calimeter) impinging on the same pixel crossed by the primary particle.

Micro-strip silicon detectors in PAMELA

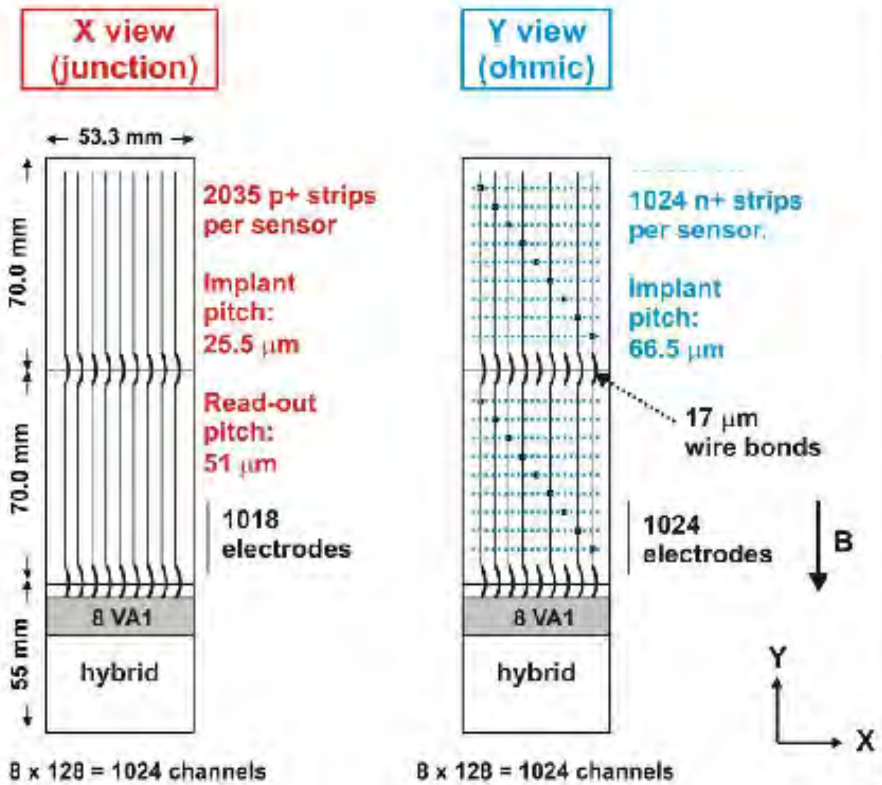

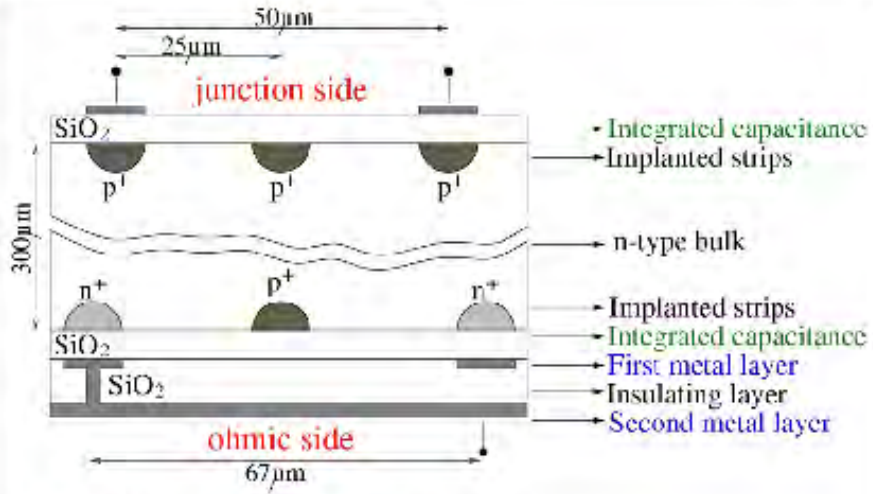

Silicon sensors (Hamamatsu):

- 300 µm, double sided - x & y view
- AC coupled (no external chips)
- double metal (no kapton fanout)
- 1024 read-out channels per view

Spatial resolution:

- junction side (X): 3 µm @0°, < 4 µm up to 10°
- ohmic side (Y) 8÷13 µm

courtesy of
E. Vannuccini
ISSS-2017

courtesy of
E. Vannuccini
ISSS-2017

The AMS-02 tracking system

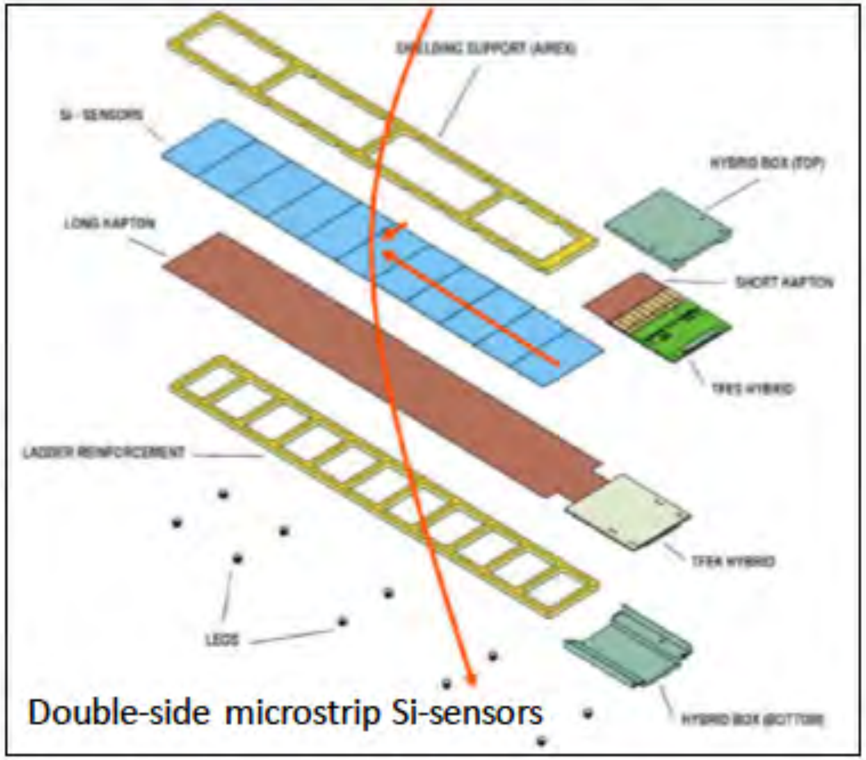

- 0.15 T magnetic field @ center
- ~ **10 μm** resolution on the bending direction
- ~ 3 m track-length

→ MDR ~ 2 TV

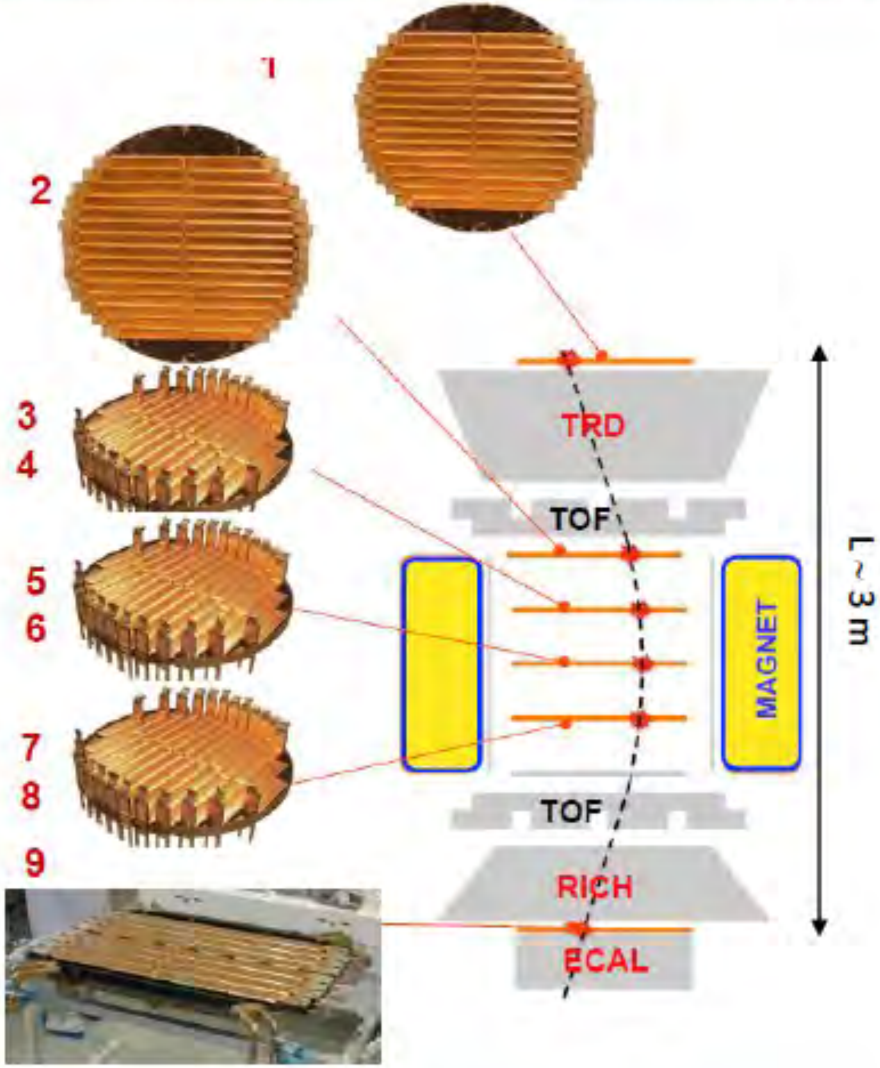

Magnetic spectrometers are limited by their Maximum Magnetic Rigitidy (MDR) to a few TeV while e.m. calorimeters have good resolution in the multi-TeV region

E.M. CALORIMETERS: ENERGY RESOLUTION

Energy resolution, σ_E/E, can be parametrized as

$$a/\sqrt{E} \oplus b \oplus c/E$$ E in GeV

- $a/E^{1/2}$ = **stochastic term**: statistical fluctuations (photostatistics, sampling fluctuations, shower fluctuations..)

For sampling calorimeters a = $\sqrt{t/f}$ (f = sampling fraction , t = sampling frequency). A few % for homogeneous calorimeters and about 10% for sampling calorimeters.

- b = **constant term** due to calibration, non uniformity of calorimeter etc... STABILITY vs. time of calibrations is important.

- c/E = **electronics noise contribution** summed on all readout channels. Includes contribution from PILEUP.

Homogeneous calorimeters: absorber is the active medium for detection

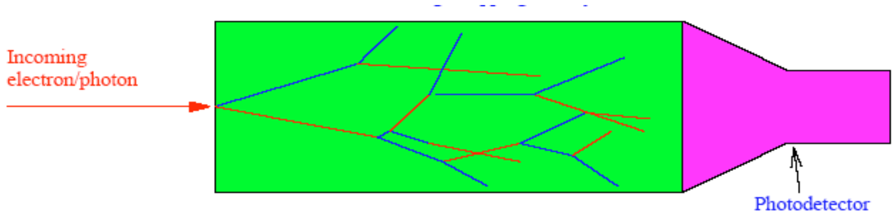

Absorber detector
e.g.: BGO, CsI crystals, Lead Glass etc...

crystal calorimeters are more expensive

Sampling calorimeters: alternate structure absorber + active medium

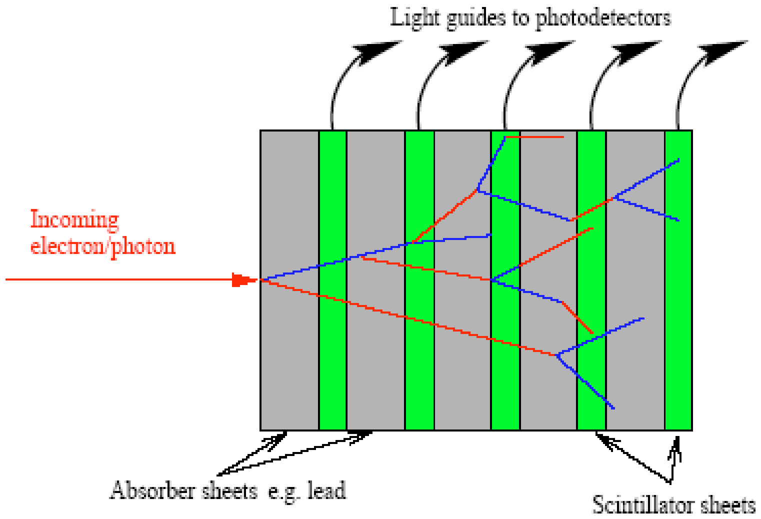

Absorber
Pb, Tungsten, Uranium, etc...

Detector
e.g.: scintillators, SciFibers, silicon pads, MWPC, etc...

cost effective

- Shower sampled by layers of **active media (low-Z)** alternated with **dense (high-Z)** passive absorbers
- Only a fraction of the shower energy is collected by the active media
- Energy resolution affected by <u>fluctuations in energy deposited in the active layers</u>: **sampling fluctuations**

ELECTROMAGNETIC SHOWERS

When an electron/positron/photon interacts with matter a cascade of e^+e^-, γ is initiated.

Simple model for average shower properties, assuming **1 X_0** as generation length:

- electrons lose ~2/3 of their E
- high energy photons: 7/9 probability to convert into one e^+e^- pair

In each generation the number of charged particles doubles

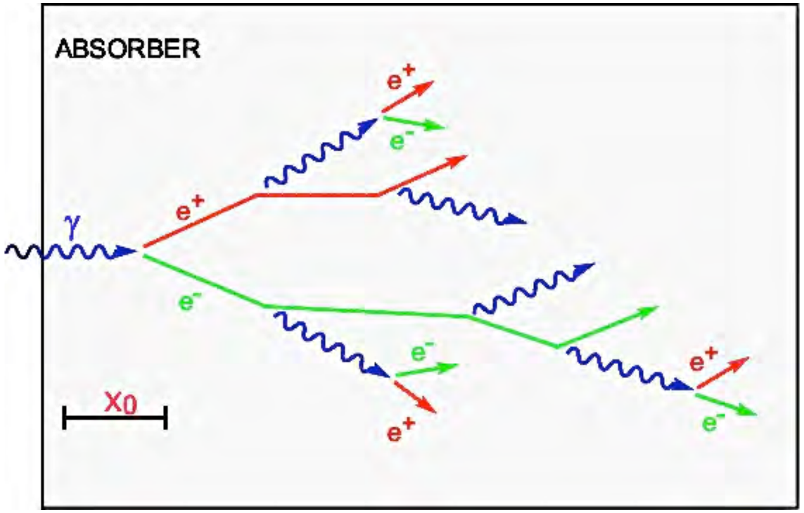

Define the *scale variables*: $t = x/X_o$ — thickness *in* ***radiation length*** (X_0) *units*

$y = E/E_c$ — deposited energy in *units of critical energy*

After t–generation: average energy/particle **drops below E_c** and shower growth drops.

Average number of particles: $N(t) \sim 2^t$

Average energy of a shower particle $N(t) \sim E_o / 2^t$

Shower maximum *(log E dependence)* $t_{max} \sim \ln(E_o/E_c) / \ln 2$

E.M. SHOWERS: ***LONGITUDINAL PROFILE***

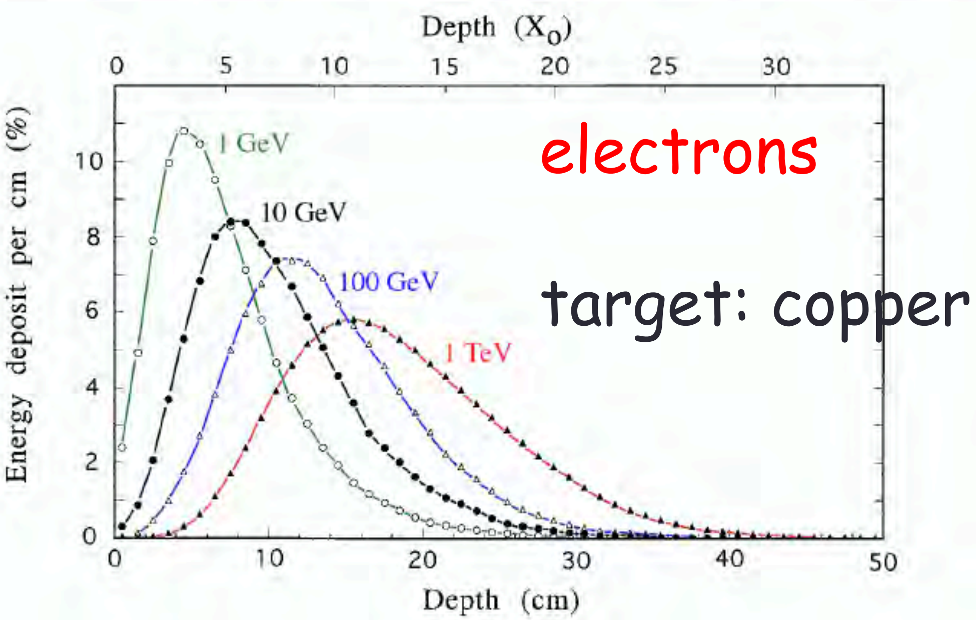

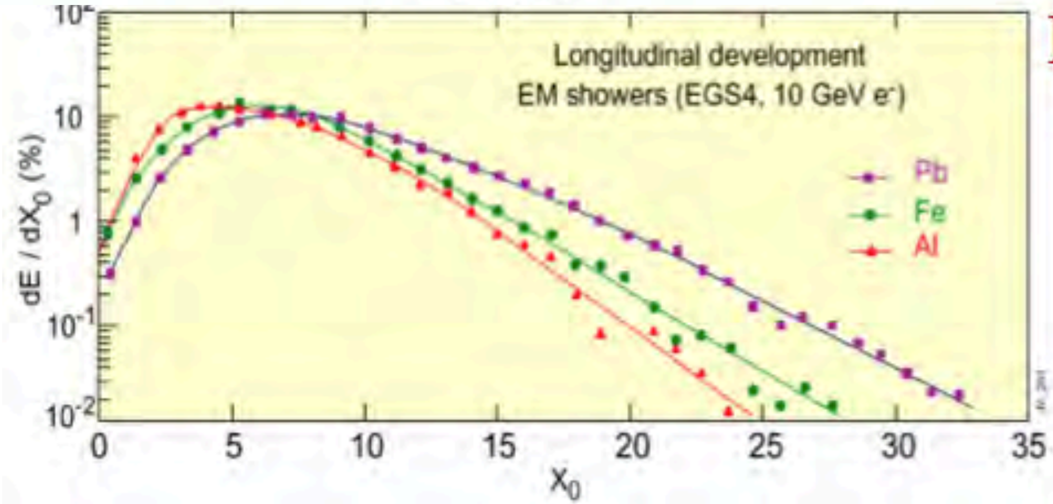

Shower energy dep parametrization:

$$\frac{dE}{dt} \propto E_0 t^{\alpha} e^{\beta t}$$

β material dependent

$$t_{max} = 1.4 \ln(E_0/E_c)$$

$$N_{tot} \propto E_0/E_c$$

E_c α 1/Z ➡ •shower max •shower tail

Longitudinal containment:

$$t_{95\%} = t_{max} + 0.08Z + 9.6$$

*E.M. SHOWERS: **LATERAL PROFILE***

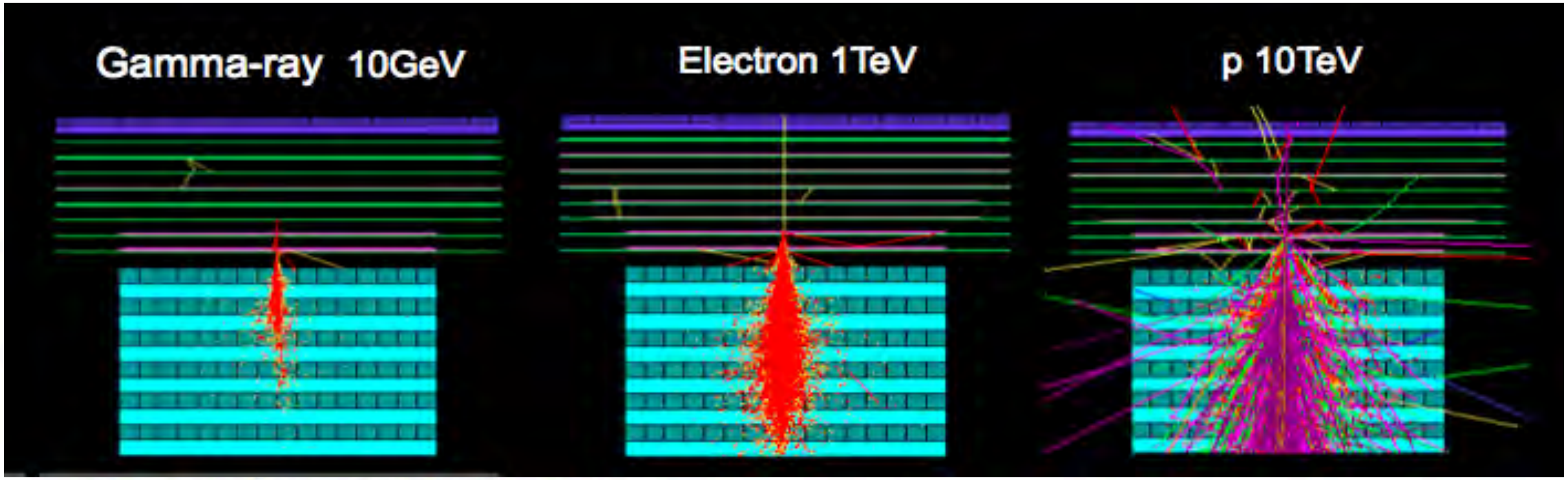

Molière radius sets transverse shower size, it gives the average lateral deflection of critical energy electrons after traversing $1X_0$

$$R_M = \frac{21\text{MeV}}{E_C} X_0$$

$$R_M \propto \frac{X_0}{E_C} \propto \frac{A}{Z} (Z >> 1)$$

90% E_0 within $1R_M$, 95% within $2R_M$, 99% within $3.5R_M$

Balloon-borne calorimetric experiments

ATIC

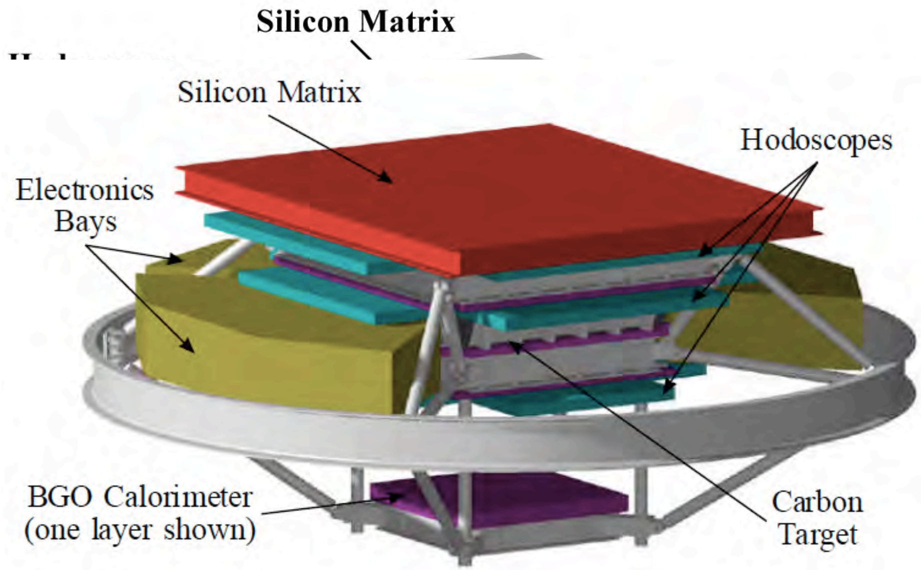

Si-Matrix: 4480 pixels (each 2 cm x 1.5 cm) to measure GCR charge in presence of backscattered shower particles.

Plastic scintillator hodoscope, embedded in Carbon target, provides event trigger, charge and particle tracking.

Calorimeter: 10 layers BGO crystals, 40 per layer. Total depth 22 X_0, 1.14 λ. Measure the electromagnetic core of the nuclear shower.

- Geometrical factor: 0.45 m^2 sr (calorimeter top) to 0.24 m^2 sr (calorimeter bottom)
- 3 successful antarctic flights: 2000, 2002, 2007 (~57 days in total)

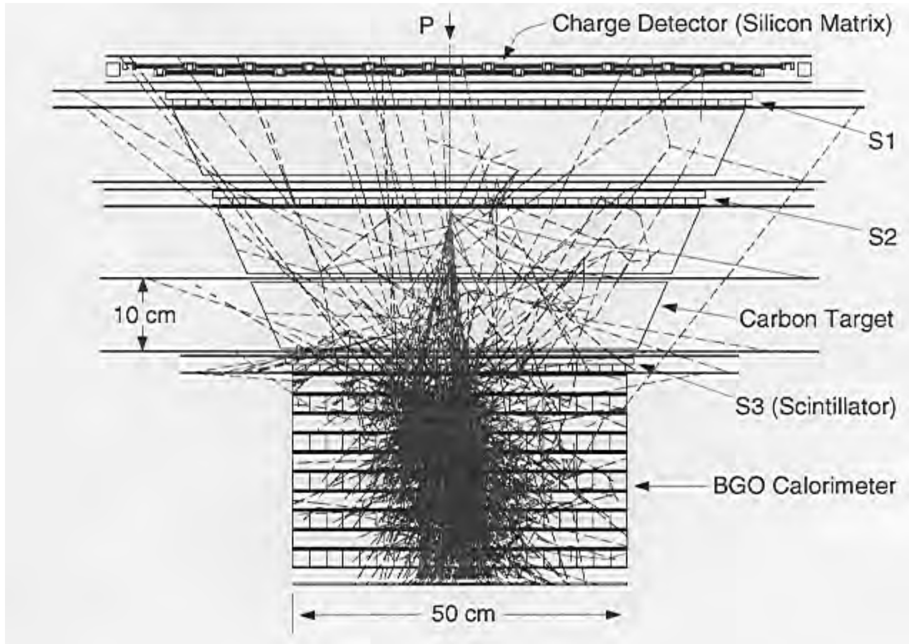

Advanced Thin Ionization Calorimeter (ATIC)

J.H. Adams[2], H.S. Ahn[3], G.L. Bashindzhagyan[4], K.E. Batkov[4], J. Chang[6,7], M. Christl[2], A.R. Fazely[5], O. Ganel[3], R.M. Gunasingha[5], T.G. Guzik[1], J. Isbert[1], K.C. Kim[3], E.N. Kouznetsov[4], M.I. Panasyuk[4], A.D. Panov[4], W.K.H. Schmidt[6], E.S. Seo[3], N.V. Sokolskaya[4], J. Watts, J.P. Wefel[1], J. Wu[3], V.I. Zatsepin[4]

1) Louisiana State University, Baton Rouge, LA, USA

2) Marshall Space Flight Center, Huntsville, AL, USA

3) University of Maryland, College Park, MD, USA

4) Skobeltsyn Inst. of Nucl. Phys., Moscow State Univ., RU

5) Southern University, Baton Rouge, LA, USA

6) Max Plank Institute für Space Physics, Lindau, Germany

7) Purple Mountain Observatory, China

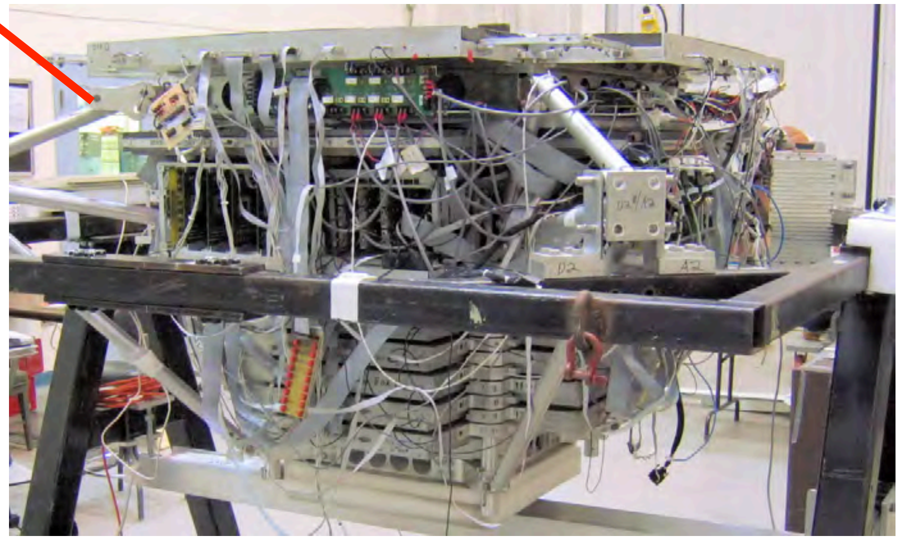

The ATIC "bump" PUZZLE

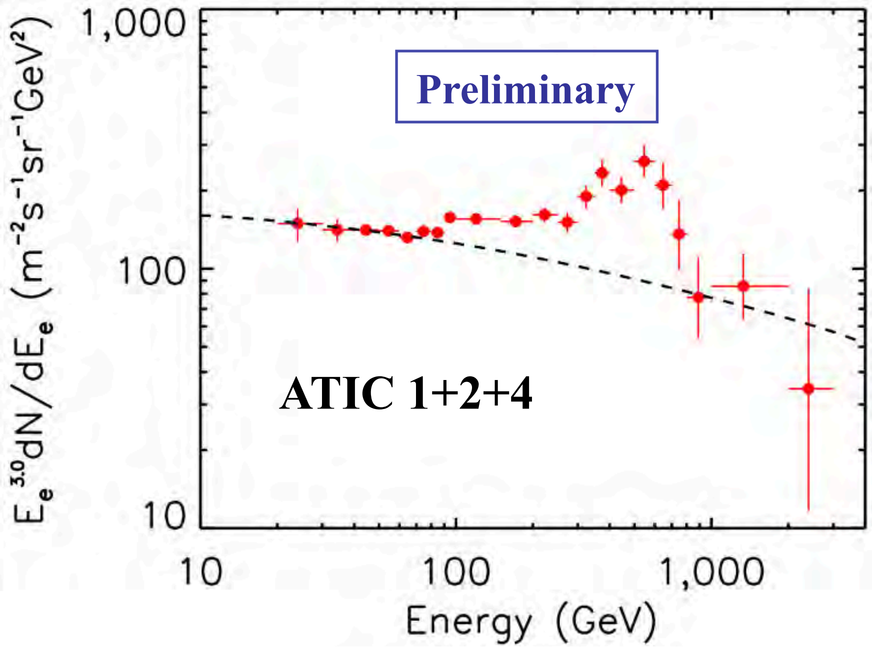

All three ATIC flights are consistent

from: Joachim Isbert RICAP 2009

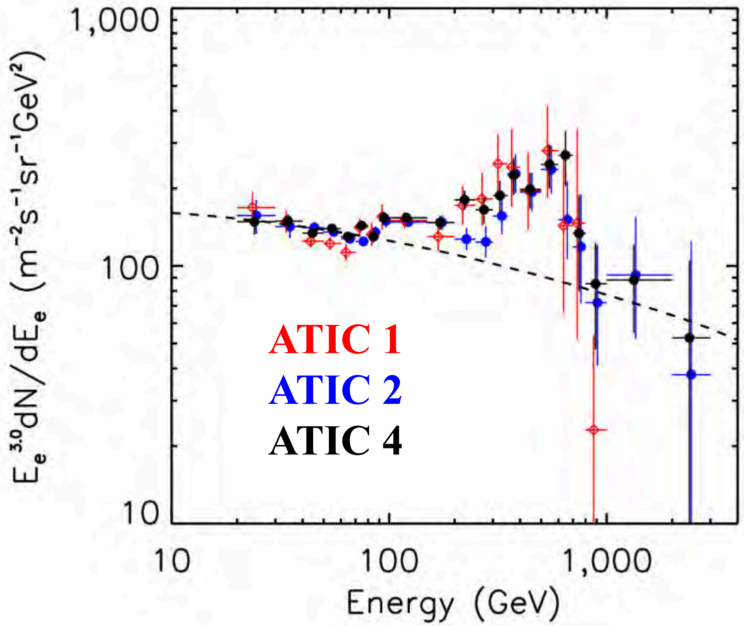

"Bump" is seen in all three flights

Significance for ATIC1+2+4 is 5.1 sigma

ATIC - atmospheric Gamma-rays:

check using the same eletron selection

→ NO BUMP seen in γ-rays

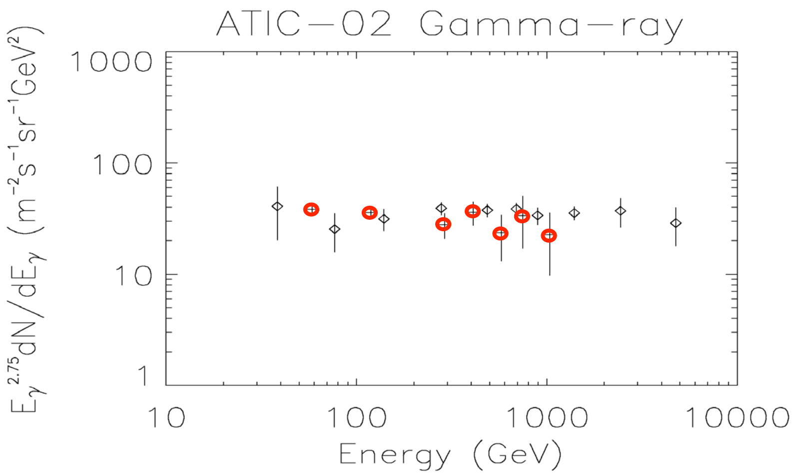

Balloon-borne calorimetric experiments

BETS

- Balloon flights in 1997,1998
  - From Sanriku, Japan
- Exposure time = ~13hr
- Altitude = ~5~6g/cm^2
- $S\Omega$ = ~320 cm^{2}sr
- e- + e+ (no separation)

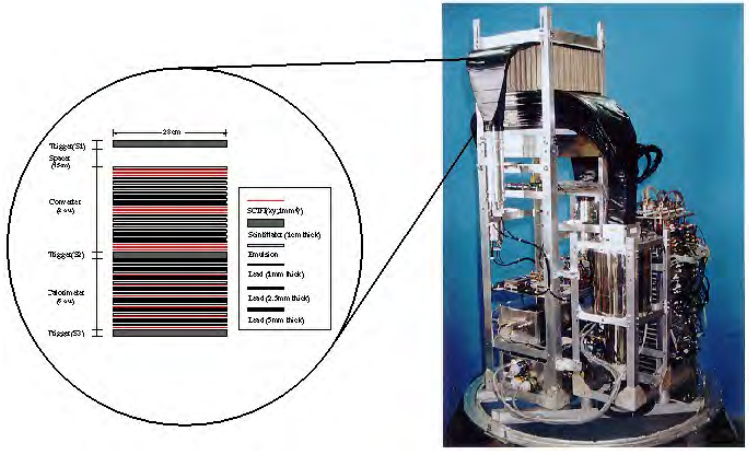

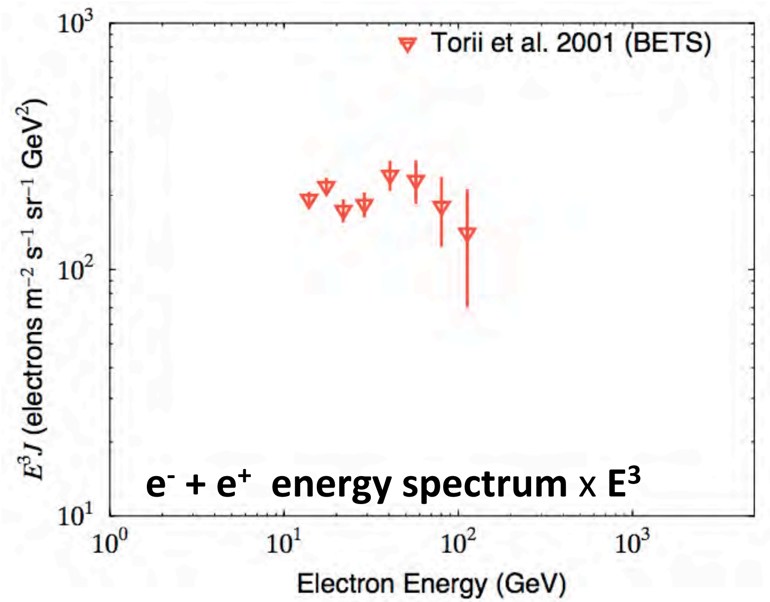

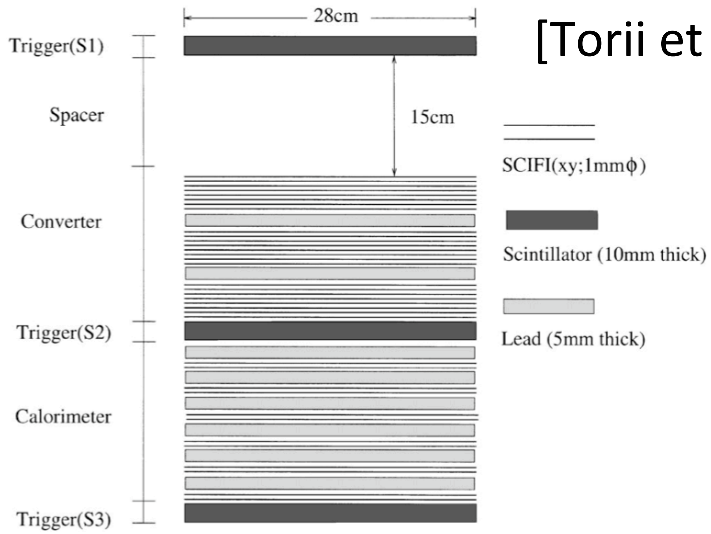

[Torii et al. 2001]

fibers readout with ICCD

Balloon-borne calorimetric experiments

CREAM

- 3 independent charge measurements
  - Timing-based Charge Detector (TCD)
  - Pixelated Silicon Detector (SCD)
  - Cerenkov counter (CD) and Camera (w/o TRD)
- 2 independent energy measurements + tracking
  - Transition Radiation Detector (Z > 3)
  - Tungsten Sci-Fi calorimeter (Z ≥ 1)
- GF ~ 0.3 m^2 sr for Z=1,2; ~ 1.3 m^2 sr for Z>3

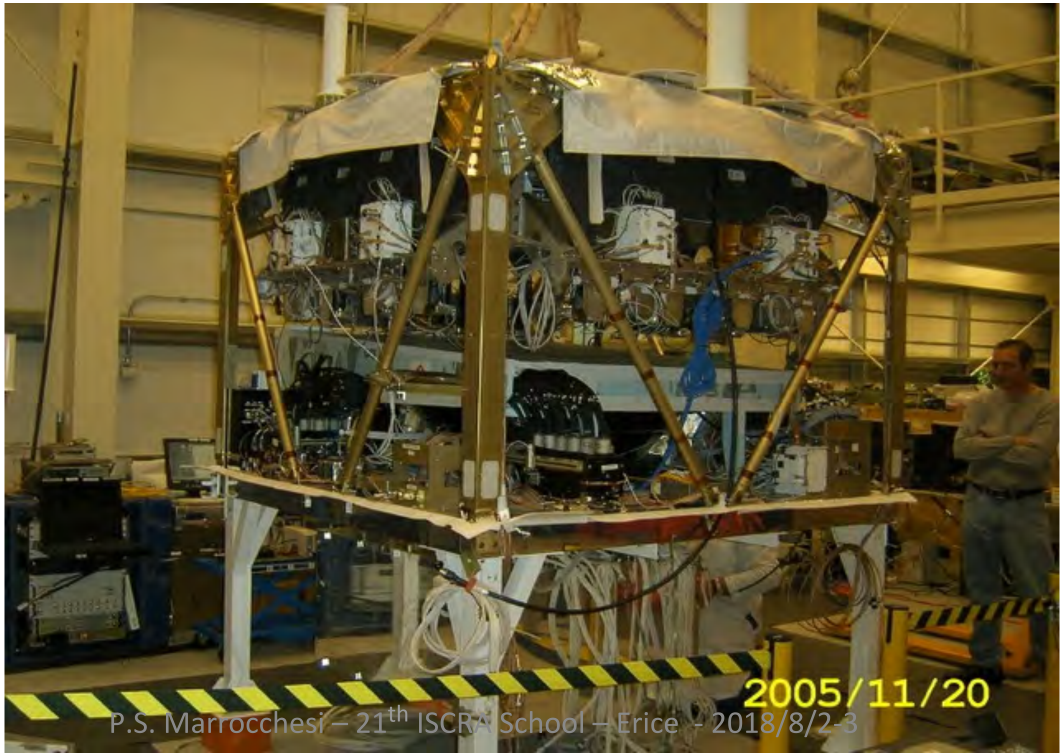

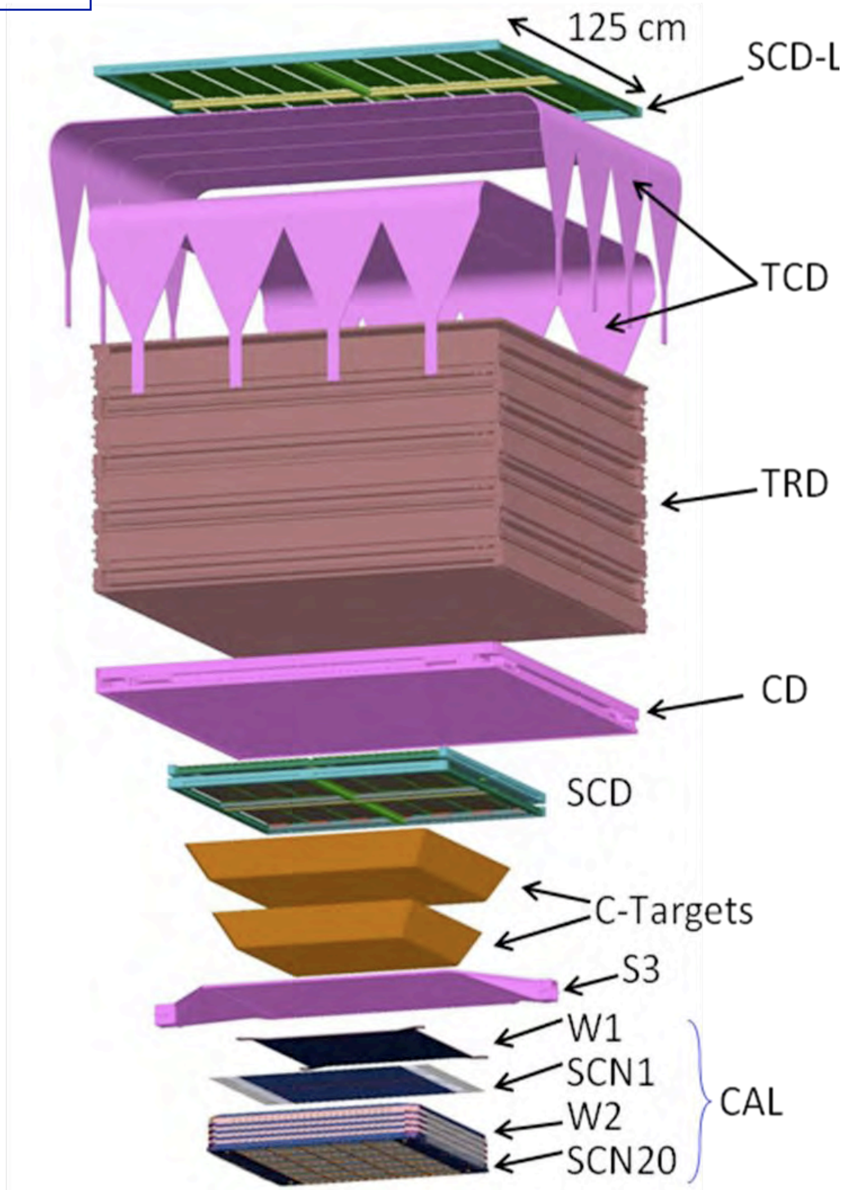

Exploded view: configuration with TRD

Ahn et al., NIM A, 579, 1034, 2007

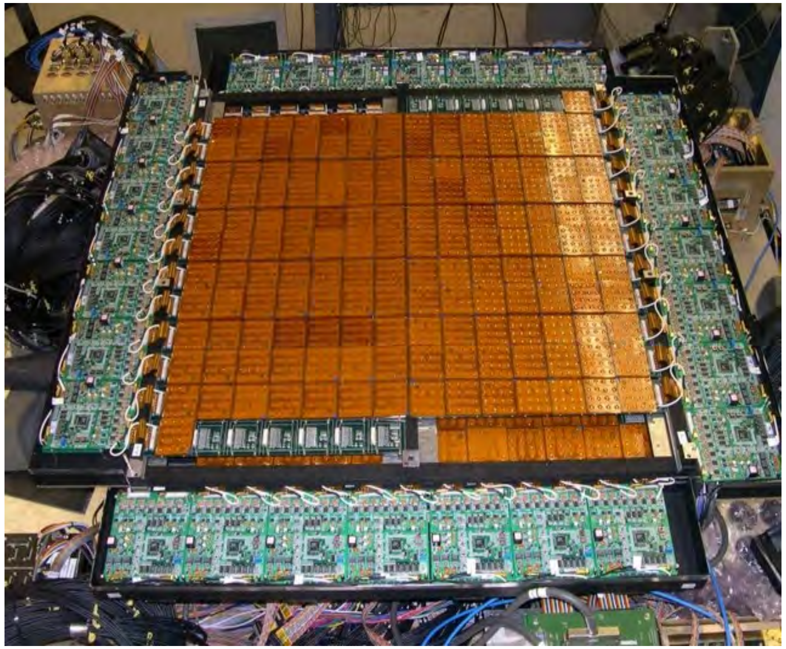

Silicon Charge Detector (SCD)

particle-ID by charge measurement
from Z = 1 to Z ~ 33 (σ ~ 0.1 - 0.2 e)

- **2 layers** of sensors
- pixel size ~ 2.1 cm^2
- **16 pixels per sensor**
- 380 mm thick Si sensor
- depletion at 70 V
- Active area per layer ~ 0.52 m^2
- 2496 chans/layer were readout

Tungsten Scintillating-Fibers Sampling Calorimeter

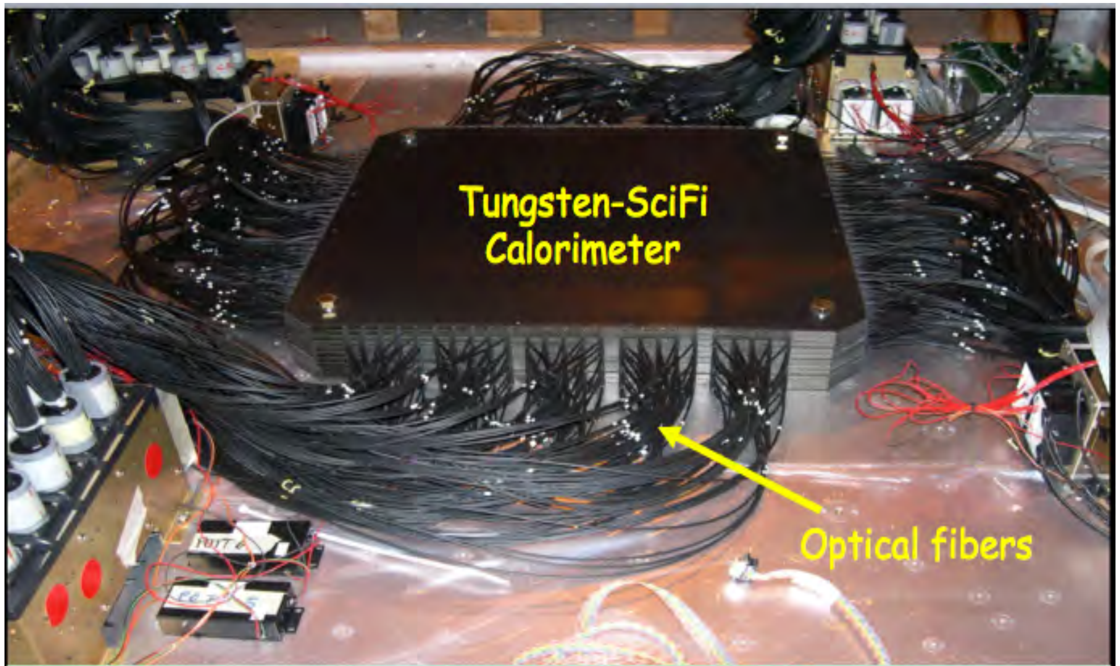

Preceded by a **graphite target** (~ 0.5 λ_{INT}) to induce an hadronic interaction
Active area 50 x 50 cm^2 : 2560 channels (3 gain ranges) readout by 40 HPDs
Longitudinal sampling : 3.5 mm Tungsten (1 X_0) + 0.5 mm SciFi ribbons
Total of 20 layers (20 X_0 ~ 0.7 λ_{INT}) : alternate x-y views
Transverse granularity : scintillating fiber ribbons 1 cm ~ 1 Moliere radius

Charge measurement with SCD

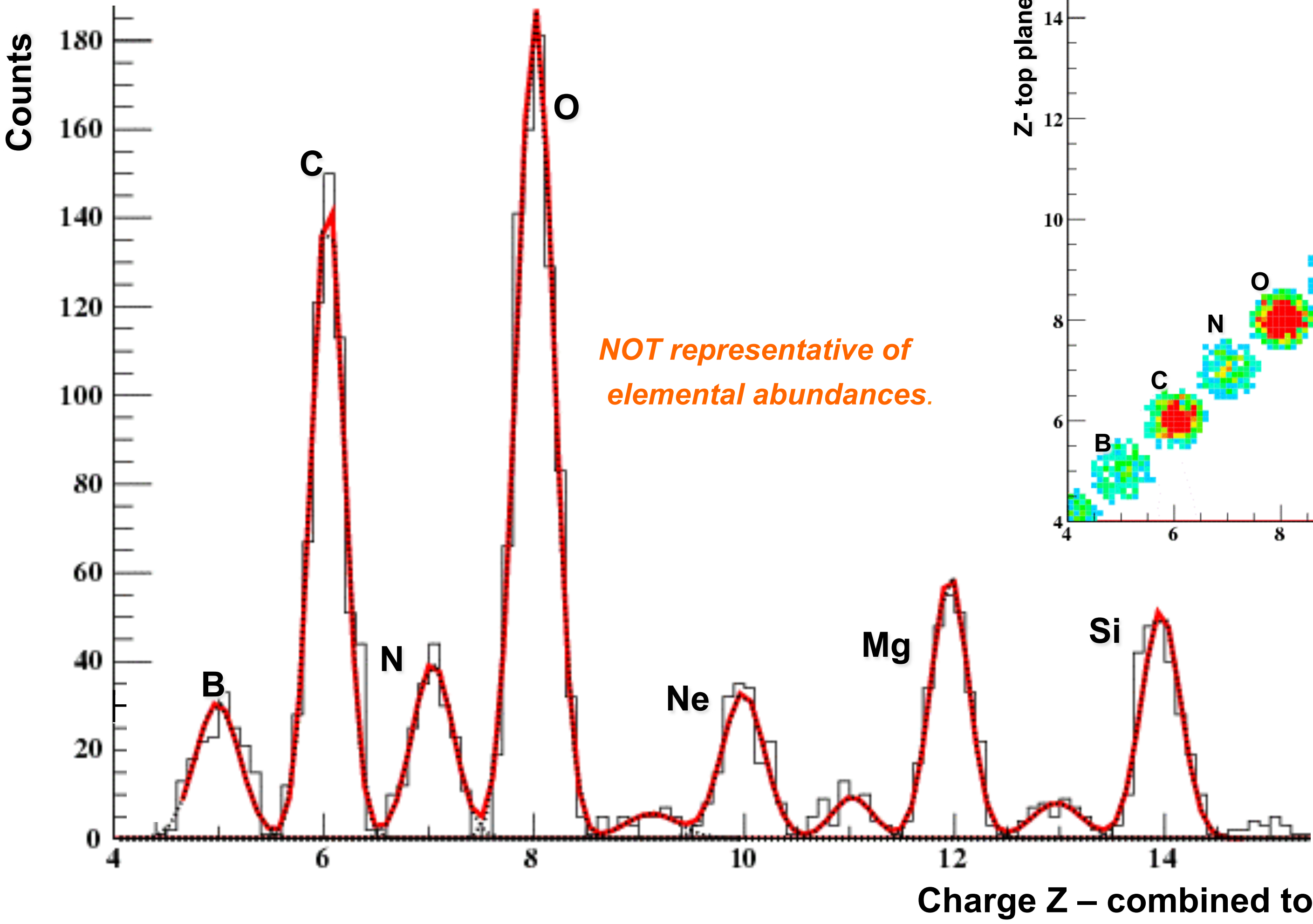

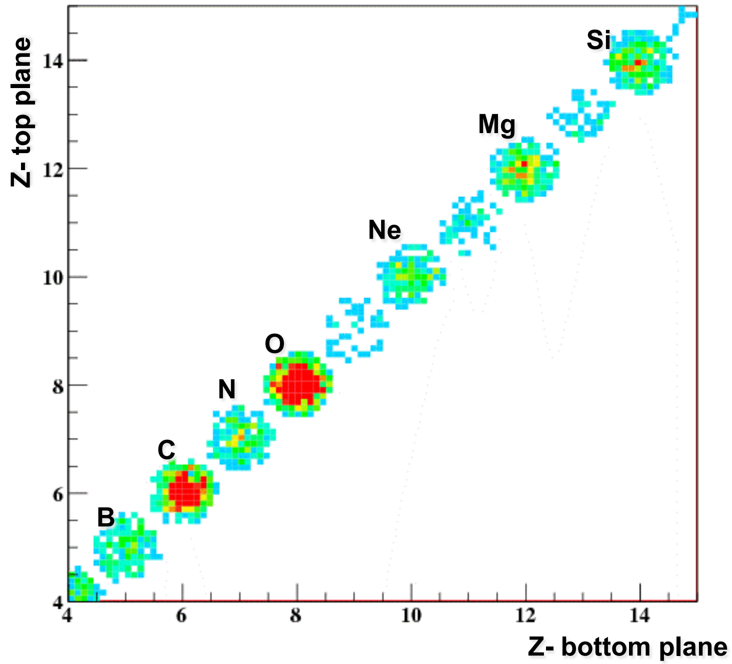

Excellent charge resolution: ~ 0.2 e from C to Si

Flight I: Dec 2004 - Jan 05

- 42 days - Balloon Record at that time
- (54 days by ULDB, now 55 days by Super-TIGER in 2013)
- ~ 40 million Hi-Z Triggers

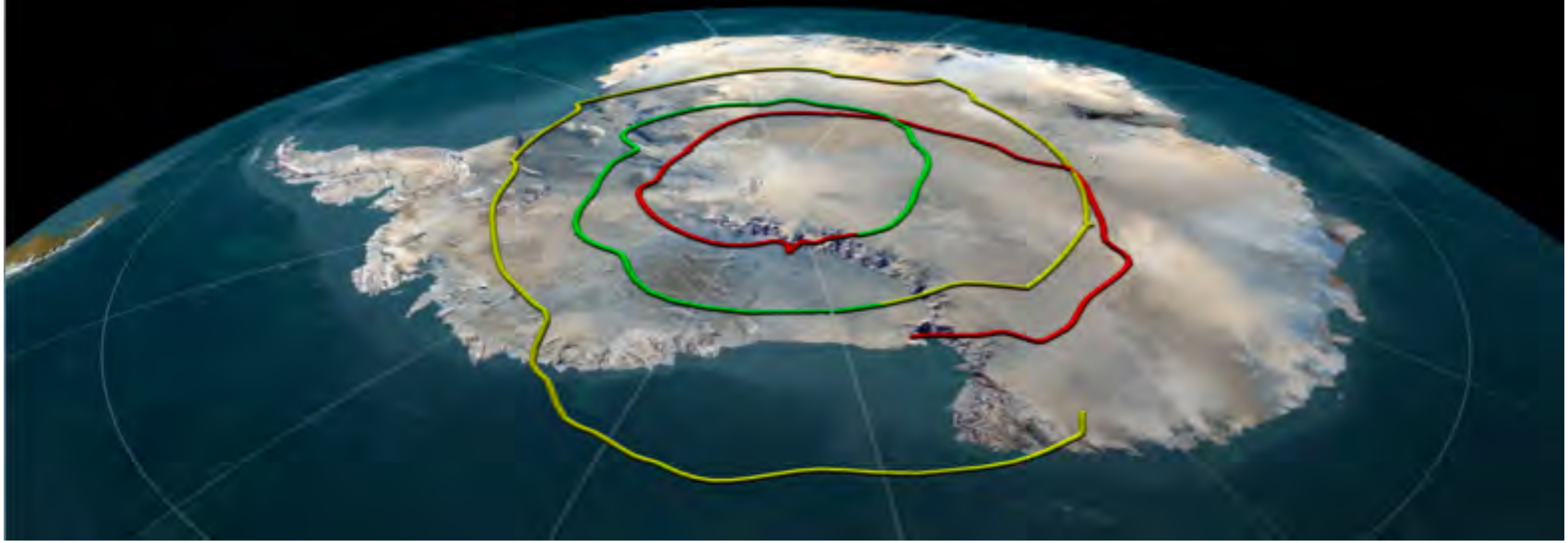

CREAM flights

CREAM-I
12/16/04 – 1/27/05
42 days

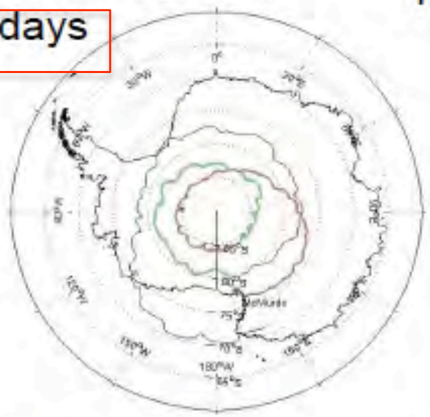

CREAM-II
12/16/05-1/13/06
28 days

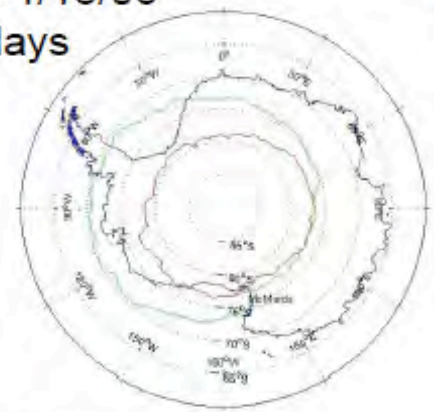

CREAM-III
12/19/07-1/17/08
29 days

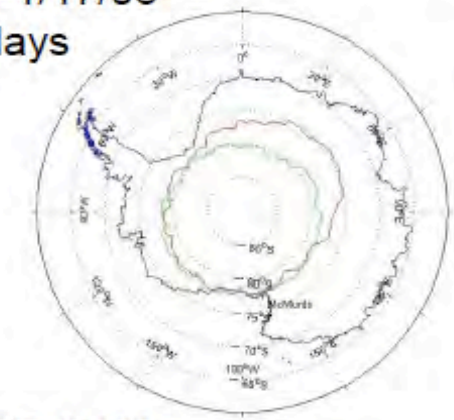

CREAM-IV
12/19/08 - 1/7/09
19 days 13 hrs

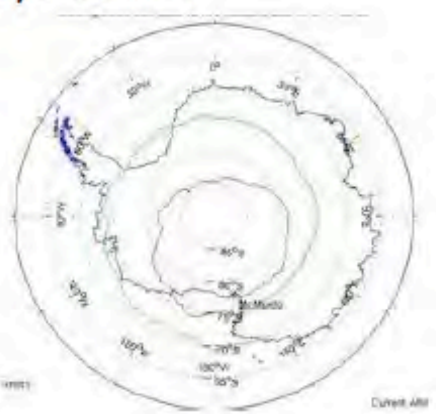

CREAM-V
12/1/09 – 1/8/10
37 days 10 hrs

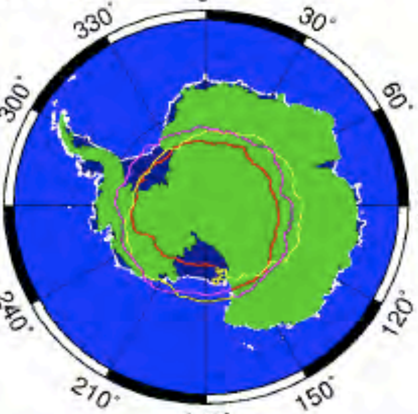

CREAM-VI
12/21/10 – 12/26/10
5 days 16 hrs

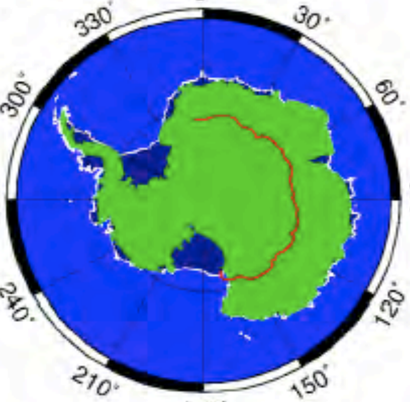

Six Flights: ~161 days cumulative exposure

Recovery operations

From balloon flights to space

Nowadays direct measurements of electron + positron fluxes are carried out in space by experiments that can provided the required **LARGE EXPOSURE**
(e.g.: PAMELA, AMS, FERMI, CALET, DAMPE)

PAMELA launched on 15th June 2006 – satellite mission

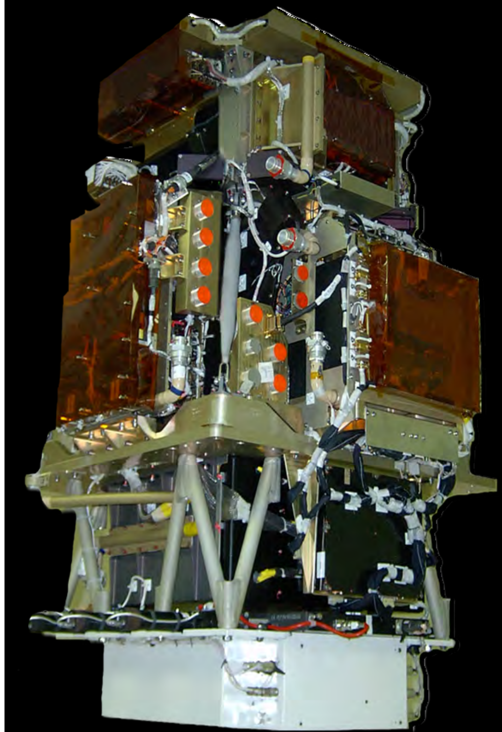

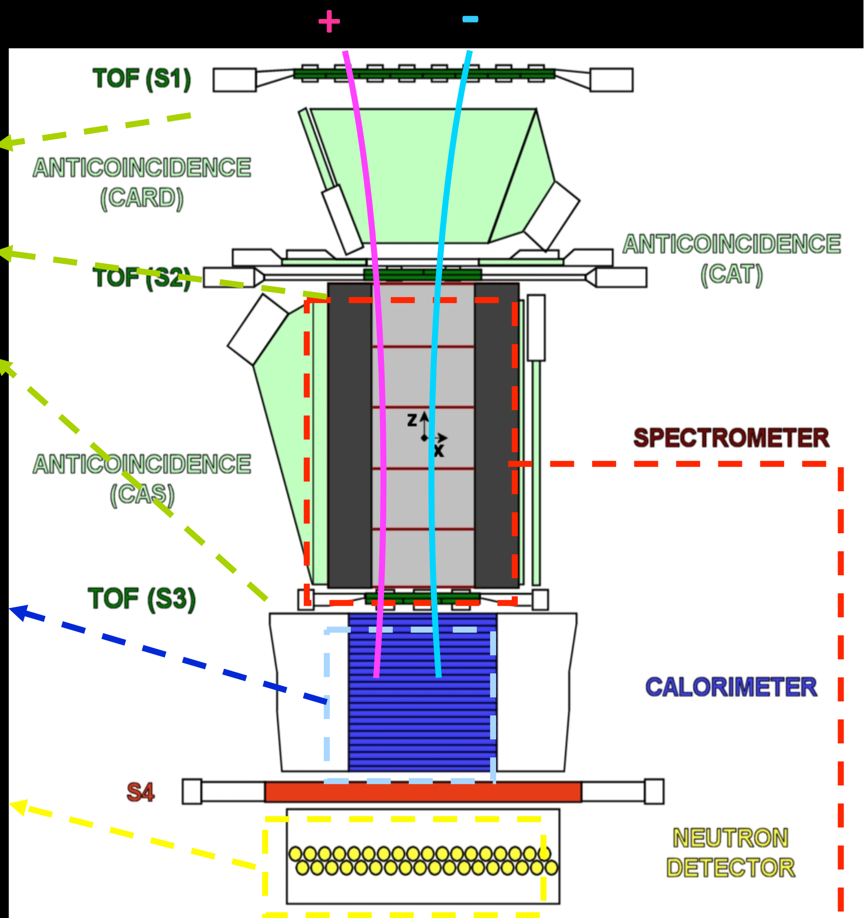

Time-Of-Flight

plastic scintillators + PMT:
Trigger
- Albedo rejection;
- Mass identification up to 1 GeV;
- Charge identification from dE/dX

Electromagnetic calorimeter

W/Si sampling (16.3 X_0, 0.6 λI)
Discrimination e+ / p, anti-p/e^-
(shower topology)
- Direct E measurement for e^-

Neutron detector

^{3}He tubes + polyethylene moderator:
- High-energy e/h discrimination

GF: 21.5 cm^2 sr
Mass: 470 kg
Size: 130x70x70 cm^3
Power Budget: 360W

Elliptical orbit 350 – 610 km
70^o inclination
in operation at 560 km

microstrip silicon tracking system + permanent magnet
provides: - ***Magnetic rigidity*** → R = pc/Ze
- ***Charge sign***
- ***Charge value from dE/dx***

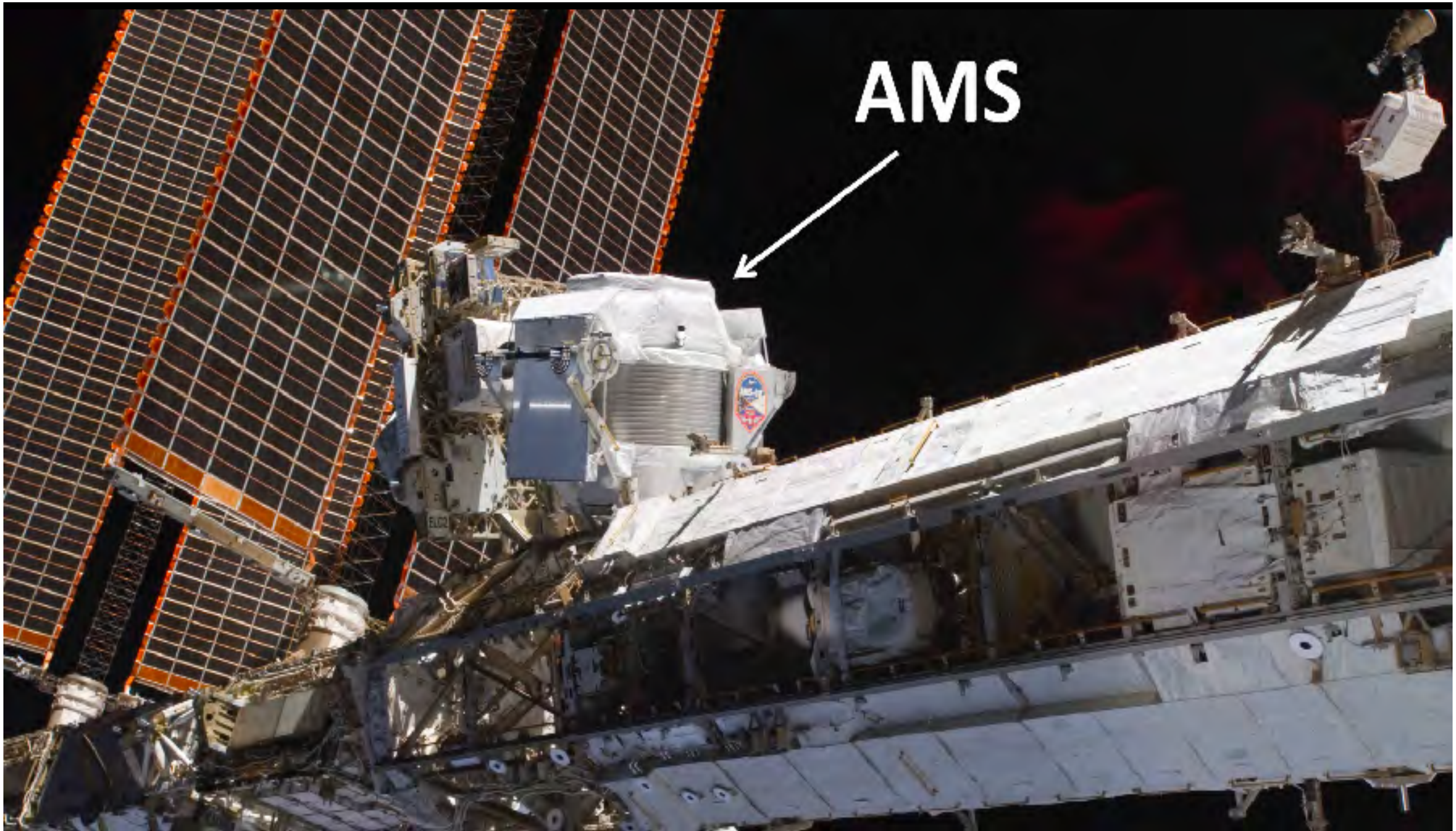

ALPHA Magnetic Spectrometer (AMS) on the ISS - launched in 2011

AMS-02: A TeV precision, multipurpose spectrometer

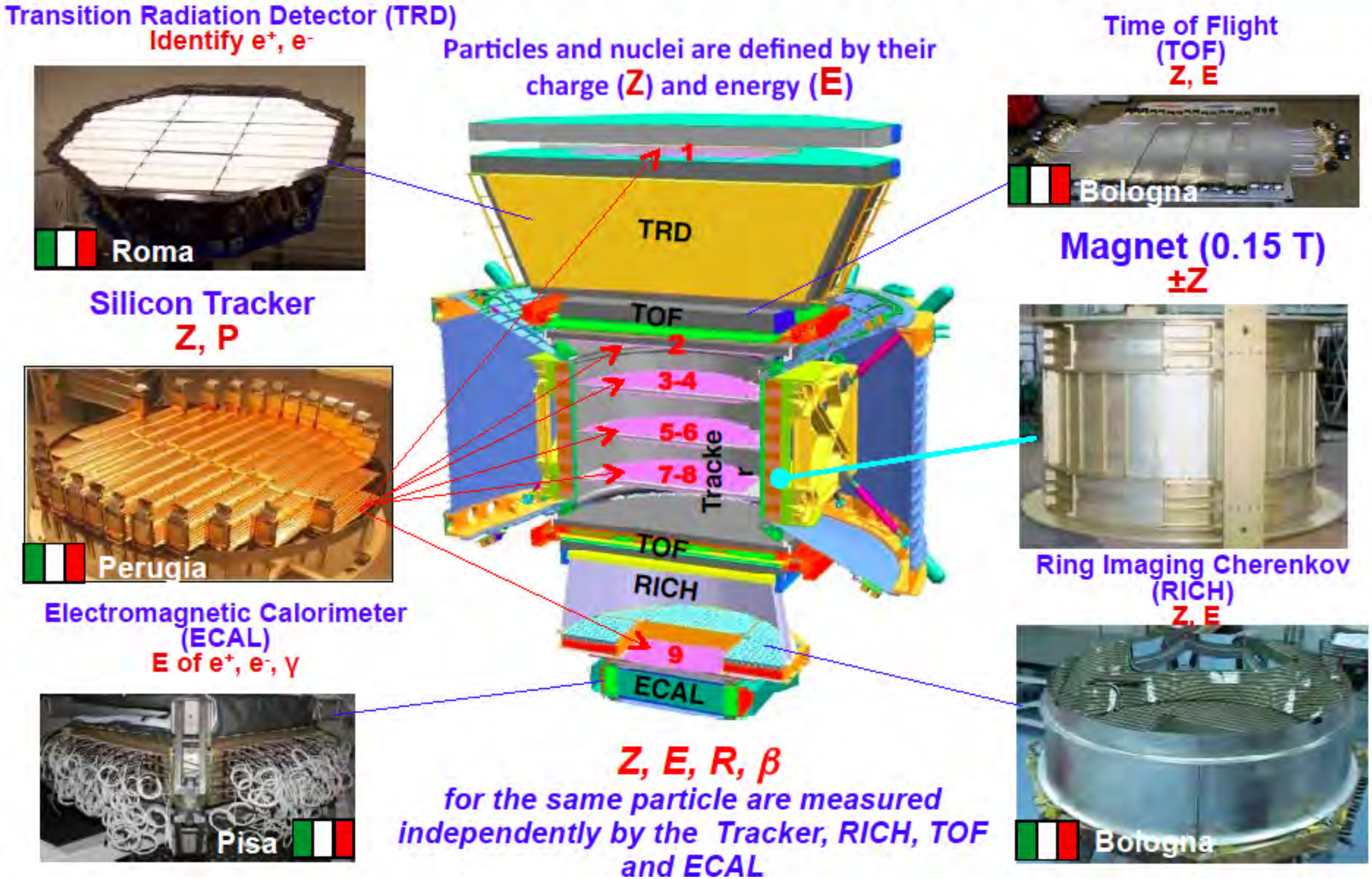

Crab Nebula

Charged cosmic-ray leptons

electron and positron direct measurements

PAMELA (2009) : first unambiguous evidence of the rise of the **positron fraction** $e^+/(e^-+e^+)$ above 10 GeV

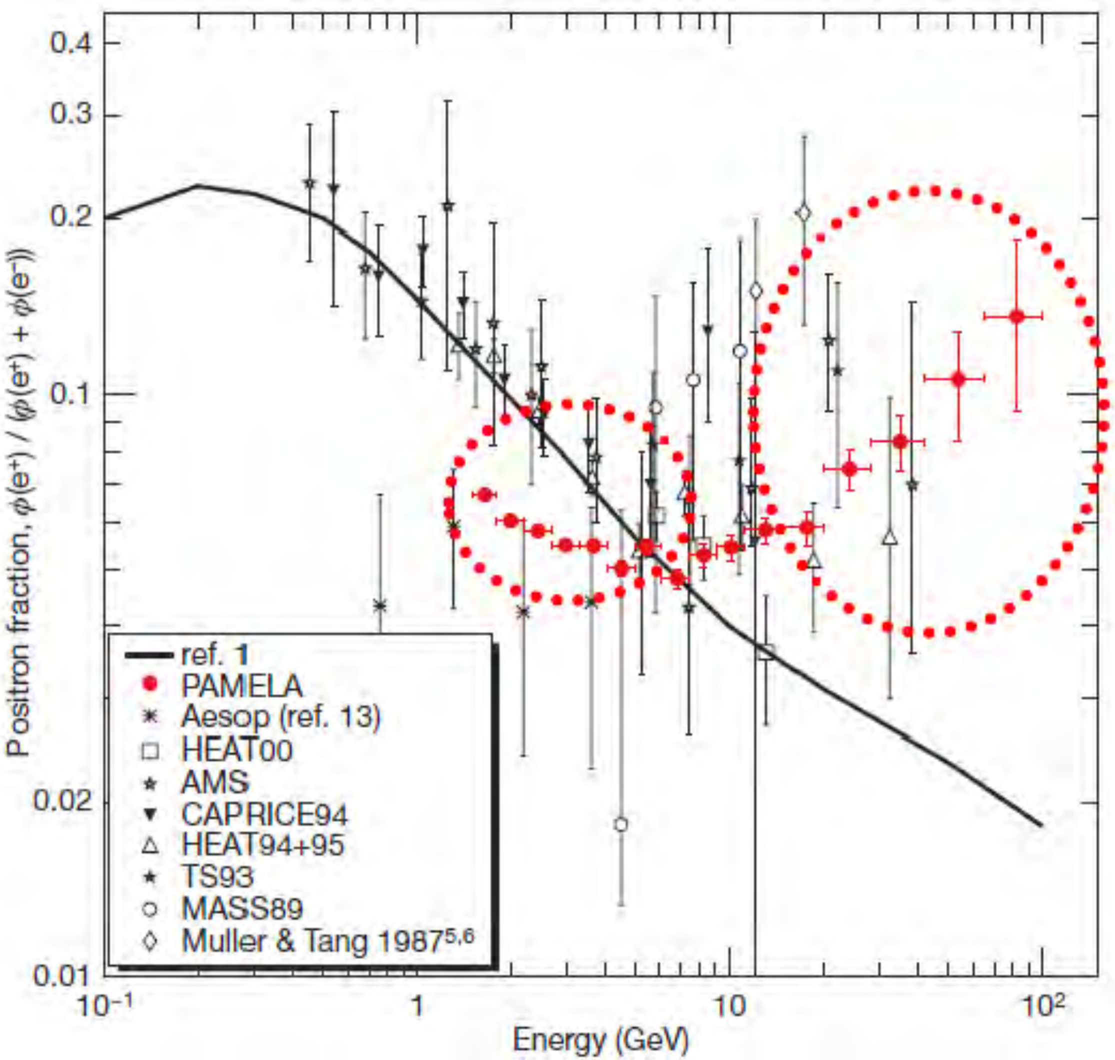

August 2009

An anomalous positron abundance in cosmic rays with energies 1.5–100 GeV

Citations: 1338

2011 PAMELA Results: Positrons

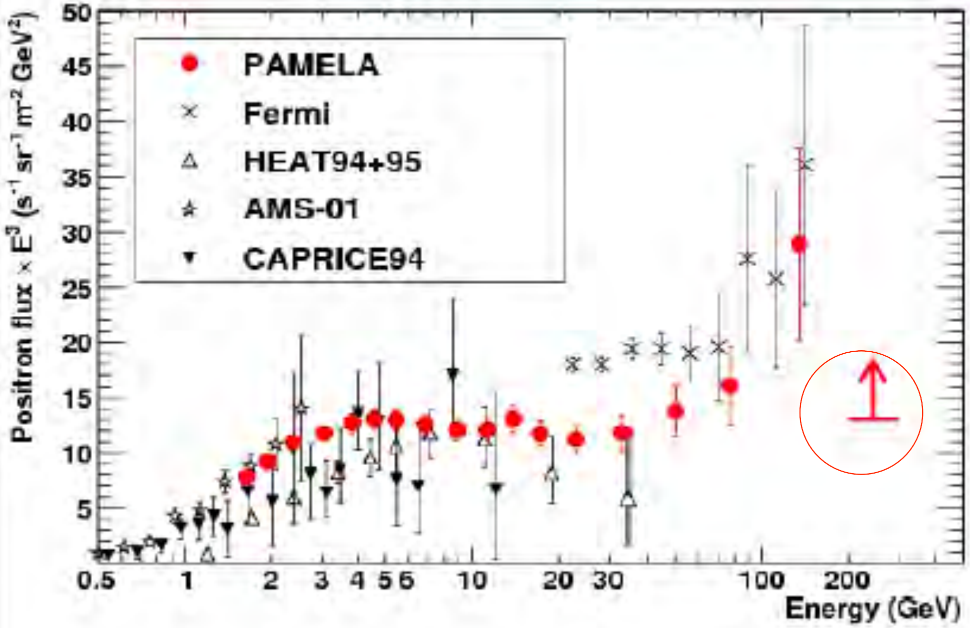

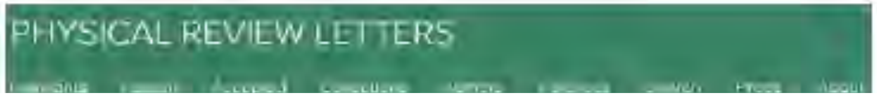

O. Adriani et al. , PRL 106 (2011) 201101

- PAMELA positron spectrum to 300 GeV

- AMS-02 positrons to 500 GeV

Results confirmed by AMS-02!

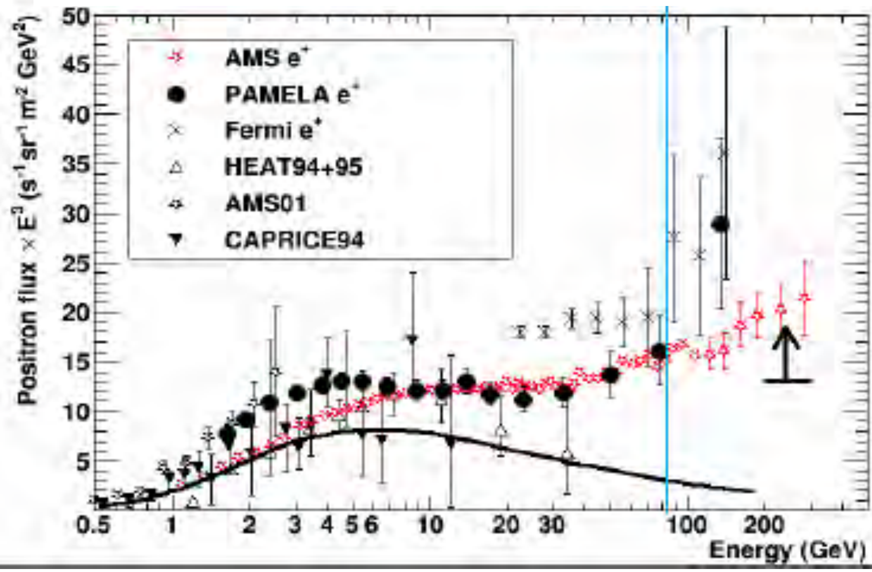

2015 PAMELA Results: Electrons

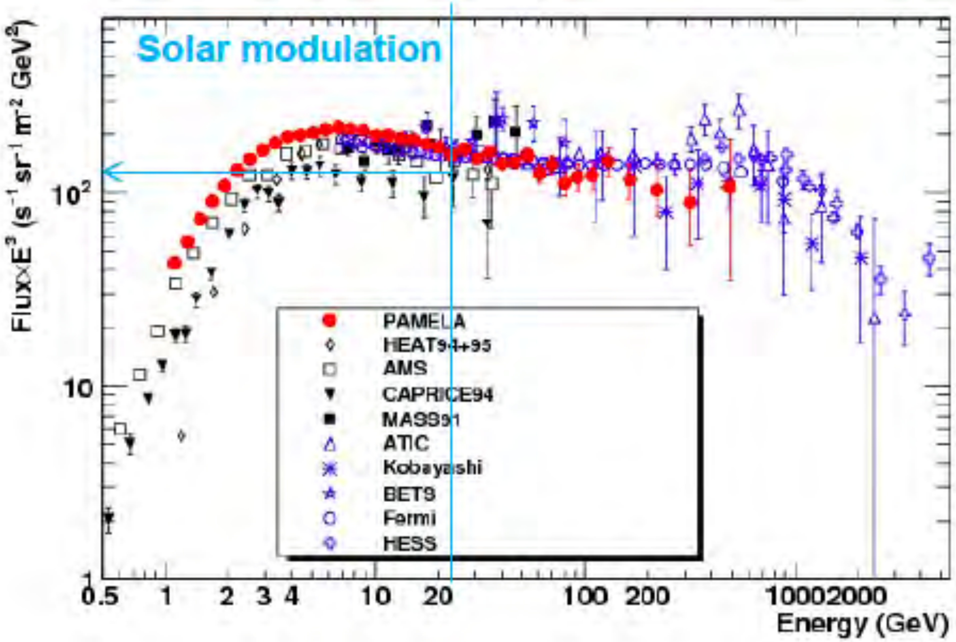

O. Adriani et al., PRL 106, 201101

- PAMELA electron spectrum (published data to 625 GeV)
- AMS-02 electrons to 700 GeV

Study of low energy data (affected by solar modulation)

O. Adriani et al., ApJ 810 (2015) 142

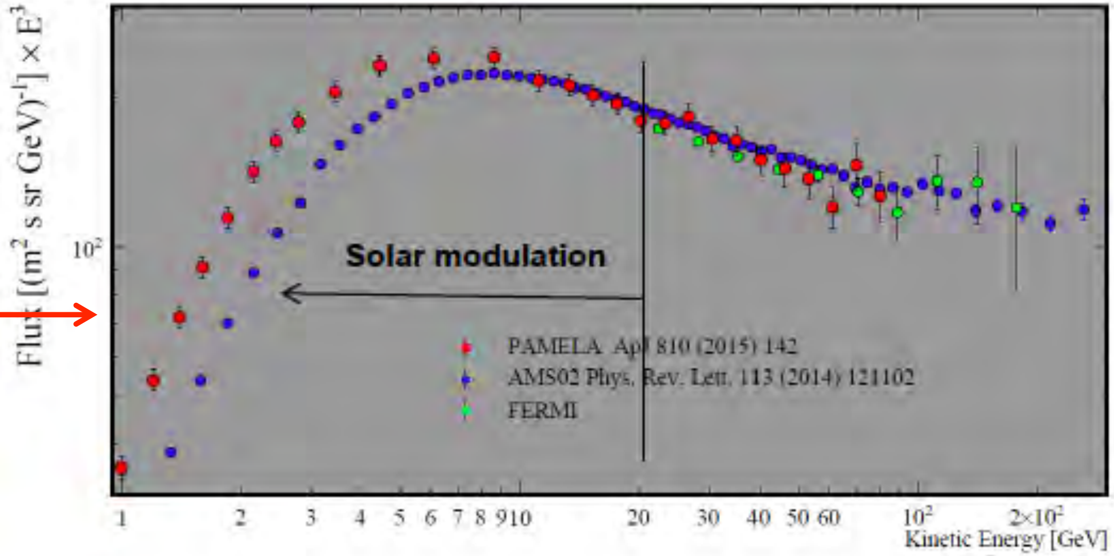

Anisotropy in e^+ and e^- data

- PAMELA

  Study of arrival directions of e^+ and e^- taking into account the effects of the Earth's geomagnetic field:

- No anisotropy observed at all angular scales
- $\delta = 0.076$ at 95% confidence level

  [Panico @ICRC 2015]

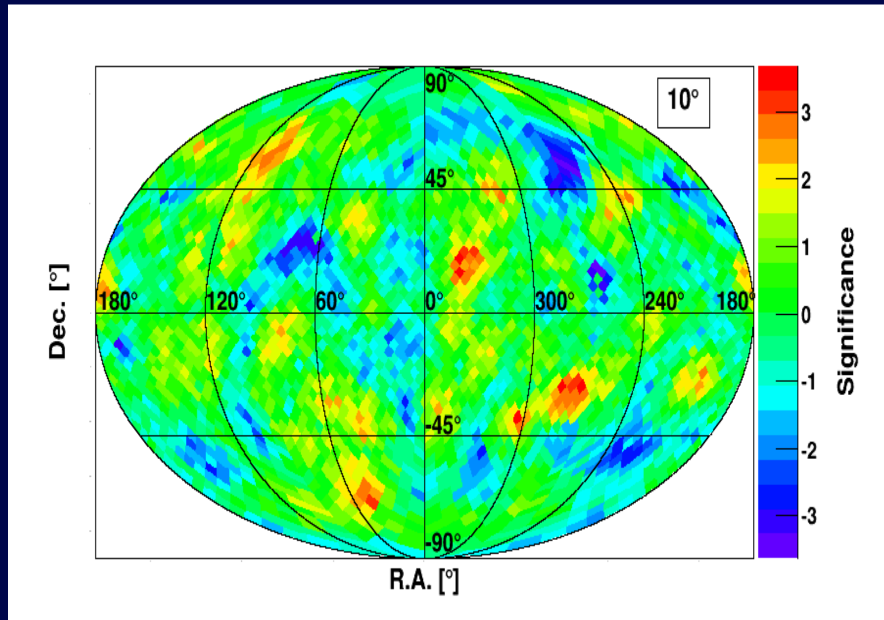

PAMELA Significance sky maps

- AMS-02 (preliminary 2018)

AMS has measured the e+ anisotropy in the energy range from 16 GeV to 350 GeV as being consistent with isotropy

AMS results on the Positron Fraction

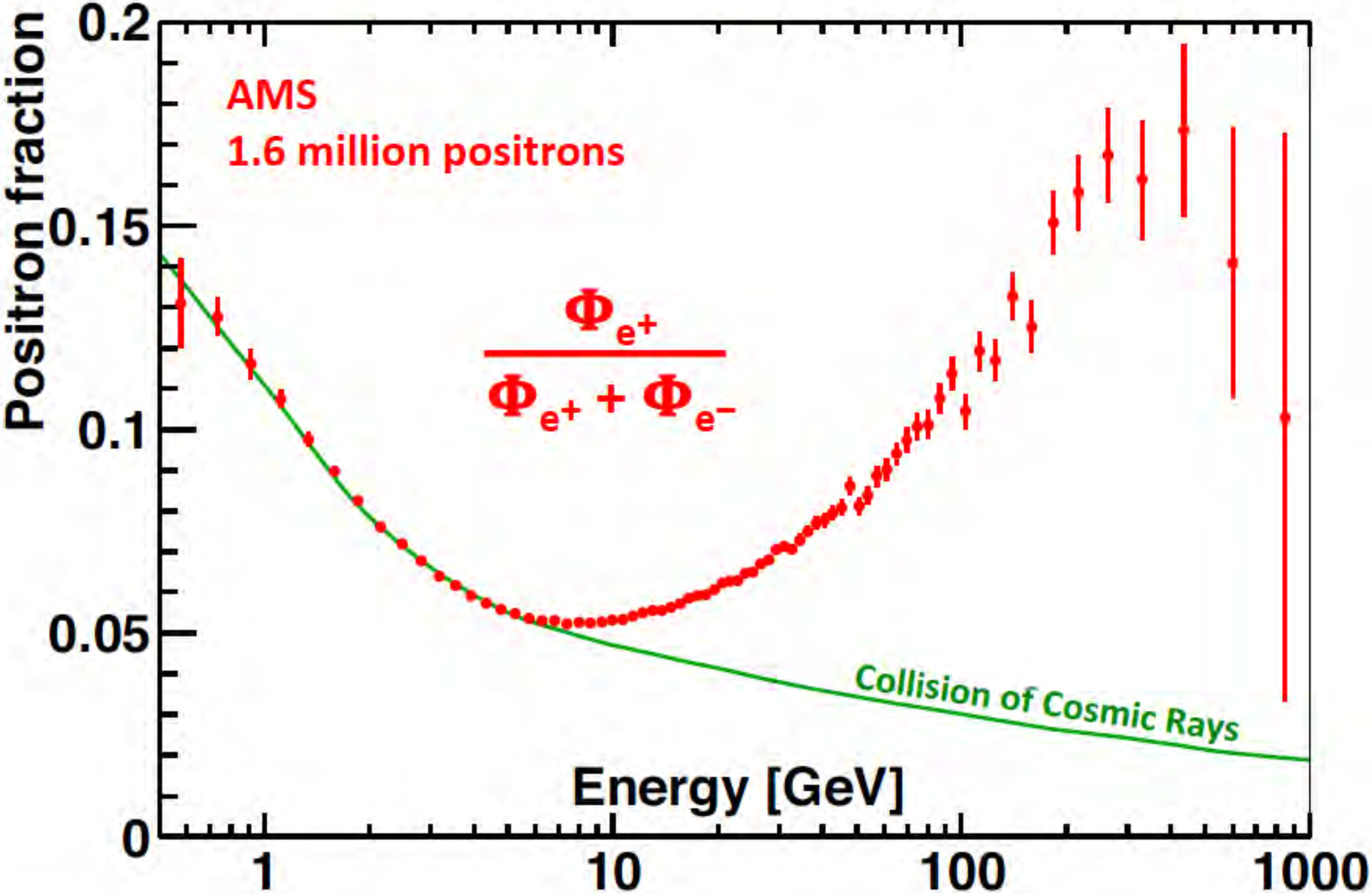

Measurements of the Electron and Positron spectra

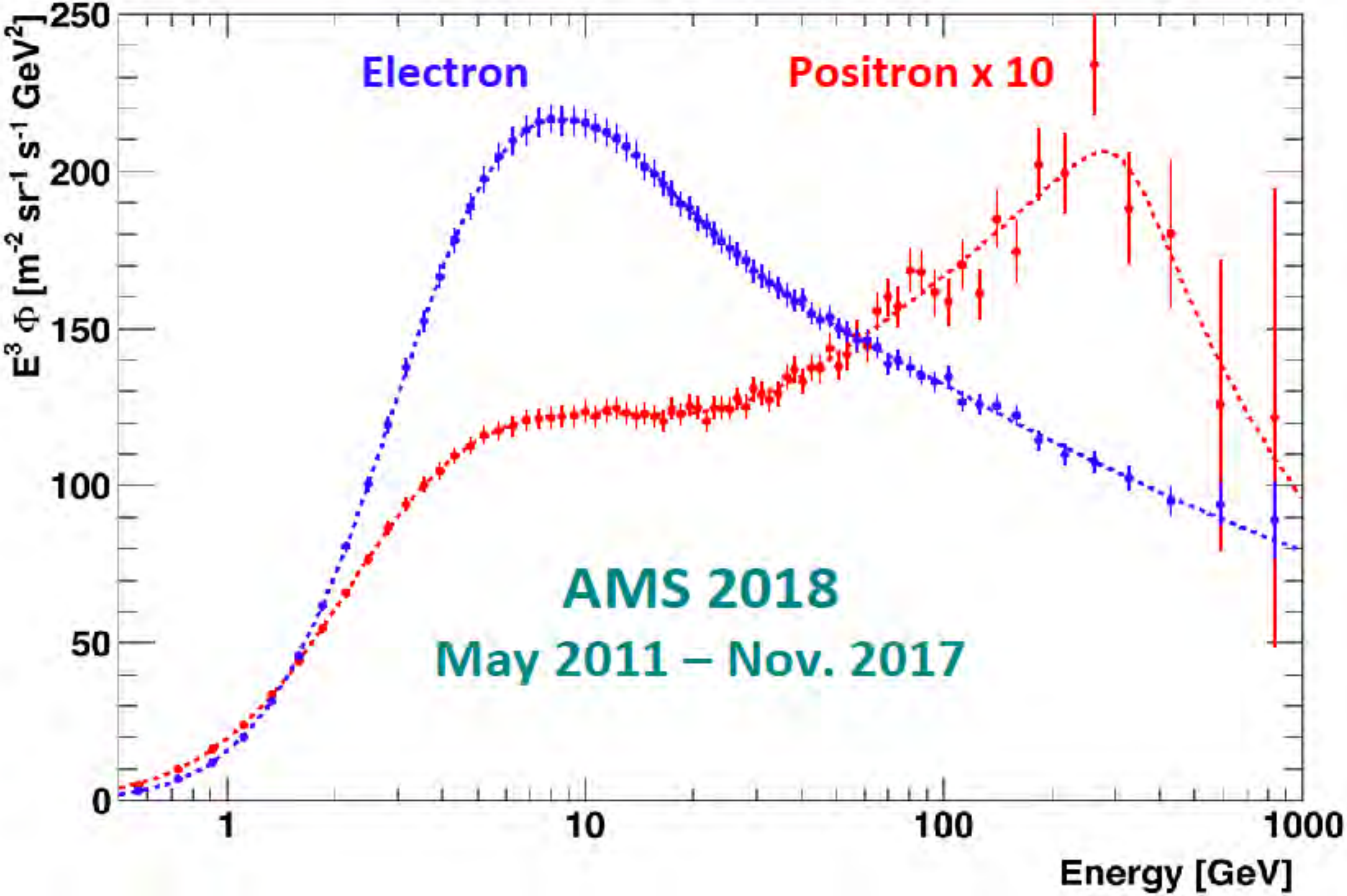

Fluxes of e^+, e^-, p and anti-p as measured by AMS-02

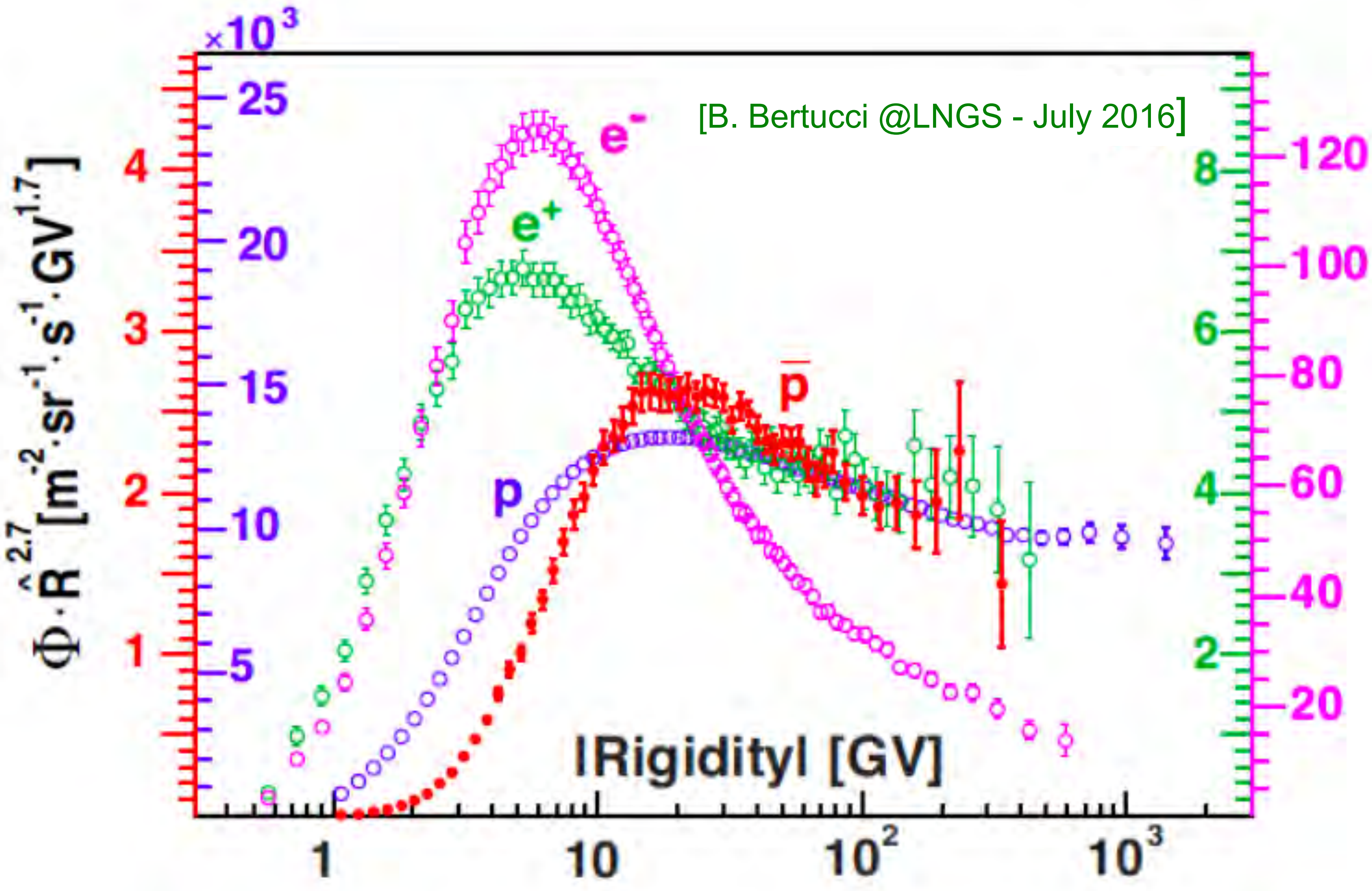

- Above ~60 GV the rigidity dependence of e^+, p and anti-p are **almost identical**
- BUT electrons behave differentlly.

The CR leptonic sector puzzle *(observations)*

① Positron spectrum: *harder than e^-* above 50 – 60 GeV and has *similar Rigidity dependence as proton (and anti-proton).* Incompatible with secondary origin since at these energies radiative losses are dominant during propagation.

② Electron spectrum: *featureless* above 30 GeV up to ~ 1 TeV and *steeper than e^+*

③ Inclusive $e^+ + e^-$ spectrum: direct measurements < 1 TeV => power law index ~ -3.17

Spectrum above 1 TeV from HESS (indirect Cherenkov measurement in the atmosphere)

FERMI data + new direct measurements by CALET and DAMPE.

④ Anisotropy in e^+ and e^- data: *no anisotropy observed* at all angular scales by PAMELA

Electron measurements at high energy are challenging due to the large proton background. High proton rejection power (> 10^5) is required.

A sample of Theoretical Models explaining AMS data

Dark Matter

1) J. Kopp, Phys. Rev. D 88, 076013 (2013);
2) L. Feng, R.Z. Yang, H.N. He, T.K. Dong, Y.Z. Fan and J. Chang Phys.Lett. B728 (2014) 250
3) M. Cirelli, M. Kadastik, M. Raidal and A. Strumia ,Nucl.Phys. B873 (2013) 530
4) M. Ibe, S. Iwamoto, T. Moroi and N. Yokozaki, JHEP 1308 (2013) 029
5) Y. Kajiyama and H. Okada, Eur.Phys.J. C74 (2014) 2722
6) K.R. Dienes and J. Kumar, Phys.Rev. D88 (2013) 10, 103509
7) L. Bergstrom, T. Bringmann, I. Cholis, D. Hooper and C. Weniger, PRL 111 (2013) 171101
8) K. Kohri and N. Sahu, Phys.Rev. D88 (2013) 10, 103001
9) A. Ibarra, A.S. Lamperstorfer and J. Silk, Phys.Rev. D89 (2014) 063539
10) Y. Zhao and K.M. Zurek, JHEP 1407 (2014) 017
11) C. H. Chen, C. W. Chiang, and T. Nomura, Phys. Lett. B 747, 495 (2015)
12) H. B. Jin, Y. L. Wu, and Y.-F. Zhou, Phys.Rev. D92, 055027 (2015)
13) M-Y. Cui, Q. Yuan, Y-L.S. Tsai and Y-Z. Fan, arXiv:1610.03840 (2016)
14) A. Cuoco, M. Krämer and M. Korsmeier, arXiv:1610.03071 (2016)
15) A. Reinert and M. W. Winkler JCAP 01 (2018) 055

and many other excellent papers ...

Propagation

1) R.Cowsik, B.Burch, and T.Madziwa-Nussinov, Ap.J. 786 (2014) 124
2) K. Blum, B. Katz and E. Waxman, Phys.Rev.Lett. 111 (2013) 211101
3) R. Kappl and M. W. Winkler, J. Cosmol. Astropart. Phys. 09 (2014) 051
4) G.Giesen, M.Boudaud, Y.Gènolini, V.Poulin, M.Cirelli, P.Salati and P.D.Serpico, JCAP09 (2015) 023;
5) C.Evoli, D.Gaggero and D.Grasso, JCAP 12 (2015) 039.
6) R.Kappl, A.Reinert, and M.W.Winkler, arXiv:1506.04145 (2015)

and many other excellent papers ...

Astrophysical Sources

1) T. Linden and S. Profumo, Astrophys.J. 772 (2013) 18
2) P. Mertsch and S. Sarkar, Phys.Rev. D 90 (2014) 061301
3) I. Cholis and D. Hooper, Phys.Rev. D88 (2013) 023013
4) A. Erlykin and A.W. Wolfendale, Astropart.Phys. 49 (2013) 23
5) P.F. Yin, Z.H. Yu, Q. Yuan and X.J. Bi, Phys.Rev. D88 (2013) 2, 023001
6) A.D. Erlykin and A.W. Wolfendale, Astropart.Phys. 50-52 (2013) 47
7) E. Amato, Int.J.Mod.Phys.Conf.Ser. 28 (2014) 1460160
8) P. Blasi, Braz.J.Phys. 44 (2014) 426
9) D. Gaggero, D. Grasso, L. Maccione, G. DiBernardo and C Evoli, Phys.Rev. D89 (2014) 083007
10) M. DiMauro, F. Donato, N. Fornengo, R. Lineros and A. Vittino, JCAP 1404 (2014) 006
11) K. Kohri, K. Ioka, Y. Fujita, and R. Yamazaki, Prog. Theor. Exp. Phys. 2016, 021E01 (2016)

and many other excellent papers ...

The positron excess puzzle *(theoretical interpretations)*

✧ Positron excess from Astrophysical sources including:

- **Pulsar Wind Nebulae** (PWN) where the pulsar produces e^+e^- pairs
  + acceleration away from the neutron star (at termination shock)
- **SuperNova Remnants** (SNR) for a recent eview e.g.: [P.Serpico, Astropart. Phys. 39-40 , 2]
- **Local source(s)**: order 0.1% anisotropy expected at ~ 100 GeV

✧ Positron excess from Dark Matter for a recent review e.g.: [M. Cirelli - Dark Matter phenomena - Rapporteur Talk at ICRC2015]

Astrophysical interpretation(s)

- try to fit simultaneously all observables with a single model.
- Large number of papers. An example below from [M.Di Mauro @ICRC2015] :

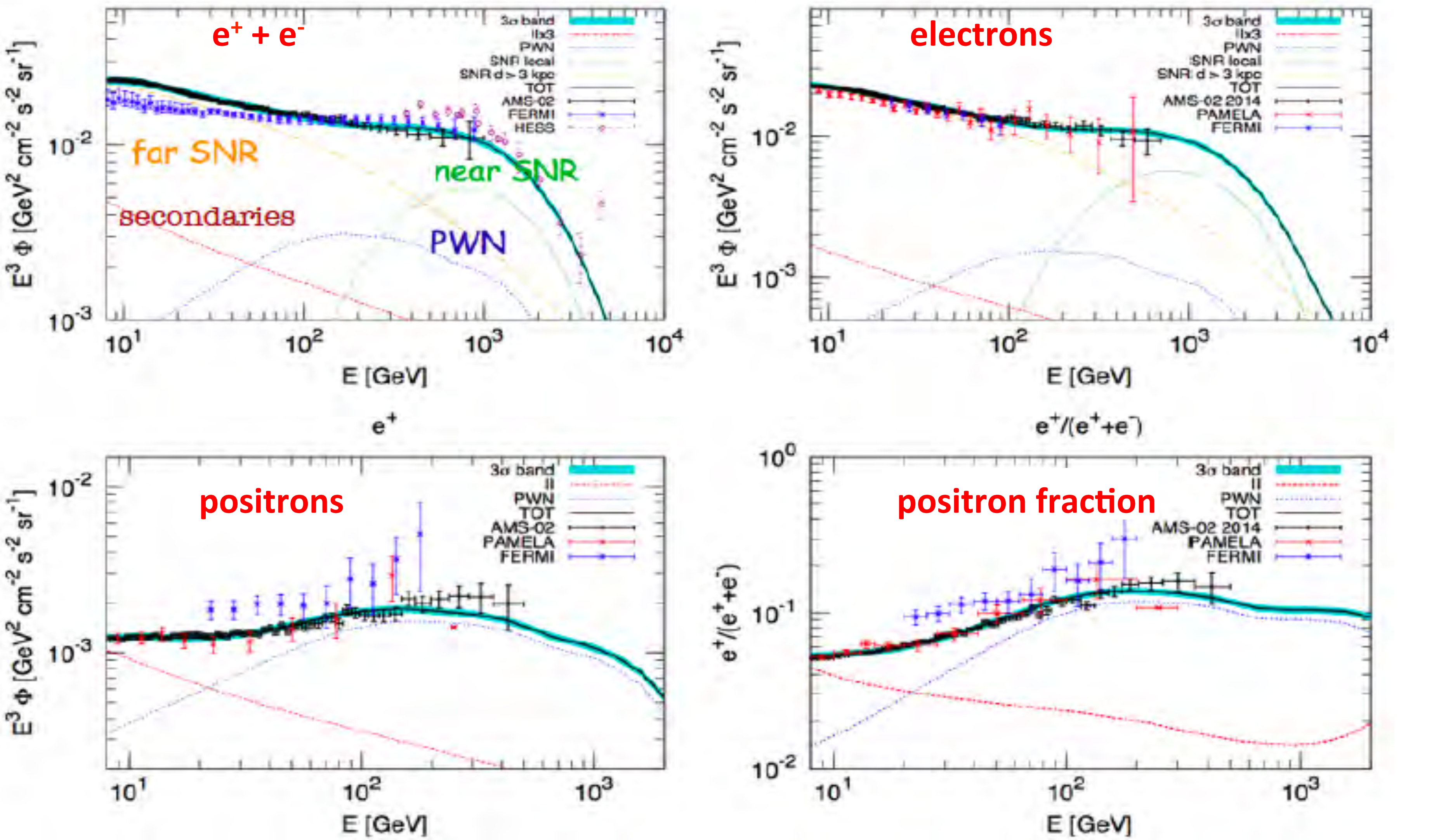

WANTED ! electron spectrum above 1 TeV

Precision measurements expected from new missions CALET and DAMPE

Some nearby sources, e.g. Vela SNR, might have unique signatures
in the electron energy spectrum in the TeV region (Kobayashi et al. ApJ 2004)

Expected flux for 5 year mission

> 10 GeV	~ 2.7 x 10^7
>100 GeV	~ 2.0 x 10^5
>1000 GeV	~ 1.0 x 10^3

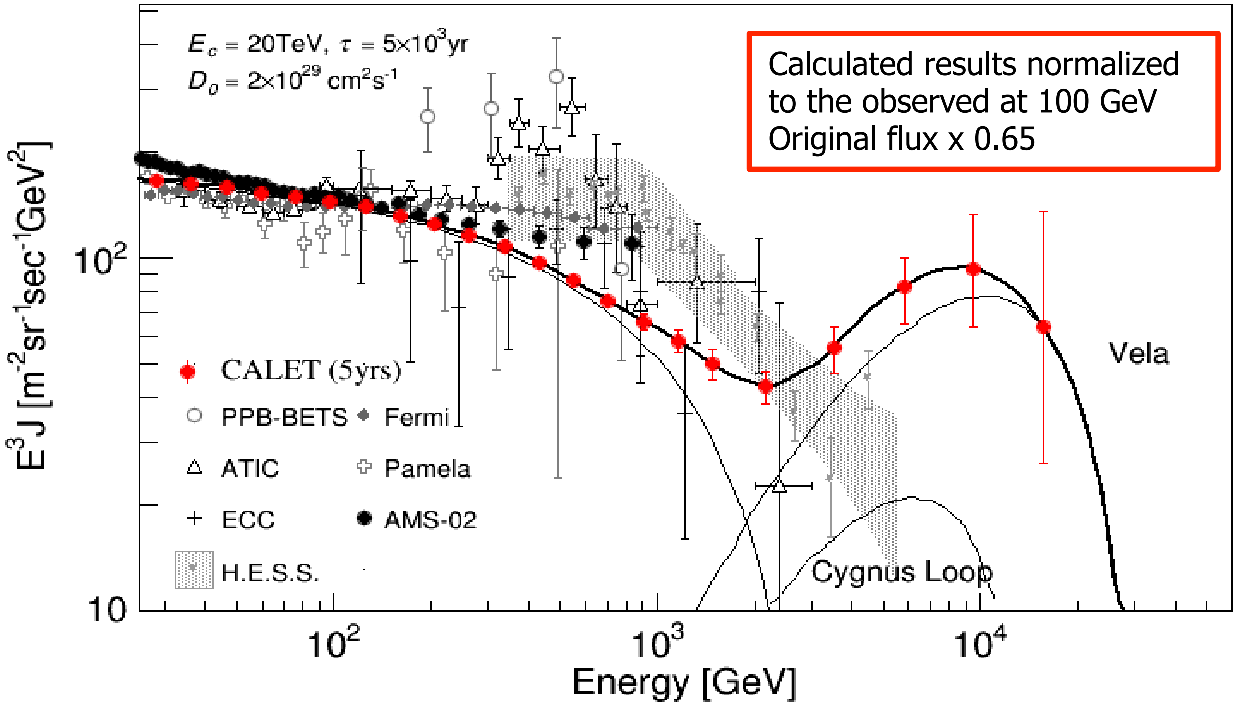

Identification of the unique signature from nearby SNRs, such as Vela in the electron spectrum by CALET

Expected Anisotropy from Vela SNR

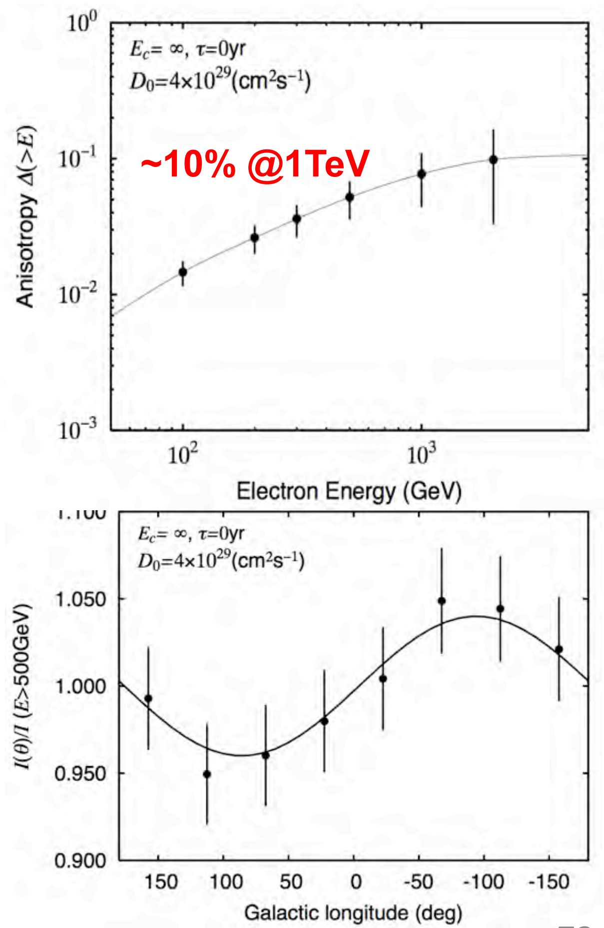

CALET

Calorimetric Electron Telescope

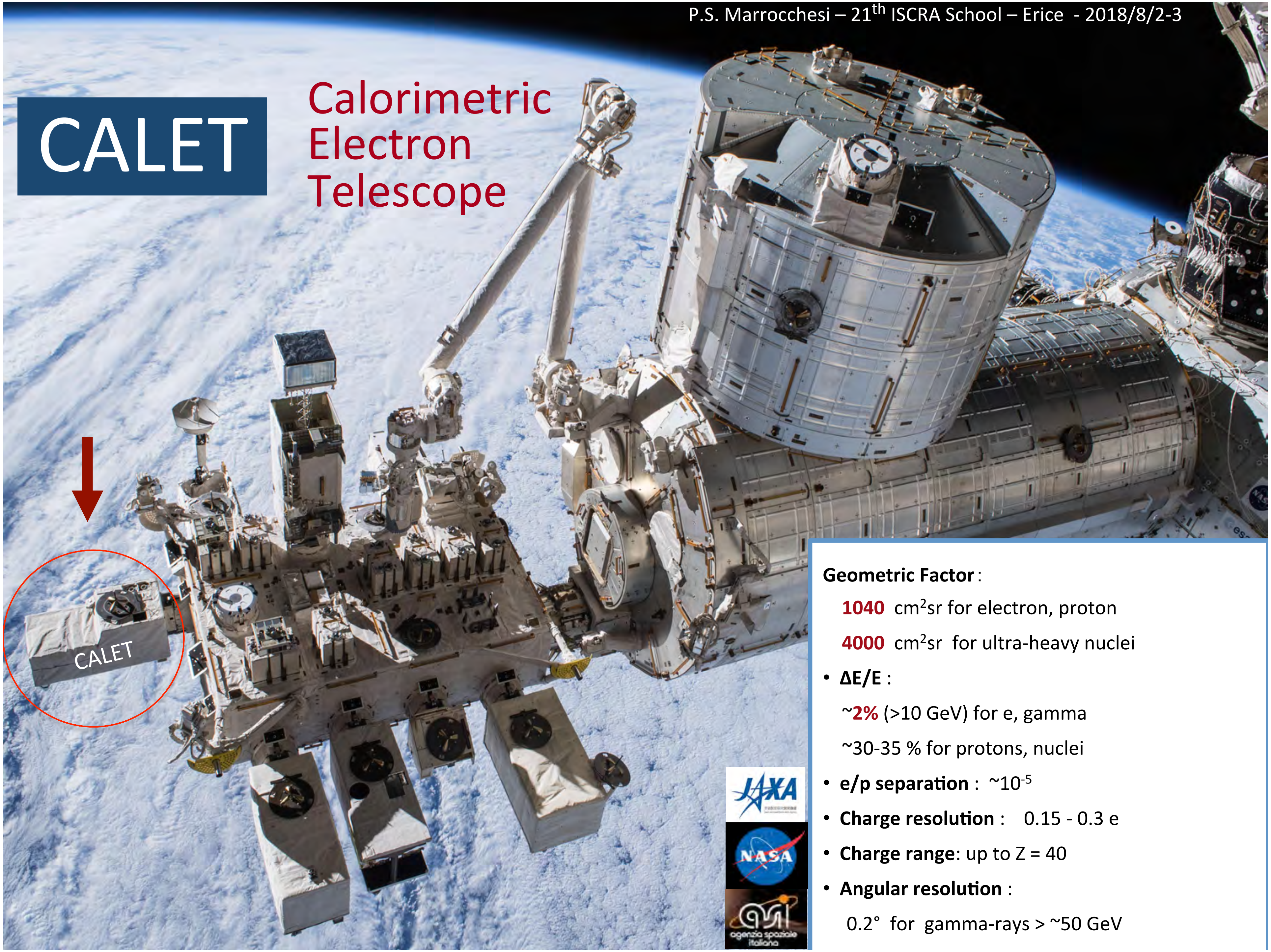

Geometric Factor :

1040 cm^2sr for electron, proton

4000 cm^2sr for ultra-heavy nuclei

- **ΔE/E** :

  ~**2%** (>10 GeV) for e, gamma

  ~30-35 % for protons, nuclei
- **e/p separation** : ~10^{-5}
- **Charge resolution** : 0.15 - 0.3 e
- **Charge range**: up to Z = 40
- **Angular resolution** :

  0.2° for gamma-rays > ~50 GeV

CALET Payload

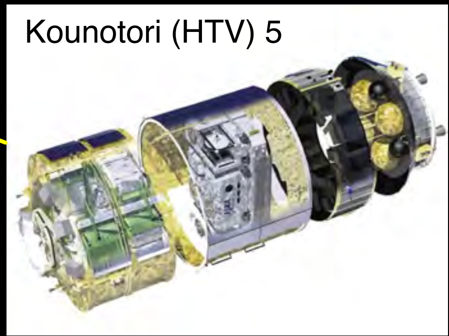

Launched on Aug. 19^{th}, 2015
by the Japanese H2-B rocket

- Mass: 612.8 kg
- Power: 507 W (max)
- Telemetry: Medium 600 kbps (6.5GB/day)

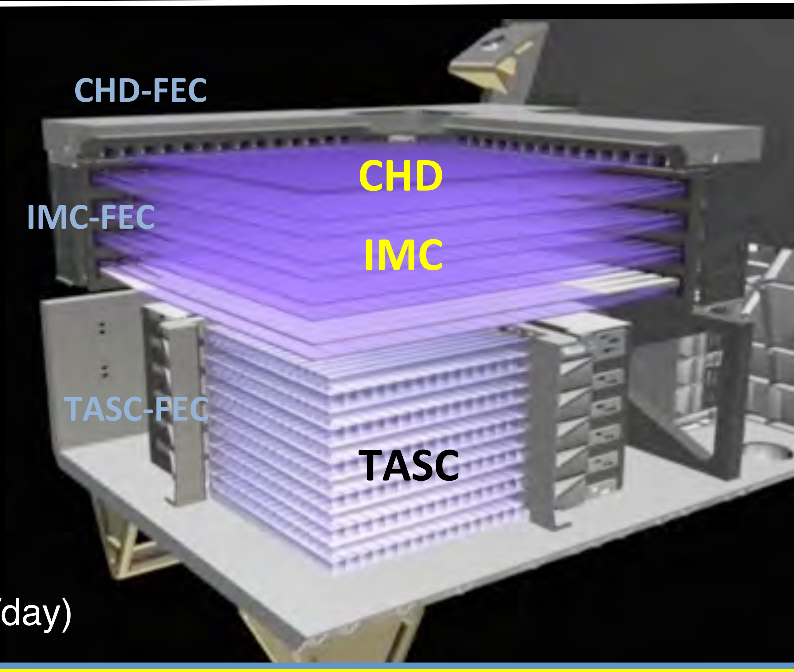

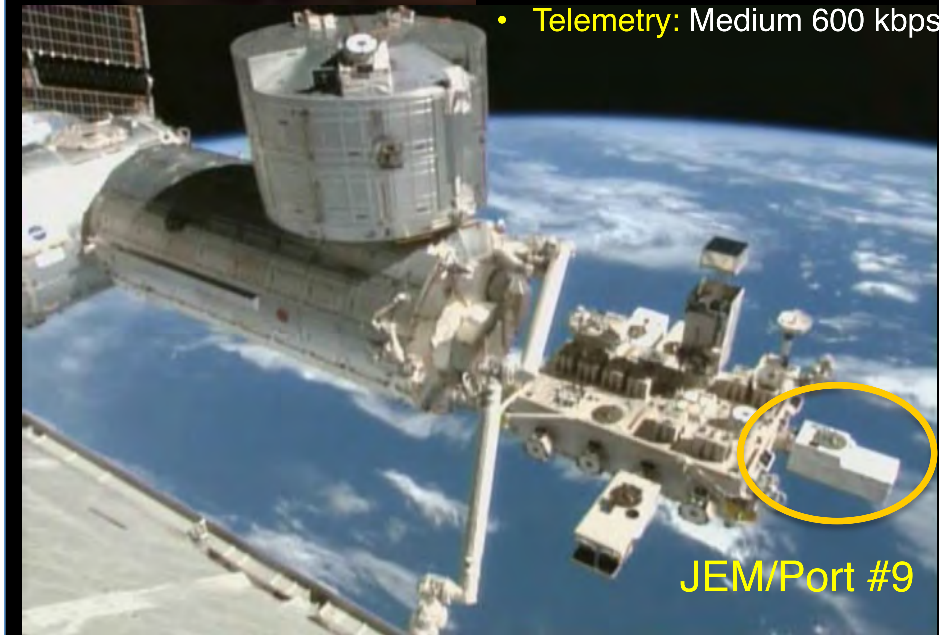

CALET: a unique set of key instruments.

- ❑ **TASC**: a **thick, homogeneous calorimeter** allows to extend electron measurements into the TeV energy region with ~2% energy resolution.
- ❑ **IMC:** a **high granularity (1mm) imaging pre-shower with tracking capabilities** identifies the starting point of electromagnetic showers.
- ❑ TASC+IMC **(30 X_0, 1.3 λ_I)** provide a **strong rejection power ～10^5** to separate electrons from the abundant protons.
- ❑ **CHD: a charge detector** combined with multiple dE/dx samples from IMC identifies individual elements.

DAMPE

Dark Matter Explorer Satellite (Launched on Dec 17, 2015)

- Large geometric factor instrument (0.3 m^2 sr for p and nuclei)
- Precision Si-W tracker (40μm , 0.2°)
- Thick calorimeter (32 X_0 , σ_E/E better than 1% above 50 GeV for e/γ , ~35% for hadrons)
- "Mutiple" charge measurements (0.2-0.3 e resolution)
- e/p rejection power > 10^5 (topology alone, plus neutron detector)

	DAMPE
e/γ Energy res.@100 GeV (%)	1.5
e/γ Angular res.@100 GeV (°)	0.1
e/p discrimination	10^5
Calorimeter thickness (X_0)	32
Geometrical accep. (m^2sr)	0.29

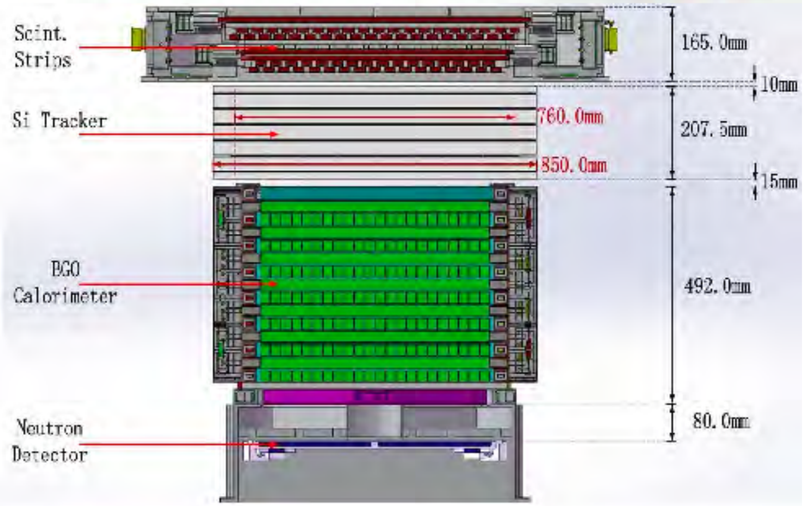

Comparison with AMS-02 and FERMI

	DAMPE	AMS-02	Fermi LAT
e/γ Energy res.@100 GeV (%)	1.5	3	10
e/γ Angular res.@100 GeV (°)	0.1	0.3	0.1
e/p discrimination	10^5	10^5 - 10^6	10^3
Calorimeter thickness (X_0)	32	17	8.6
Geometrical accep. (m^2sr)	0.29	0.09	1

[I. De Mitri, LNGS 2015]

- **Satellite ≈ 1900 kg, payload ≈1300kg**
- **Power consumption ≈640W**
- **Lifetime > 3 years**
- **Launched by CZ-2D rockets**

- **Altitude 500 km**
- **Inclination 97.4°**
- **Period 95 minutes**
- **Sun-synchronous orbit**

The DAMPE Detector

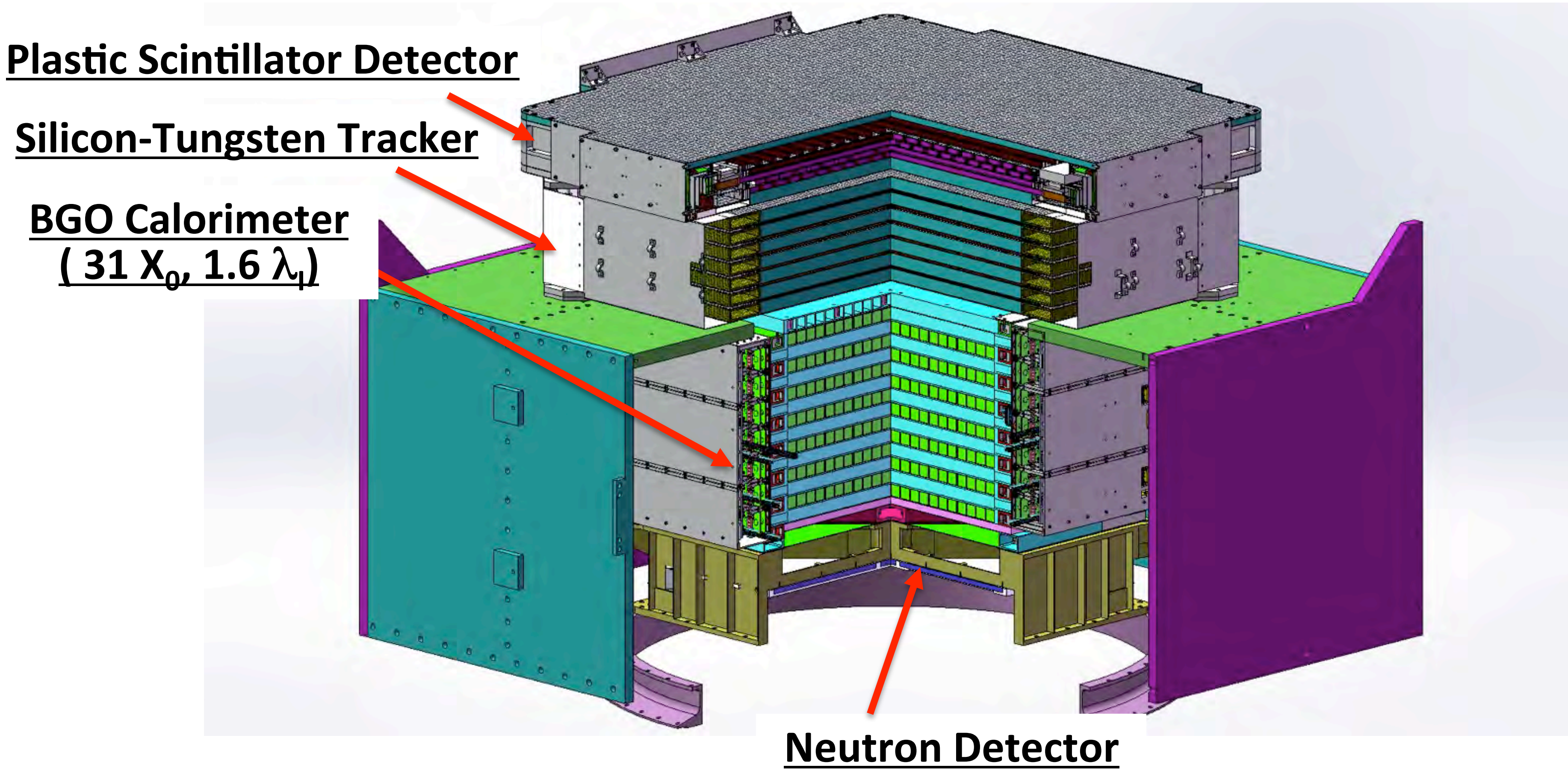

W converter + thick calorimeter (total 33 X_0) + precise tracking + chargemeasurement

high energy gamma-ray, electron and CR telescope

Measurements of the electron spectrum

Comparison of CALET with DAMPE and other experiments in space

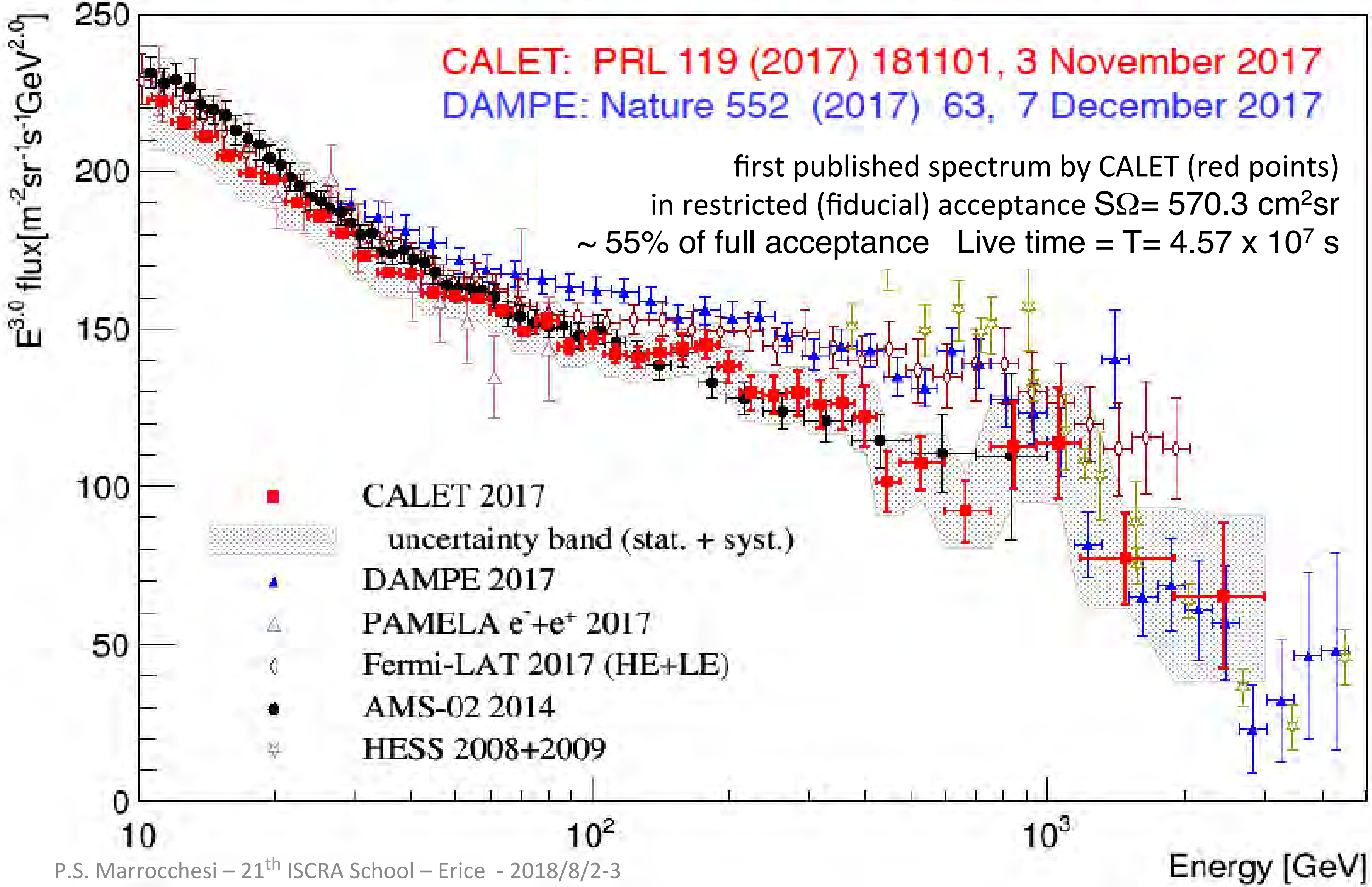

Extended Measurement by CALET

Approximately doubled statistics above 500GeV by using full acceptance of CALET

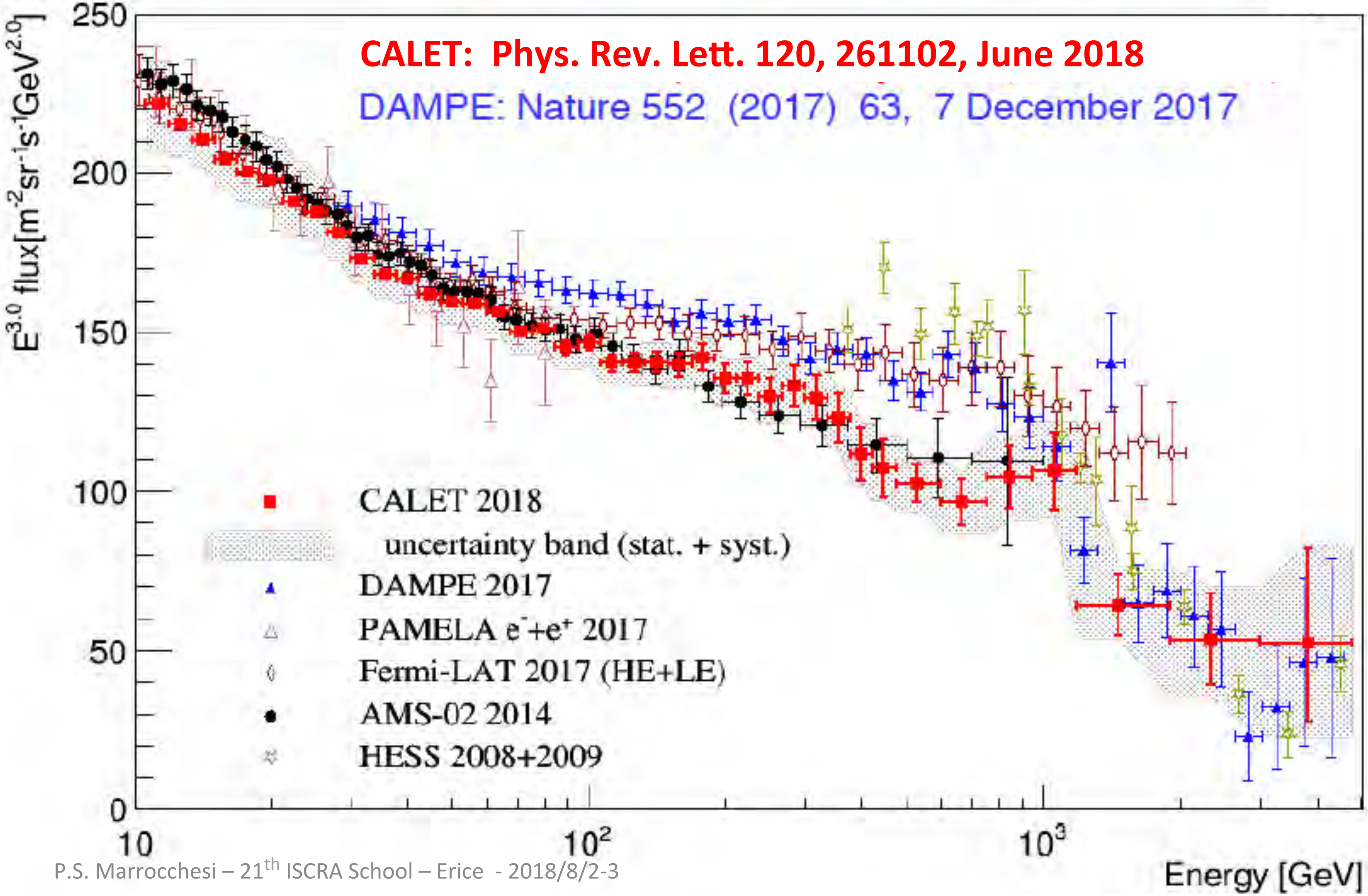

Extended Measurement by CALET

Approximately doubled statistics above 500GeV by using full acceptance of CALET **[11 GeV, 4.8 TeV]**

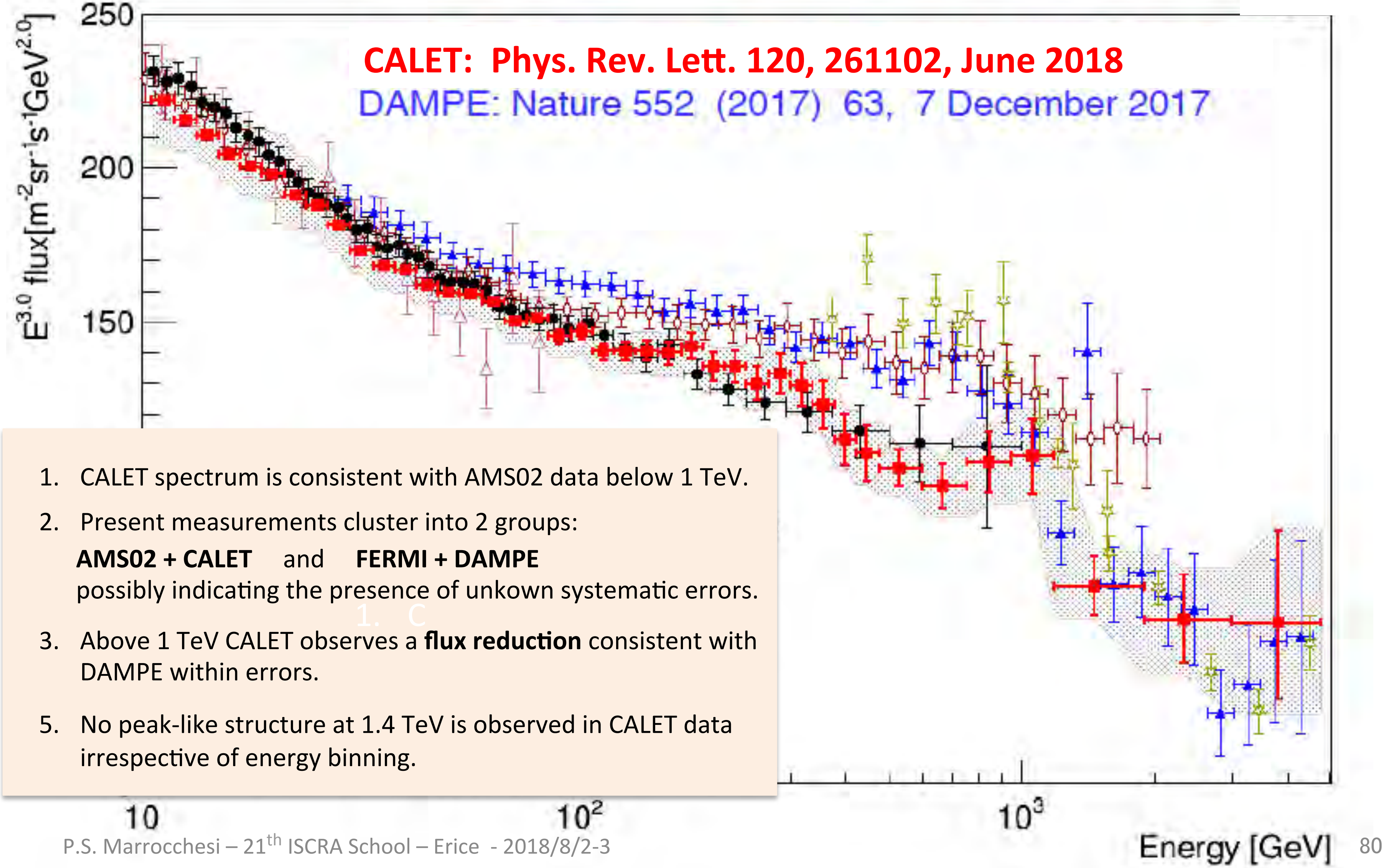

1. CALET spectrum is consistent with AMS02 data below 1 TeV.
2. Present measurements cluster into 2 groups:
   AMS02 + CALET and **FERMI + DAMPE**
   possibly indicating the presence of unkown systematic errors.
3. Above 1 TeV CALET observes a **flux reduction** consistent with DAMPE within errors.
5. No peak-like structure at 1.4 TeV is observed in CALET data irrespective of energy binning.

Comparison of CALET and DAMPE

Is there a peak-like spectral structure at 1.4 TeV ?